

## REPORT DOCUMENTATION PAGE

Form Approved  
OMB No. 0704-0188

The public reporting burden for this collection of information is estimated to average 1 hour per response, including the time for reviewing instructions, searching existing data sources, gathering and maintaining the data needed, and completing and reviewing the collection of information. Send comments regarding this burden estimate or any other aspect of this collection of information, including suggestions for reducing the burden, to Department of Defense, Washington Headquarters Services, Directorate for Information Operations and Reports (0704-0188), 1215 Jefferson Davis Highway, Suite 1204, Arlington, VA 22202-4302. Respondents should be aware that notwithstanding any other provision of law, no person shall be subject to any penalty for failing to comply with a collection of information if it does not display a currently valid OMB control number.

**PLEASE DO NOT RETURN YOUR FORM TO THE ABOVE ADDRESS.**

1. REPORT DATE (DD-MM-YYYY) 7/Dec/2001	2. REPORT TYPE THESIS	3. DATES COVERED (From - To)		
4. TITLE AND SUBTITLE CLIMATOLOGICAL LIGHTING CHARACTERISTICS OF THE SOUTHERN ROCKY AND APPALACHIAN MOUNTAIN CHAINS, A COMPARISON OF TWO DISTINCT MOUNTAIN EFFECTS			5a. CONTRACT NUMBER	
			5b. GRANT NUMBER	
			5c. PROGRAM ELEMENT NUMBER	
6. AUTHOR(S) CAPT PHILLIPS STEPHEN E			5d. PROJECT NUMBER	
			5e. TASK NUMBER	
			5f. WORK UNIT NUMBER	
7. PERFORMING ORGANIZATION NAME(S) AND ADDRESS(ES) TEXAS A&M UNIVERSITY			8. PERFORMING ORGANIZATION REPORT NUMBER CI01-310	
9. SPONSORING/MONITORING AGENCY NAME(S) AND ADDRESS(ES) THE DEPARTMENT OF THE AIR FORCE AFIT/CIA, BLDG 125 2950 P STREET WPAFB OH 45433			10. SPONSOR/MONITOR'S ACRONYM(S)	
			11. SPONSOR/MONITOR'S REPORT NUMBER(S)	
12. DISTRIBUTION/AVAILABILITY STATEMENT Unlimited distribution In Accordance With AFI 35-205/AFIT Sup 1			DISTRIBUTION STATEMENT A: Approved for Public Release Distribution Unlimited	
13. SUPPLEMENTARY NOTES				
14. ABSTRACT				
15. SUBJECT TERMS				
16. SECURITY CLASSIFICATION OF: a. REPORT		17. LIMITATION OF ABSTRACT	18. NUMBER OF PAGES 142	19a. NAME OF RESPONSIBLE PERSON 19b. TELEPHONE NUMBER (Include area code)

20020204 079

**CLIMATOLOGICAL LIGHTNING CHARACTERISTICS OF THE SOUTHERN  
ROCKY AND APPALACHIAN MOUNTAIN CHAINS, A COMPARISON OF TWO  
DISTINCT MOUNTAIN EFFECTS**

A Thesis

by

STEPHEN EDWARD PHILLIPS

Submitted to the Office of Graduate Studies of  
Texas A&M University  
in partial fulfillment of the requirements for the degree of

MASTER OF SCIENCE

December 2001

Major Subject: Atmospheric Sciences

## ABSTRACT

Climatological Lightning Characteristics of the Southern Rocky and Appalachian Mountain Chains: A Comparison of Two Distinct Mountain Effects. (December 2001)

Stephen Edward Phillips, B.S., Texas A&M University

Chair of Advisory Committee: Dr. Richard Orville

This study presents a high-resolution lightning climatology for southern portions of both the Rocky Mountains and the Appalachian Mountains. Data from the National Lightning Detection Network (NLDN) are analyzed to produce maps of average annual lightning flash density, positive flash density, percent positive flashes, median peak current, and multiplicity. Three-hourly increments are used to demonstrate the annual average diurnal evolution of flash density. Data are also divided into seasonal averages for the same three-hourly increments to describe the daily evolution of flash density for each of the four seasons: December-January-February, March-April-May, June-July-August, and September-October-November.

The flash density analyses reveal opposite mountain-valley effects. In the Rocky Mountains, flash density enhancements occur over and near mountains and flash density minima occur in the valleys. In the Appalachians, the enhancements occur in the valleys, while minimums are noted over the mountains. The eastern edge of the Appalachian lightning suppression is determined to be a result of faster propagation of mountain-initiated convection. Weaker mountain breezes in the Appalachians are theorized to be the catalysts for this. The western edge of the suppression is the cumulative effect of

consistent flash density gradients at the Appalachian's western slopes. A theory is presented which links this gradient to observations of high median peak currents.

Statistical tests on flash density means show that the Appalachian suppression is significant. Multiple regressions predict lightning flash density from terrain characteristics.

Vertical wind and thermodynamic profiles, horizontal temperature differences at summit levels, and average annual precipitation complete the study. From these data, a conceptual model is presented to describe the nature of the lightning evolution in each region, and explain the processes that lead to the end state.

This study concludes that the differences between the patterns of lightning characteristics in the Southern Rockies and the Southern Appalachians are the cumulative effects of subtle differences in the diurnal evolution patterns. Furthermore, the Appalachian lightning suppression is a product of lightning propagation and storm evolution, rather than a suppression of convective initiation.

## ACKNOWLEDGMENTS

I present my most heartfelt thanks to my committee chair, Dr. Orville, and committee members Dr. Nielsen-Gammon and Dr. Cline. Without their advice and direction, this work would not have been possible.

I also thank the United States Air Force for selecting me to this program and funding my studies.

To my peers and officemates, I offer my sincere appreciation for their help in classes, research, and computer support.

Finally, I owe my deepest debt of gratitude to my wife, Amy. Without her advice, support, and encouragement, this experience would have been a monumental struggle.

## TABLE OF CONTENTS

	Page
ABSTRACT .....	iii
ACKNOWLEDGMENTS .....	v
TABLE OF CONTENTS .....	vi
LIST OF FIGURES .....	viii
LIST OF TABLES.....	x
LIST OF EQUATIONS.....	xi
<b>CHAPTER</b>	
I. INTRODUCTION AND BACKGROUND .....	1
1.1. Introduction .....	1
1.2. Previous Studies .....	2
II. DATA AND METHODS .....	8
2.1. National Lightning Detection Network.....	8
2.2. Regions and Terrain .....	13
2.3. Statistical Methods .....	16
2.4. Upper Air.....	17
2.5. Precipitation Data .....	19
III. RESULTS .....	21
3.1. Lightning Characteristics .....	21
3.2. Precipitation Patterns.....	53
3.3. Statistical Analysis .....	54
3.4. Upper Air Analysis.....	61

CHAPTER	Page
IV. SUMMARY AND CONCLUSION .....	66
4.1. Discussion .....	66
4.2. Conclusion.....	80
REFERENCES .....	85
APPENDIX .....	87
VITA.....	142

## LIST OF FIGURES

FIGURE	Page
1 SW Region Annual Flash Density .....	2
2 SE Region Annual Flash Density.....	3
3 Leeside Convergence Mechanism.....	4
4 NLDN Sensor Locations.....	8
5 Radiation Field Signatures .....	11
6 Key Terrain: Southwest Region.....	14
7 Key Terrain: Southeast Region.....	15
8 SW Positive Flash Characteristics (All Seasons / All Times) .....	23
9 SW Median Peak Currents (All Seasons / All Times) .....	24
10 SW Multiplicities (All Seasons / All Times) .....	25
11 SE Positive Flash Characteristics (All Seasons / All Times).....	27
12 SE Median Peak Currents (All Seasons / All Times) .....	28
13 Distance Between DF Sensors In NLDN.....	29
14 SE Multiplicities (All Seasons / All Times).....	31
15 SW Region By-Times Analysis: Increasing Periods .....	33
16 SW Region By-Times Analysis: Decreasing Periods .....	37
17 SE Region By-Times Analysis: Increasing Periods.....	39
18 SE Region By-Times Analysis: Decreasing Periods .....	40
19 MAM SW Region Three-Hourly Flash Densities.....	45
20 MAM SE Region Three-Hourly Flash Densities.....	46
21 JJA SW Region Three-Hourly Flash Densities.....	47

FIGURE	Page
22 JJA SE Region Three-Hourly Flash Densities .....	48
23 SON SW Region Three-Hourly Flash Densities.....	49
24 SON SE Region Three-Hourly Flash Densities.....	50
25 DJF SW Region Three-Hourly Flash Density .....	51
26 DJF SE Region Three-Hourly Flash Densities .....	52
27 Annual Average Precipitation Overlaid On Annual Flash Density .....	54
28 Flash Density Anomalies Versus Elevation Anomalies.....	57
29 SW Multiple Regression Output .....	58
30 SE Multiple Regression Output .....	60
31 Wind Profiles .....	63
32 Propagation Of Thunderstorm Activity Due To Cold Pool / Mountain Breeze Interactions.....	79

**LIST OF TABLES**

TABLE	Page
1     Southwest Region Flash Counts.....	34
2     Southeast Region Flash Counts.....	41
3     Thermodynamic Data.....	65

**LIST OF EQUATIONS**

EQUATION	Page
1      Electric Field Vector .....	9
2      Magnetic Flux Density Vector .....	9
3      Peak Channel Current .....	10

## CHAPTER I

### INTRODUCTION AND BACKGROUND

#### 1.1. Introduction

Climatological lightning studies have been an area of rising interest over the last fifteen years. Extensive research has been performed on the western portions of the United States, mainly in Arizona and New Mexico, where it has been found that the rugged terrain of the Rocky Mountains aids convective initiation and establishes a pattern of high lightning flash density (fig. 1) over the mountain peaks and ridges (Reap, 1986). In the Appalachian Mountain region, however, the mountainous terrain appears to drive a different result. Huffines and Orville (1999) noted a pattern of minimum lightning flash density in the Appalachian Mountain region (fig. 2), which was in stark contrast to the maximum noted in the Rocky Mountains. The contour intervals in figures 1 and 2 were selected to best display the observed mountain and river effects. Even though the Appalachian chain has a significant effect on the weather patterns of the Eastern United States (O'Handley and Bosart, 1996), the effects of these mountains on cloud-to-ground (CG) lightning has sparked very little research. Because the Appalachians are more often subjected to synoptic scale weather systems, it is much more difficult to isolate the primary catalyst for convection. The purpose of this study is to document the lightning suppression over the Appalachian region, and to provide insight into the cause of the pattern.

## 1.2. Previous Studies

The first strides in climatological lightning research through remote observations were made after Radio Detection And Ranging (RADAR) data became available. Precipitation patterns in Arizona, which showed a positive correlation between elevation and rainfall amounts, prompted Braham (1958) to initiate a study of radar echoes in the Tucson area. By comparing the locations and timing of radar echoes to terrain elevation data (spatial resolution of 30 seconds), Braham showed that diurnal mountain echoes occurred more often and earlier than valley echoes, but were less vigorous and produced lower rainfall rates. He suggested that the annual precipitation pattern in the Tucson area resulted from the higher frequency of smaller showers over the mountains giving higher rainfall totals. His main problem was the need for more data. Attempting to analyze the echo data at the same scale as his 30-second terrain data produced statistically poor results.

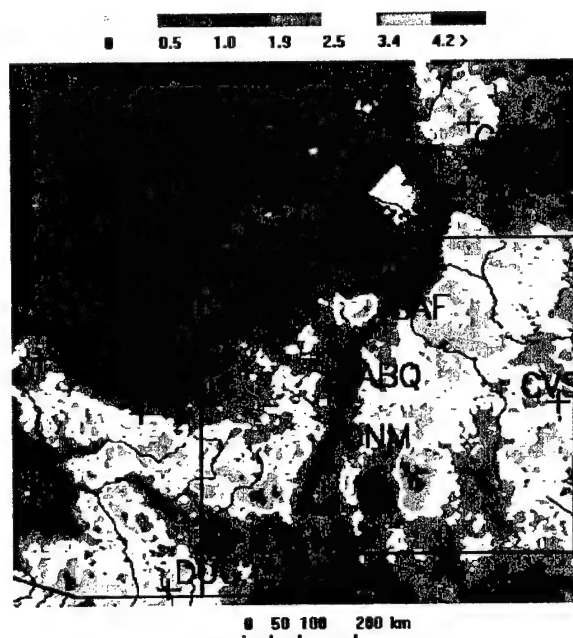


Fig. 1. SW Region Annual Flash Density. Contours are flashes  $\text{km}^{-2} \text{ yr}^{-1}$ .

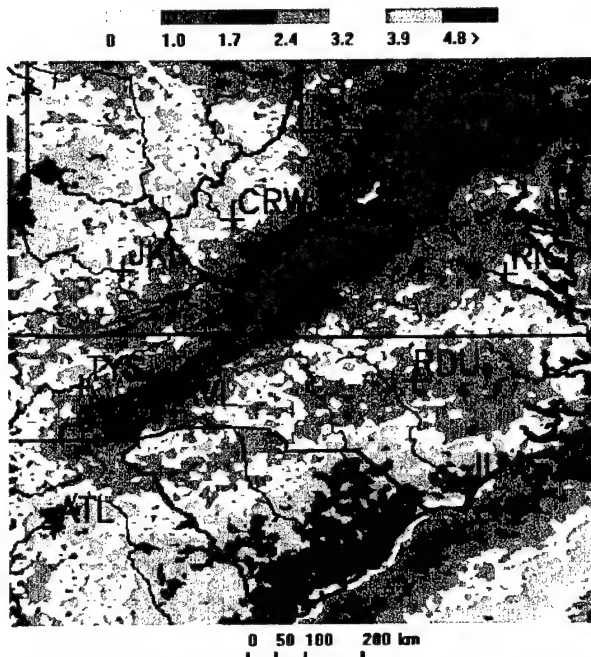


Fig 2. SE Region Annual Flash Density. Contours are flashes  $\text{km}^{-2} \text{ yr}^{-1}$ .

Meteorological satellites further advanced thunderstorm research by allowing scientists to “trace back” thunderstorm clouds to their initial cumulus form. Klitch et al. (1985) and Weaver and Kelly (1982) showed that Colorado summertime cumuli initiated over mountain peaks and ridges. Banta and Schaaf (1987) used this method to identify convective initiation points in the southern Rocky Mountains. They demonstrated that the initiation points cluster in certain “genesis zones,” and that these zones vary according to the direction of the ridge-top winds. Banta (1984) introduced the leeside convergence mechanism as a theory for explaining the location and timing of mountainous convective initiation. This mechanism initiates convection when strong solar heating on the mountain slopes lee of the ridge top winds creates a thermally direct circulation with surface winds blowing up the mountain slope. Where these surface winds meet the ridge-top winds (just lee of the ridge) a convergence zone is born (fig. 3). Banta (1986) explored mountainous convective initiation processes by comparing CG lightning data to ridge-top wind speeds

and directions. This study showed that when the winds at ridge-top were less than about  $12 \text{ ms}^{-1}$ , the lee-side convergence mechanism was effective in triggering thunderstorm development. Other mechanisms, such as orographic lifting, channeling, and wake effects also contribute to convective initiation (Banta 1984), but the leeside convergence mechanism remains the primary explanation for convective initiation in the southern Rocky Mountains.



Fig. 3. Leeside Convergence Mechanism. (Banta and Schaaf, 1987)

Still more advances in climatological lightning research were made possible as the economic impact of cloud-to-ground (CG) lightning strikes necessitated the establishment of a National Lightning Detection Network (NLDN). What would become the NLDN began as three regional networks, funded by three different entities. The U.S. Bureau of Land Management (BLM) established the network in the West with the interest of the country's national parks and forests in mind. Meanwhile, the Midwest network was brought about by the National Severe Storms Laboratory (NSSL) (Cummins et al., 1995), and the East Coast network was put in place by the State University of New York at Albany (SUNYA) (Orville et al., 1983). By 1983, the electric utility industry recognized the operational benefit of the network (Cummins et al., 1998), and funded the expansion of the East Coast network. Nationwide commercial interest followed, ultimately consolidating the three regional networks and prompting the establishment of a

commercial data service company. This company, GeoMet Data Services, Inc. (GDS), has recently combined with another parent company (Lightning Location and Protection, Inc.) to become Global Atmospherics, Inc. (GAI), which currently operates the national network (Cummins et al., 1998). The NLDN began in 1987, and provided accurate CG lightning data for the entire United States by 1989 (Cummins et al., 1995). Since dependable data sources and financial supporters have become more widespread, progress in the field of lightning study has progressed rapidly.

By the mid 1980's, the BLM network in the Southwest United States was providing dependable and accurate CG lightning data (Krider et al., 1996). Since the proposal of the leeside convergence mechanism, several studies (Lopez and Holle, 1985, Schaaf et al., 1988, Reap, 1986, and Liner et al., 1999) have analyzed lightning data from the BLM and NLDN, stratified these data by ridge-top winds, and revealed thunderstorm genesis zones similar to those found by Banta and Schaaf (1987). Reap (1986) used western United States CG lightning patterns from mid-June through mid-September to demonstrate a positive correlation between elevation and lightning flash density. He also suggested that the very stable seasonal and geographical distribution of CG lightning in the southern Rockies, due to the strong terrain influence, potentially allows for good objective convective forecasts (given a large enough data sample).

The current study expands the previous works to cover a twelve-year data sample (1989-2000), and includes a study of the Southern Appalachian Mountains. The primary objective is to thoroughly document, at high resolution, the lightning characteristics of the Southern Rockies and the Southern Appalachians. To quantify the statistical relations, multiple regressions were performed for each region. These regressions predicted

lightning flash density from the two independent variables of elevation and elevation gradient. The expected result was that a quadratic curve, with a peak in the middle elevations, would best fit the flash density-versus-elevation relation in the Rockies. This relation was predicted since the lowest terrain lacks a trigger mechanism and the highest terrain lacks moisture. For the Appalachians, an inverse relation with a peak of lightning flash density in the valleys and a minimum over the mountain ridges was expected, in support of the observations of Huffines and Orville.

This study also reviews the convective initiation mechanisms that are accepted in the Southern Rockies, especially the leeside convergence mechanism, and searches for evidence of their validity in the Southern Appalachians. Finally, this paper seeks to explain the suppression of lightning in the Appalachian chain.

The hypothesis explaining the lightning suppression over the Appalachians is two-fold. First, the theory must explain the inability for pre-existent thunderstorms to enter the mountain region, and secondly, must explain why convective initiation over the mountains does not lead to the same lightning enhancements as seen in the SW. The hypothesis for the first question predicts that the southwest to northeast orientation of the Appalachian chain limits the moisture available to preexistent thunderstorms. As storm complexes approach the mountain chain from the west, the storms' warm, moist southerly low level jet would be forced to cross the southwest to northeast oriented mountain chain. On the northwest side of the mountains, the low-level flow would then be a descending flow, with a decrease in relative humidity. Thunderstorms that enter this region, west-northwest of the Appalachians would therefore be fed by this drier low-level inflow. The second part of the hypothesis is that the ridge top winds in the Southern Appalachians are, on average,

greater than the  $12 \text{ ms}^{-1}$  threshold established by Banta (1986), and that the equivalent potential temperature difference between mountain tops and valleys is significantly less in the Appalachians than in the Rockies. Combining these two factors would stifle the leeside convergence convective initiation process by creating too sheared of an environment at the ridge-top and weakening the mountain breeze circulation, thus leading to a much shallower leeside convergence zone. A hypothesis explaining why thunderstorms that do develop via the leeside convergence mechanism assumes that the Appalachians are more subject to upper level steering flow than the Southern Rockies, therefore thunderstorms that initiate over the ridges and peaks in the SE region will quickly advect away from the mountains.

## CHAPTER II

### DATA AND METHODS

#### 2.1. National Lightning Detection Network

The primary data source for this study was the U. S. National Lightning Detection Network (NLDN) cloud-to-ground lightning data. The NLDN consists of a combination of magnetic direction finder (DF) and time of arrival (TOA) sensors. The network is currently comprised of 59 TOA sensors and 47 improved accuracy from combined technology (IMPACT) sensors, which combine TOA and DF technology (Cummins et al., 1998). The current configuration of these sensors is given by figure 4, taken from Orville and Huffines (2001).

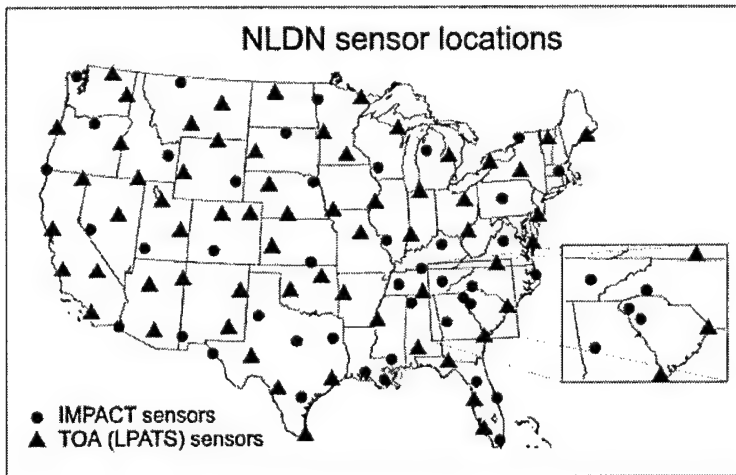


Fig. 4. NLDN Sensor Locations. (Orville and Huffines, 2001.) Filled circles represent locations of sensors with both TOA and DF capabilities. Filled triangles depict locations of DF only sensors. The inset shows the high concentration of IMPACT sensors in the SE.

### 2.1.1. Lightning Detection Theory

Since lightning is the electrical breakdown between two oppositely charged regions, the characteristics of the resulting electrical and magnetic field changes must be understood before lightning can be remotely detected. Because the focus of this study is only cloud-to-ground lightning, the following discussion applies to such flashes.

Like all electrical discharges, lightning emits electromagnetic radiation. The nature of this radiation is described by Maxwell's equations, and assuming a vertical lightning channel, is manifested at the earth's surface as a change in electric field ( $E_z$ ) and an azimuthal magnetic flux density ( $B_\phi$ ). Uman (1987, p.137) gives the following equations for these vectors:

$$\mathbf{E}(r, \phi, 0, t) = \frac{1}{2\pi\epsilon_0} \left[ \int_{H_B}^{H_T} \frac{2z'^2 - r^2}{R^5} \int_0^t i(z', \tau - R/c) d\tau dz' + \int_{H_B}^{H_T} \frac{2z'^2 - r^2}{cR^4} i(z', t - R/c) dz' - \int_{H_B}^{H_T} \frac{r^2}{c^2 R^3} \frac{\partial i(z', t - R/c)}{\partial t} dz' \right] \mathbf{a}_z \quad (1)$$

$$\mathbf{B}(r, \phi, 0, t) = \frac{\mu_0}{2\pi} \left[ \int_{H_B}^{H_T} \frac{r}{R^3} i(z', t - R/c) dz' + \int_{H_B}^{H_T} \frac{r}{cR^2} \frac{\partial i(z', t - R/c)}{\partial t} dz' \right] \mathbf{a}_\phi \quad (2)$$

where the above symbols and variables are defined as:

$\mathbf{E}(r, \phi, 0, t)$  = Electric field at ground level

$R$  = Range to a point on channel

$\epsilon_0$  = Permittivity of a vacuum

$H_T$  = Height of top of channel

$\mathbf{a}_z$  = Unit vector in  $r$  direction

$\phi$  = Azimuth

$t$  = Time

$c$  = Speed of Light

$z'$  = Height of charged region

$\mathbf{B}(r, \phi, 0, t)$  = Magnetic field at ground level

$r$  = Radial distance to channel

$\mu_0$  = Permeability of a vacuum

$H_B$  = Height of base of channel

$\mathbf{a}_\phi$  = Unit vector in  $\phi$  direction

$i$  = Return stroke current

$\tau$  = Retarded time ( $t - R/c$ )

Performing a scale analysis shows that the third term of equation (1) and the second term of equation (2) both diminish by  $r^{-1}$ , and therefore dominate their respective equations.

Both of these terms represent the radiative terms; thus, the radiative terms can be used to approximate the electric and magnetic fields at distances greater than about 100 km.

Wacker and Orville, (1999) show that by making the far-field approximation ( $r \gg z'$ ,  $R \approx r$ ), the peak channel current can be determined by the following proportionality between measured fields and channel current:

$$i_{peak} \approx \frac{2\pi c}{\mu_0 v} r B_{peak} \approx \frac{2\pi}{\mu_0 v} r E_{peak} \quad (3)$$

where:

$i_{peak}$  = Peak current of the return stroke       $v$  = Velocity of the return stroke

From the above equations, measurements of the electromagnetic field can be converted to radiation field signatures as seen in figure 5 (from Krider et al., 1980). This figure shows that the shapes of the radiation field signatures are different and can be used to distinguish between cloud and cloud-to-ground discharges. By discarding those lightning discharges whose measured radiation field signatures resemble the radiation field signature of cloud flashes, the NLDN records only CG lightning. The one exception to our acceptance criteria is that all positive flashes, initially accepted as CG discharges due to their wave forms, but whose peak current is less than 10 kA, are assumed to be cloud discharges, as recommended by Cummins et al. (1998).

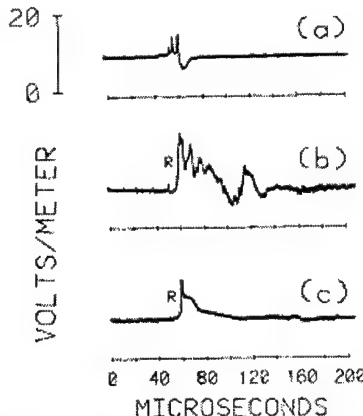


Fig. 5. Radiation Field Signatures. (a) Cloud flash (b) First return stroke (c) Subsequent return stroke (Krider et al., 1980).

The relationships discussed above have given rise to the three types of sensors now employed by the NLDN to detect, locate, and measure CG lightning strikes. The first sensor type is the magnetic direction finder (DF). This sensor consists of two orthogonal magnetic loop antennas. A lightning discharge induces a current in the antennas, which is proportional to the electric current in the lightning channel, and inversely proportional to the range from the channel, and the direction to the channel. From the ratio of the signals measured by the two loops, an azimuth is determined. Two DF sensors can be used to estimate the location of a CG flash; however, triangulating the measured directions from three sensors produces a more accurate location. The second type of sensor used in the current network is the time-of-arrival (TOA) sensor. As the name suggests, the TOA sensor records the time at which the peak radiation wave passes the sensor. As explained by Cummins et al. (1993), the relative time difference measured by a pair of TOA sensors gives a hyperbola of possible locations. If a lightning strike is detected by at least four TOA sensors, an unambiguous location can be determined. The third sensor type, the improved accuracy from combined technology (IMPACT) sensor combines the equipment

and techniques of the DF and the TOA sensors to provide a more accurate estimation of location and time of a lightning flash. In 1994 the NLDN was upgraded through the installation of a network of IMPACT sensors, thus resulting in improved overall performance of the NLDN (Cummins et al., 1998). Since the network-wide upgrade, this network measures CG lightning flash location with an accuracy of 500 m, and a detection efficiency between 80% and 90% for events with peak currents above 5 kA (Cummins et al., 1998). The lightning measurements directly provide location, polarity, magnetic field, electric field, and flash multiplicity. From these measurements, the following data variables were derived: flash density, positive flash density, percent flashes with positive polarity, median peak currents, and flash multiplicity.

### *2.1.2. NLDN Analysis*

Interactive Data Language (IDL) programs, created by Dr. Gary Huffines (currently at the Air Force Institute of Technology), allowed for graphical analysis of the CG lightning characteristic variables. The data were analyzed at 5 km resolution, square root of the sum of squares of location errors before and after the system-wide upgrade of 1994 (Orville et al., 2001). Twelve-year (1989-2000) annual maps were created for all seven variables for both the Southern Rocky Mountain and Southern Appalachian regions. The annual data were also divided into seasonal data, providing maps of all seven variables for the twelve-year period for each of the four seasons, December-January-February (DJF), March-April-May (MAM), June-July-August (JJA), and September-October-November (SON). A “by-times” analysis was also performed on both the annual and the seasonal data. This consisted of analyzing CG flash density for three-hourly increments first for the

entire year, and then for each season. Eight three-hour increments were created, beginning with 0000-0300 Universal Time Coordinated (UTC). The by-times analysis demonstrated the climatological diurnal evolution of the lightning patterns for the two regions. These maps also depict the location and timing of climatologically favored lightning initiation.

## **2.2. Regions and Terrain**

Before discussing additional data sources and methodology, it is important to understand the two regions under investigation, especially with respect to their key terrain features. Furthermore, similarities and differences between the characteristics of each region are of vital importance to understanding the problem statement and results of this study.

The first (and the more understood) region is the Southern Rocky Mountains (fig. 6). This area covers the entire state of New Mexico (NM), and portions of Colorado (CO), Arizona (AZ), and Utah (UT). Specifically, it was taken to be the area bounded by 30.25 and 41.25 degrees north latitude, and 102.0 and 113.0 degrees west longitude. For the remainder of the paper, this region will also be referred to as the Southern Rockies or the Southwest (SW). Several cities are labeled as geographical reference points; these cities are listed in the caption for figure 1. Key terrain features of the Southern Rockies include the following: the San Juan and Sangre de Cristo Mountains in Southern CO and Northern NM, the Mogollon Rim and White Mountains in Central AZ, and the Sacramento Mountains in Central NM. Important river valleys include the Rio Grande Valley in central NM, and the Colorado River, San Juan, and Gunnison River Valleys from western

CO through northern AZ. The average elevation for the SW region was about 1700 m, and the maximum elevation was 4395 m in Central CO (Mt. Elbert).

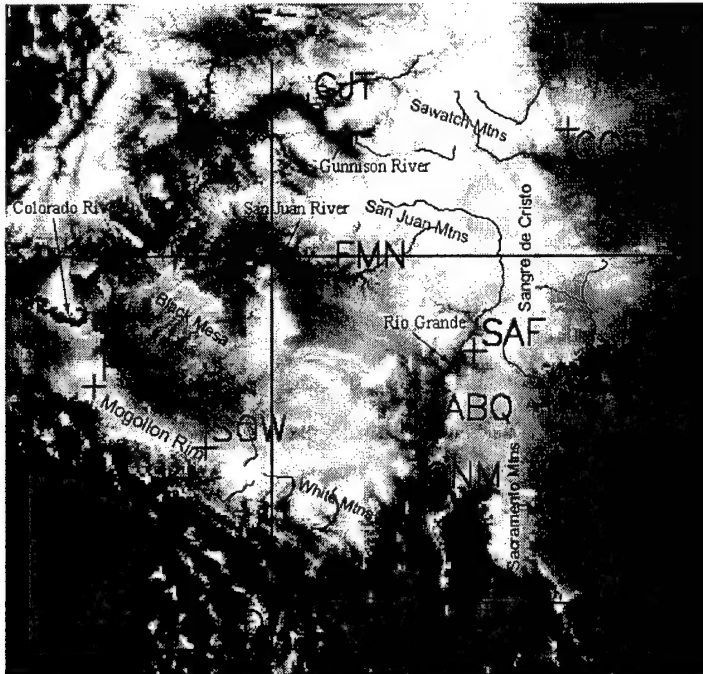


Fig. 6. Key Terrain: Southwest Region. Bright white represents highest elevations.

Reference cities include Grand Junction, CO (GJT), Colorado Springs, CO (COS), Farmington, NM (FMN), Santa Fe, NM (SAF), Albuquerque, NM (ABQ), Socorro, NM (ONM), Clovis, NM (CVS), Flagstaff, AZ (FLG), Show Low, AZ (SOW), and Douglas, AZ (DUG).

The second region, the Southern Appalachian Mountains (fig. 7), includes all of South Carolina (SC), North Carolina (NC), Virginia (VA), and West Virginia (WV), as well as portions of Georgia (GA), Tennessee (TN), Kentucky (KY), Ohio (OH), and Pennsylvania (PA). The area plotted was that bounded by 31.25 and 42.25 degrees north latitude and 75.0 and 86.0 degrees west longitude. This region will also be referenced in this paper as the Southern Appalachians, or the Southeast (SE). Reference cities are also

included for SE, and are listed in the caption for figure 7. The important terrain features in the Southern Appalachians include the Piedmont Region in central NC, the Cumberland Plateau in TN, the Blue Ridge Mountains in NC, VA, and WV, and the Allegheny Mountains in WV. Two other important features are the Tennessee River in western VA and eastern TN and the Yadkin River in western NC. The average elevation for the region is about 300 m, and the maximum elevation is 2037 m in the Blue Ridge Mountains (Mt. Mitchell) of Western NC.

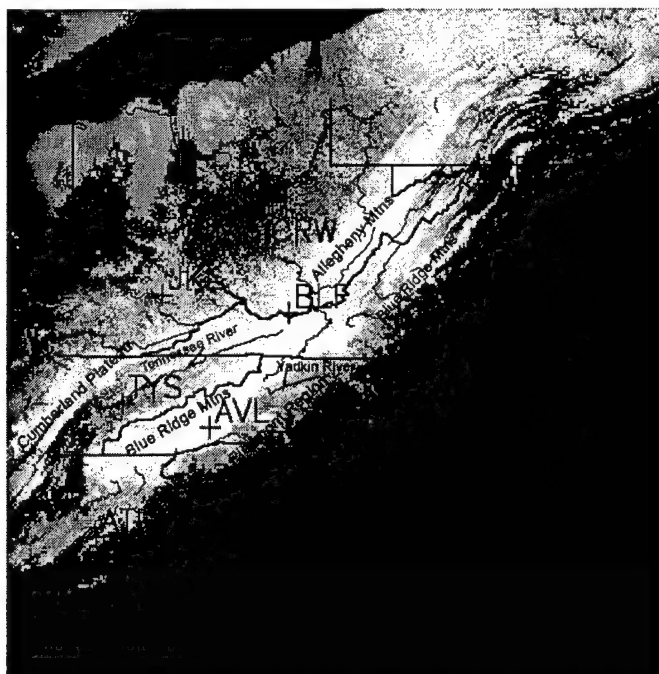


Fig. 7. Key Terrain: Southeast Region. Bright white represents highest elevations.

Reference cities include Martinsburg, WV (MRB), Charleston, WV (CRW), Bluefield, WV (BLF), Jackson, KY (JKL), Richmond, VA (RIC), Knoxville, TN (TYS), Asheville, NC (AVL), Raleigh/Durham, NC (RDU), Wilmington, NC (ILM), and Atlanta, GA (ATL).

Terrain elevation data were obtained from the National Oceanic and Atmospheric Administration's (NOAA) National Geophysical Data Center (NGDC). These data, produced by the Global Land One-km Base Elevation (GLOBE) project, were downloaded from the NGDC website. These text format data were analyzed for maximum, minimum, and average elevation for both the entire SW and SE regions. The sub-region in the SW bounded by 32 and 37 degrees north and 112 and 105 degrees west was divided into grids of 0.5 by 0.5 degree boxes, as was the sub-region in the SE bounded by 34 and 39 degrees north and 85 and 78 degrees west. If a box's average elevation was greater than 2167 m in the SW or 558 m in the SE (highest 25 percent for the respective regions), the box was labeled as high terrain. The box was labeled as low terrain if its average elevation was less than 1817 m in the SW or 294 m in the SE (lowest 40 percent for its region).

### **2.3. Statistical Methods**

Statistical analysis of the data was accomplished by completing six steps. First, the average elevation, maximum elevation, average elevation gradient (at 5 km resolution), and elevation anomaly (box elevation minus the 9-box average elevation) were computed for each half-degree box as discussed in section 2.2. The elevation anomaly analysis was introduced as way to reduce possible bias of flash densities, resulting from spatial proximity of the half-degree boxes. Second, the average flash density and flash density anomaly (box flash density / 9-box average flash density) for each was computed and plotted against the above terrain characteristics. This graphically displayed the relationships between the terrain variables and flash density. Third, a t-test was performed to determine if the average flash density for low terrain is significantly different from that

of high terrain (as defined above), for high anomalies versus low anomalies for each region, and for flat terrain versus steep terrain. Fourth, a polynomial regression was performed by using Statistical Analysis Software (SAS), that regressed flash density as the dependent variable against average elevation, maximum elevation gradient, and elevation anomaly (each separately) as the independent variables. Fifth, a multiple regression was performed with both average elevation and maximum elevation gradient as predictors for flash density. Sixth, the differences between the coefficients of determination resulting from each of the best-fitting regression curves for the SW and SE were noted. Utilization of these methods allowed for a statistical comparison of the mean flash densities of low and high terrain, as well as the calculation of a coefficient of determination between flash density and terrain elevation, and between flash density and elevation gradient.

#### **2.4. Upper Air**

Upper air analyses were conducted for both the SE and SW regions. Daily CG lightning summaries were generated for several areas of both high and low terrain. In the SE, the Cumberland Plateau, the Blue Ridge Mountains, and the Allegheny Mountains represented the high terrain, while the Tennessee River Valley, the Piedmont Region, and the region north and west of CRW depicted low terrain. The daily summaries determined the top five percent and bottom fifty percent of lightning producing days (excluding days with no lightning) for both the high and low terrain. Upper air data for the period of 1990 to 2000 (obtained from Forecast Systems Laboratory and NCDC) were then analyzed to determine the mean surface, 850mb, and 500mb winds for the days identified from the daily summaries. The 850mb winds represented the ridge-top winds, while the 500mb

winds represented the upper level flow. Standard deviation of wind vectors for each level was calculated to demonstrate the amount of synoptic variability for high and low lightning episodes. The purpose of this method was to identify synoptic patterns that commonly produce high or low lightning amounts in the mountains and valleys of the SE region.

Thermodynamic characteristics of both regions were also compared by calculating the vertical equivalent potential temperature ( $\Theta_e$ ) differential between the valleys and the ridge tops, as well as the horizontal temperature differences between mountain summit and the ambient environment at the summit level, for sections of the SW and SE regions. In the SW, central AZ through central NM was chosen to represent the key area of convective initiation. In the SE, two sections were studied independently. These sections were the southern Blue Ridge Mountains and the central Allegheny Mountains. This split was chosen since the diurnal flash density climatology (discussed in section 3.1.2) suggests that the Blue Ridge Mountains act similar to the southern Rockies during convective initiation, while the Alleghenies act differently.

To determine the average vertical stability profile for each region, the  $\Theta_e(850) - \Theta_e$  (surface) difference will be calculated in the SE, while  $\Theta_e(700) - \Theta_e$  (surface) difference will be computed in the SW. From the  $\Theta_e$  differences and the differences between the average surface elevation of upper air sites and mountaintops, a vertical gradient of  $\Theta_e$  will be calculated. A weaker gradient represents a less stable environment and the potential for stronger thunderstorm updrafts and downdrafts. The expected result is that the  $\Theta_e$  patterns of the Blue Ridge Mountains and the Southern Rockies will be unstable, while the average thermodynamic profile in the Allegheny Mountains will be more stable. Upper air data from all lightning days identified by the daily lightning summaries were used to calculate

these profiles. The average  $\Theta_e$  (surface and 850) in the Blue Ridge section was computed from 1200Z upper air observation reports from Nashville, TN and Peachtree City, GA. Observations from Wilmington, OH, Roanoke, VA, and Greensboro, NC were averaged to produce the thermodynamic profile for the Allegheny Mountain section. And, in the SW, Grand Junction, CO, Tucson, AZ, and Albuquerque, NM provided the observations required to compute the  $\Theta_e$  (surface and 700mb).

By comparing the average horizontal temperature difference between mountain summits and the ambient environment at summit level, the likelihood and relative strength of a diurnal mountain breeze can be inferred. Since it is that diurnal circulation that drives the leeside convergence mechanism, this method should reveal each region's relative potential for convective initiation, due to leeside convergence. To accomplish this comparison, surface temperature observations at the summits of Mount Lemmon (elevation 2788 m) in central AZ, and Grandfather Mountain (elevation 1615 m) in northwestern NC were obtained from NCDC. 700 mb and 850 mb temperatures, also from NCDC, represented the ambient summit level environmental temperatures for Mount Lemmon and Grandfather Mountain, respectively. Since 1958 was the only year that provided observations for all of the above sites, that year's June-July-August observations were chosen to represent the climatological average.

## 2.5. Precipitation Data

Precipitation data were obtained from NOAA's National Climatic Data Center (NCDC) through its National Virtual Data System (NVDS). Monthly observations of precipitation amounts were used to compute the annual and the JJA average precipitation.

These observations were based on the normal observing period of 1961-1990. The database consisted of 6662 observing stations across the United States and surrounding locations. Precipitation reporting sites in the area of interest were typically no more than about 10 km apart. The annual average precipitation map was also obtained directly from NCDC to verify the accuracy of the contouring methods. When overlaid with the average annual flash density and/or terrain elevation plots, these data that in some locations, precipitation is high in areas of low terrain. The JJA precipitation displayed patterns very similar to the annual patterns, therefore the annual patterns were chosen to compare to the annual flash density maps. These data demonstrate that although lightning is suppressed in the Appalachians, precipitation is not.

## CHAPTER III

### RESULTS

#### 3.1. Lightning Characteristics

Lightning characteristics for two regions of the United States (SE and SW) were plotted using data obtained from the National Lightning Detection Network over the twelve-year period from 1989 through 2000. The SW region spanned that area of the Southern Rocky Mountains bounded by 30.25 and 41.25 degrees north latitude, and 102.0 and 113.0 degrees west longitude. The SE region covered the portion of the Southern Appalachian Mountains bounded by 31.25 and 42.25 degrees north latitude and 75.0 and 86.0 degrees west longitude. The following seven lightning characteristic variables were plotted: flash density, positive flash density, percentage of flashes with positive polarity, median peak current (for negative and positive polarities), and flash multiplicity (for negative and positive polarities). These variables were plotted for the entire data set, for three-hourly increments, by season, and for increments of both time and season.

##### 3.1.1. *All Seasons / All Times*

###### Southwest Region

The flash density map for the SW region (fig. 1) shows values ranging from less than 0.5 flashes  $\text{km}^{-2} \text{ yr}^{-1}$  to greater than 4.2 flashes  $\text{km}^{-2} \text{ yr}^{-1}$ . The lowest values are located in the region between the San Juan and the Sangre de Cristo Mountains. This region is classified as high terrain (due to its absolute elevation), however, since higher

mountains surround this bowl of locally lower elevations, the region is low relative to its surroundings. The highest values of flash density are found over the Sacramento and White Mountains in Southern New Mexico. The most striking features on the SW flash density map are the obvious valley and mountain effects. A continuous minimum of lightning activity follows the Rio Grande Valley from southern Colorado through western Texas. The 1.0-1.9 flashes  $\text{km}^{-2} \text{ yr}^{-1}$  shading follows the river valley almost perfectly through this region. Lower values of flash density are also seen in several other major river valleys throughout the SW region. In the northern portion of the plot, the 0.5-1.0 flashes  $\text{km}^{-2} \text{ yr}^{-1}$  shading follows the Colorado, Gunnison, and San Juan River Valleys almost exactly. Marked decreases in flash density over distances of less than 50 km are also evident along the Salt and Gila Rivers just south of SOW.

The mountain effect appears in figure 1 as localized increases in lightning flash density over and near elevated terrain. The most impressive examples of this include the local maxima over the Sacramento, White, and Sangre de Cristo Mountains of NM, the Mogollon Rim of AZ, and the isolated mountain peak just west of SAF. Flash density values of over 4.2 flashes  $\text{km}^{-2} \text{ yr}^{-1}$  are common over each of the regions. Furthermore, the only region on the map that supports flash densities this high for which mountainous terrain is not dominant is extreme southern AZ (west of DUG). This region consists of very low desert terrain, but does contain a few isolated mountain peaks. Finally, a large area of moderately high flash density values dominates the eastern portions of the map.

The SW positive flash density map (fig. 8a) shows a positive correlation between terrain elevation and positive flash density. Values in the region range from less than 0.02

strokes per flash. Negative multiplicity values tend to increase southward and eastward, to a large maximum of greater than 2.6 strokes per flash in southeast NM. The spatial pattern in figure 10b shows little evidence of a correlation between terrain elevation and multiplicity; however, a comparison to figure 9b reveals a possible relationship between median peak current and multiplicity. High multiplicity values tend to appear in regions of strong peak current gradients (with the multiplicity maximum displaced to the weaker peak currents). Examples of this are seen just east of the White Mountains, in the eastern San Juan Mountains, west of COS, and just east of SAF. Furthermore, localized maxima of peak current tend to coincide with minima in multiplicity, as demonstrated in the eastern San Mountains, southwest of SWO, the Sangre de Cristo Mountains, and west of DUG.

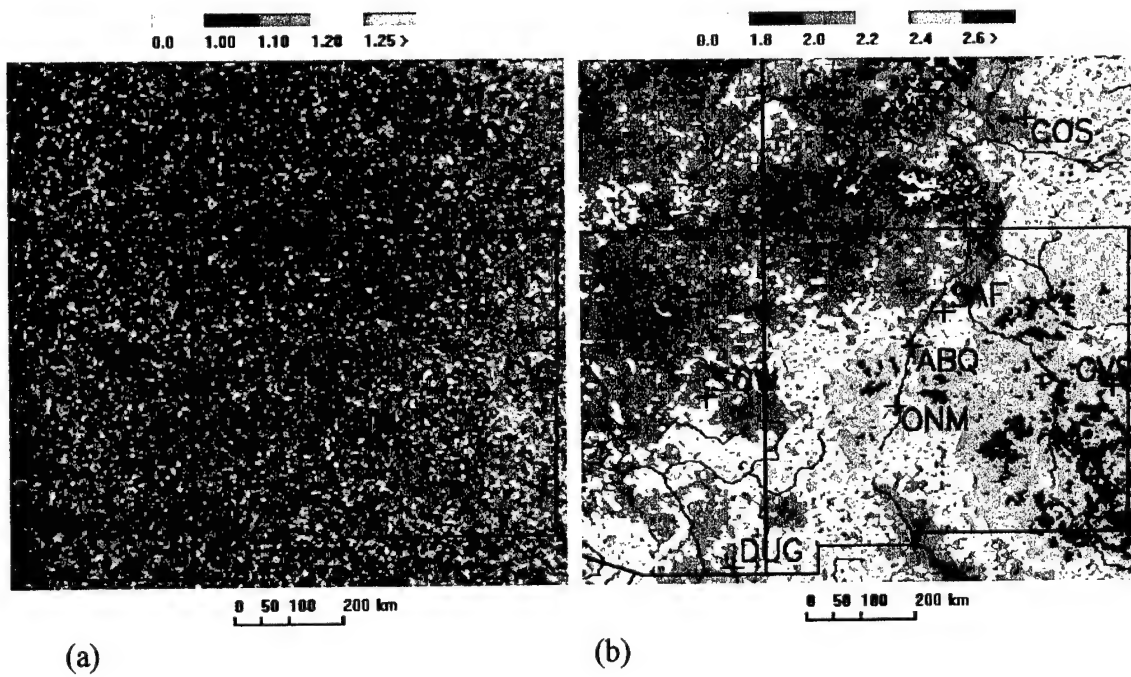


Fig. 10. SW Multiplicities (All Seasons / All Times). (a) Positive Polarity (b) Negative Polarity

values of peak negative current ranged from less than 18 to greater than 23 kilo Amperes (kA). The largest area of enhancement is the Sangre de Cristo range, with peak negative currents greater than 23 kA. Similar enhancements appear over the Sacramento and the eastern San Juan Mountains, as well as over the eastern Mogollon Rim, and the mountain ridge west through north of GJT. The most conspicuous lack of enhancement is over the area north and west of COS. Like those above regions with high peak negative currents, COS is located on the eastern edge of a mountainous feature, and is collocated with a flash density local maximum.

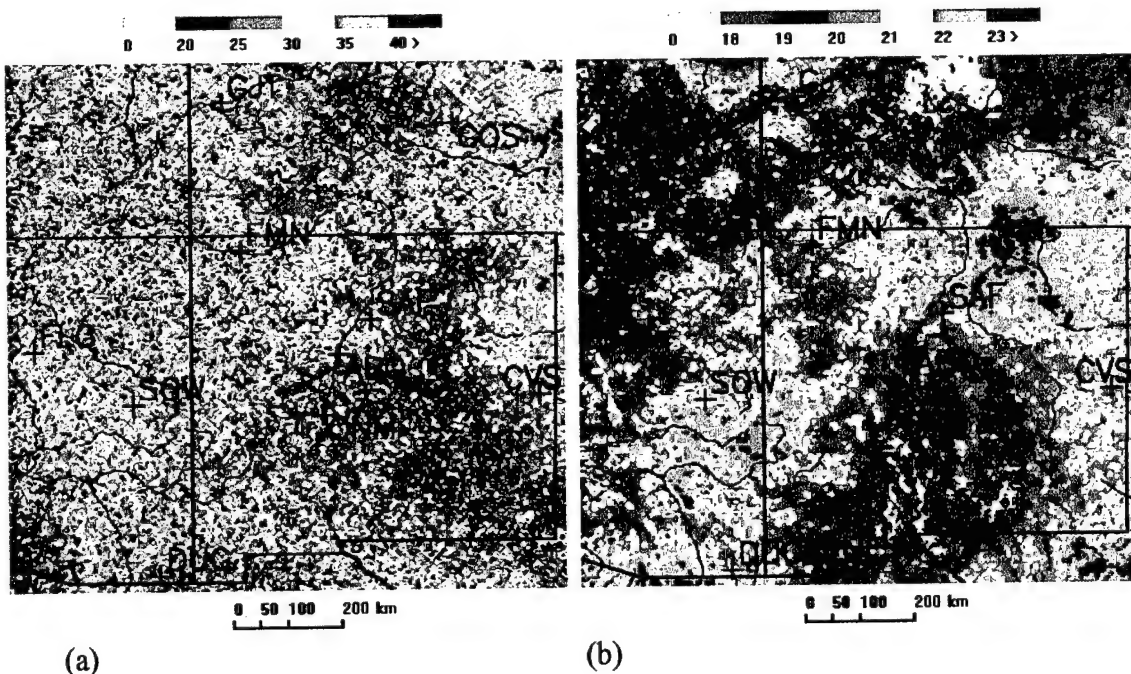


Fig. 9. SW Median Peak Currents (All Seasons / All Times). (a) Positive Polarity (b) Negative Polarity

As was found with the peak current maps, the SW multiplicity maps showed no spatial pattern at all for the positive polarity flashes, but did for the negative polarity (figs. 10a and 10b). Values of negative multiplicity ranged from less than 1.8 to greater than 2.6

flashes  $\text{km}^{-2} \text{ yr}^{-1}$  to over 0.16 flashes  $\text{km}^{-2} \text{ yr}^{-1}$ . As with flash density, high positive flash density values follow the Sacramento, White, and San Juan Mountains, and the Mogollon

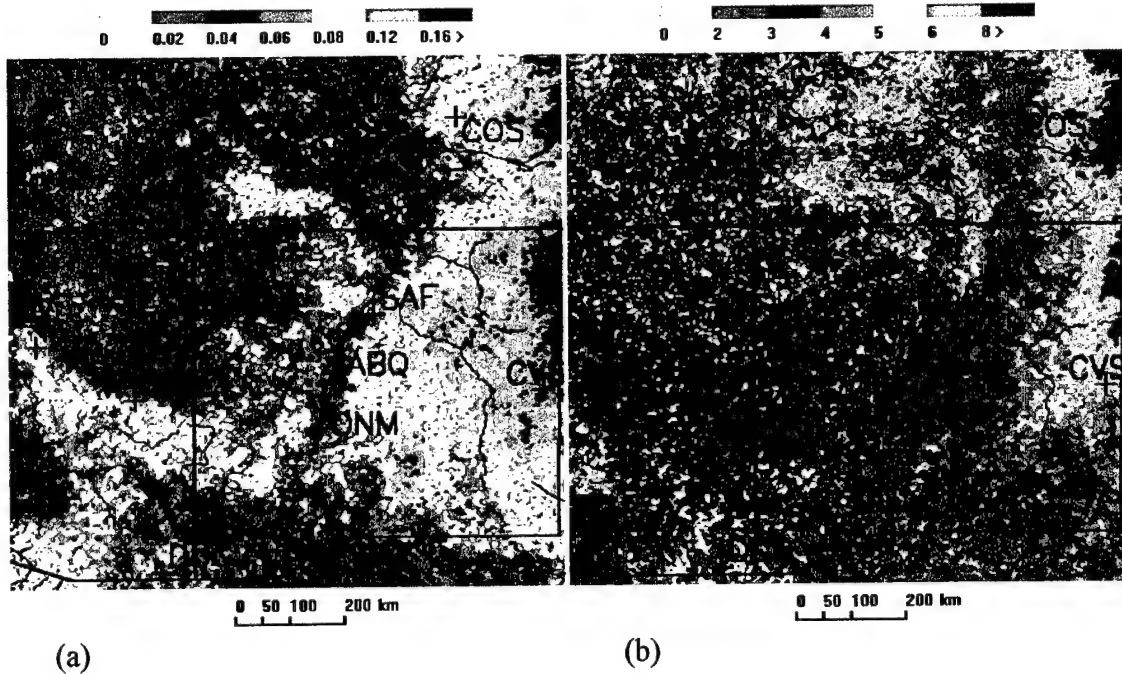


Fig. 8. SW Positive Flash Characteristics (All Seasons / All Times). (a) Positive flash density (b) Percent positive.

Rim. The same river valley effect is also seen in the vicinity of the Rio Grande, the Colorado, the San Juan, and the Gila Rivers. The eastern edge of the map reveals the highest values of positive flash density. The SW percent positive map (fig. 8b) shows an interesting pattern as well. West of the COS longitude, the locations showing high percent positive flashes display local minimums in flash density. Only in extreme eastern NM (north northeast of CVS) does the percent positive maximum coincide with relatively high values of flash density.

While the SW median positive peak current map (fig. 9a) shows no discernable pattern, the median negative peak current map (fig. 9b) reveals several localized extremes. Absolute

### Southeast Region

The flash density map for the SE region (fig. 2) shows values ranging from less than 1.0 flashes  $\text{km}^{-2} \text{ yr}^{-1}$  to greater than 4.8 flashes  $\text{km}^{-2} \text{ yr}^{-1}$ . The lowest values are located in the Allegheny Mountains. The most significant feature of this map is a large area of lightning suppression, extending from the Blue Ridge Mountains of NC to the northern Allegheny Mountains of WV. This area continues well north of the defined SE region, extending into northern Pennsylvania and southern New York. The area in figure 2 marked by the flash densities of less than 2.4 flashes  $\text{km}^{-2} \text{ yr}^{-1}$  are considered to exhibit a lightning suppression. This figure confirms, at 5 km resolution, the findings of Huffines and Orville (1999). That study showed that an area lightning suppression exists at 20 km resolution throughout the Appalachian Mountains. A second feature of importance is the area of higher flash density values along the Tennessee River Valley in eastern TN. This area is bounded on the north and west by the Cumberland Plateau and on the east by the Blue Ridge Mountains, and is significant because it is in direct contrast to the river effect of the SW region. A third key area of interest is the elongated lightning maximum stretching from southeast of AVL to north of RDU. This feature is marked by a gradual west-to-east increase in flash density, reaching maximum values between 3.9 and 4.8 flashes  $\text{km}^{-2} \text{ yr}^{-1}$ , followed by a gradual decline in lightning activity, with minimum values of less than 2.4 flashes  $\text{km}^{-2} \text{ yr}^{-1}$  in the higher plains of the RDU region. Other noteworthy features include the enhancement over ATL, an enhancement in the northwest extreme of the map, and the sea breeze-induced maximum along the SC coast.

The SE positive flash density map (fig. 11a) reveals a large area of low positive flash density over, and east of the entire Appalachian Mountain chain. Values along the

western edge of the map commonly reach  $0.25 \text{ flashes km}^{-2} \text{ yr}^{-1}$ , but rapidly decrease to  $0.04 \text{ flashes km}^{-2} \text{ yr}^{-1}$  in the Allegheny Mountain region. At the easternmost edge of the map, values have only recovered to about  $0.15 \text{ flashes km}^{-2} \text{ yr}^{-1}$ . South of the AVL latitude, however, this decrease in positive flash density is not seen. The values remain steadily greater than  $0.15 \text{ flashes km}^{-2} \text{ yr}^{-1}$ . The results shown in figure 11b (percent positive map) agree with the corresponding SW map in that the highest percent positive values (west of AVL, east of CRW, over ATL, and just off the SC/NC coast) are collocated with minimum flash density values.

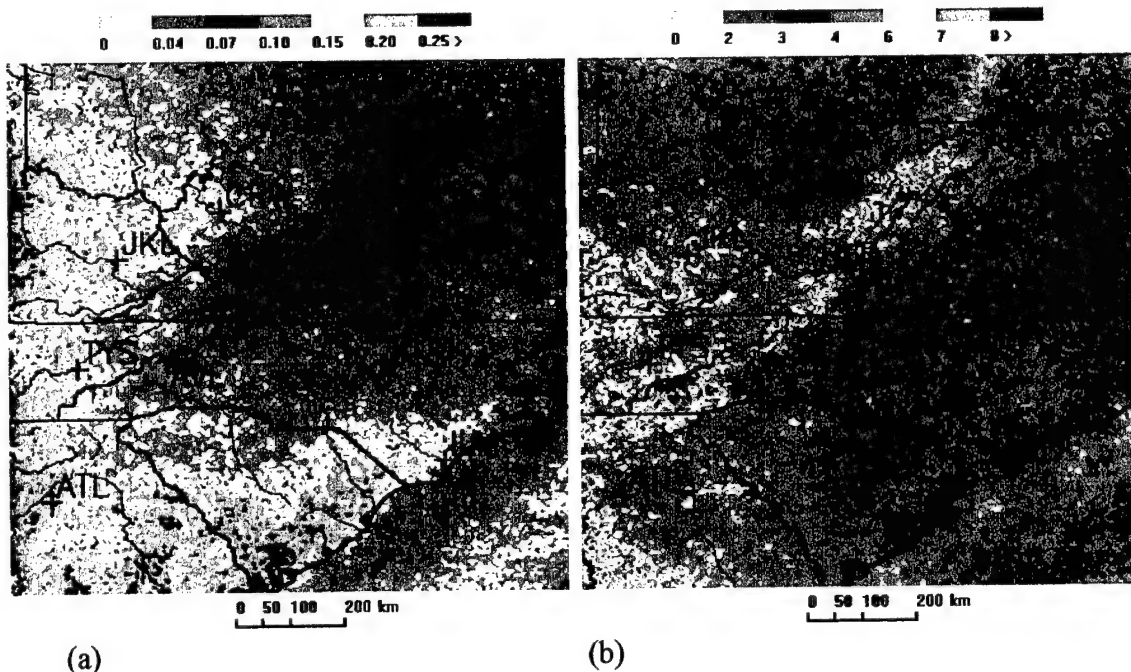


Fig. 11. SE Positive Flash Characteristics (All Seasons / All Times). (a) Positive Flash Density (b) Percent Positive Flashes

Unlike the SW region, both the positive and negative peak current maps (figs 12a and 12b, respectively) show distinct patterns in the SE. The median positive peak current reaches an elongated maximum along the Allegheny Mountain range, with currents greater

than 35 kA. This maximum extends, to a weaker degree, southward to the Blue Ridge Mountains of NC. Higher values ( $> 30$  kA) are also noted off the coast of NC and SC. In SC and GA, median positive peak currents are at a minimum of only from 15 to 20 kA.

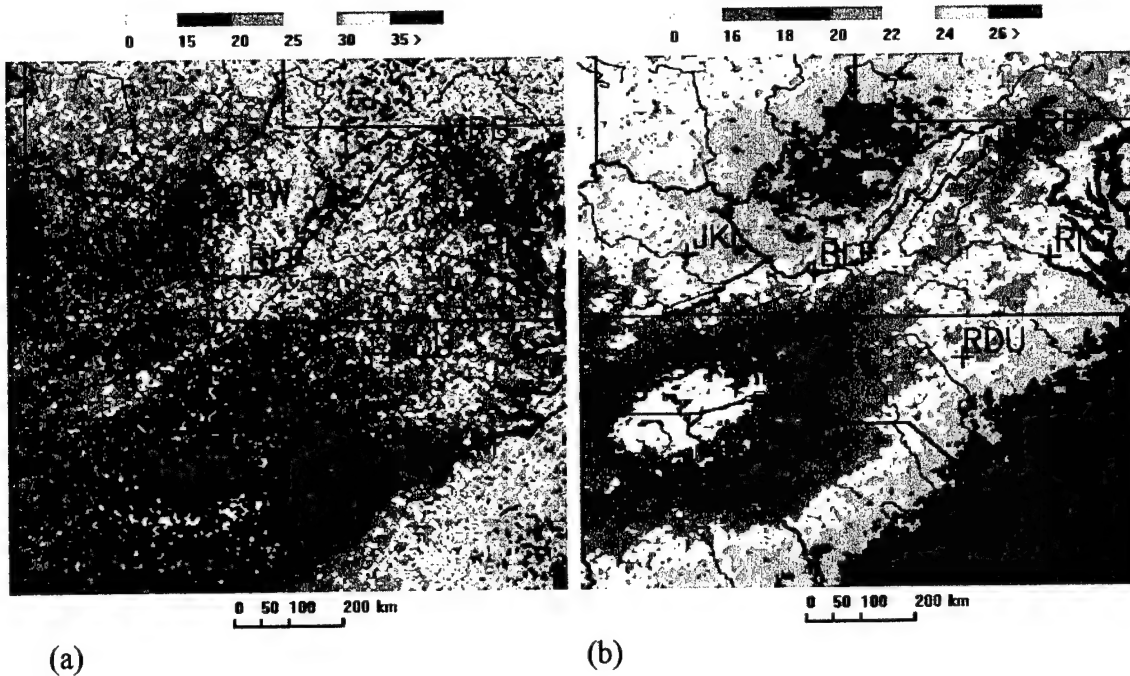


Fig. 12. SE Median Peak Currents (All Seasons / All Times). (a) Positive Polarity (b) Negative Polarity

The median negative peak current map is deceiving. The most obvious feature, the bulls-eye of low values around AVL is a by-product of the NLDN sensor density (Orville and Huffines, 1999). Since lightning flashes that are not detected by at least one IMPACT sensor are rejected by the NLDN, and since the detection range of those sensors is directly related to the median peak current, areas with a sparse arrangement of IMPACT sensors are less likely to include flashes with low median peak currents. Conversely, Orville and Huffines (1999) theorize that if IMPACT sensors are located in close proximity, lightning with lower peak currents will be detected at a higher efficiency. Figure 13, from Orville

and Huffines (1999) shows that the greatest concentration of IMPACT sensors in the US occurs in the western NC and SC. In this region, the average distance between the nearest IMPACT sensors is less than 75 km. Since the bulls-eye of low values in figure 12b is collocated with the highest density of IMPACT sensors, it will be assumed that this pattern is a result of the network configuration. Although the figure shown here displays the distance between the nearest two sensors (thus sensor density), it would be beneficial to compute the distance from each observed lightning flash to the second nearest sensor. This would provide a better representation of the detection efficiency for individual flashes, and possibly provide a strategy for eliminating the systematic bias. The high peak currents off the coast of NC and SC are attributed to a lack of coastal IMPACT sensors (figure 4). Since positive polarity flashes with median peak currents less than 10 kA were rejected to eliminate possible cloud flashes, the systematic bias due to sensor configuration was less pronounced for positive polarity flashes than for negative polarity flashes.

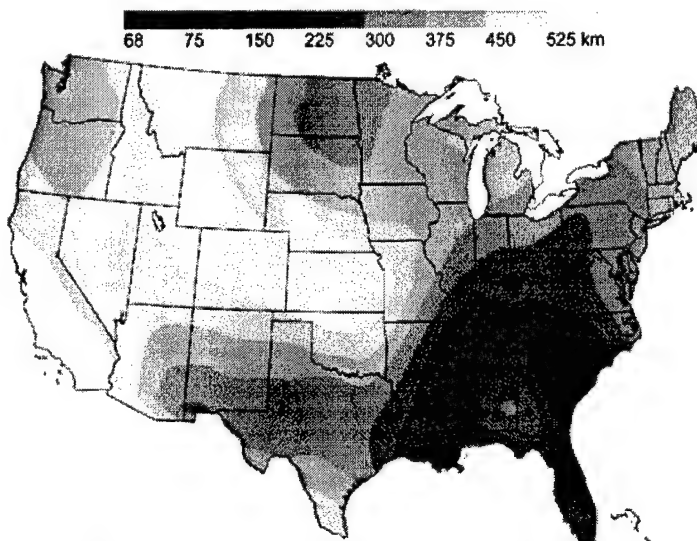


Fig. 13. Distance Between DF Sensors In NLDN. Distance between nearest two NLDN sensors with direction finders (km). (Orville and Huffines, 1999)

Looking past the peak current detection efficiency problem, patterns emerge from figure 12b. Of primary interest are the low values extending from MRB southwestward into the AVL area. Although the southwest portion of this feature is contaminated by the sensor configuration problem, the lower peak currents from PA to western VA are real. This region of low peak currents originates in the valley between the Allegheny and the northern Blue Ridge Mountains, and then extends southwestward, along the front range of the Appalachian chain. This feature has not been previously identified since 5 km resolution plots were not possible before the NLDN upgrade. A second pattern of interest is the bulls-eye of high peak currents around CRW. This is in an area of relatively dense IMPACT sensor placement; therefore, lower peak currents are expected in WV versus western OH or VA. Instead, a distinct maximum ( $> 26$  kA) is revealed. Possible explanations for this observation are discussed in section 4.1.1.

Multiplicities of positive and negative flashes are shown in figures 14a and 14b. The positive multiplicity values range from 1.00 to  $>1.25$  strokes per flash. Other than a slight trend of decreasing multiplicity from west to east, no pattern emerges from figure 14a. Figure 14b, however, does provide evidence of natural spatial patterns occurring in negative multiplicity of lightning flashes, as values range from 1.0 to  $>3.0$  strokes per flash. The most noticeable feature on this map is the low multiplicity values extending from a narrow band just west of AVL expanding to a broad region west of MRB. Other regions of low values include a small area around RDU and a band over the Gulf Stream. Enhancements are located over the western extreme of the map, in northwest SC, and in a narrow band in central VA. These patterns bring forth several questions when compared to the median peak current maps. Contrasting figure 14b to figure 12b reveals that from

CRW to BLF to MRB, the low negative multiplicity patterns correspond almost exactly with patterns of high negative peak current. The band of high negative multiplicity in central VA corresponds well (just a slight shift eastward) to an area of low negative peak currents. Unfortunately, the negative multiplicities in the southern portions of the SE region cannot be contrasted to the peak current map due to the sensor configuration problem. The negative multiplicity map appears to be almost an exact opposite of the median positive peak current map (fig. 12a). Since positive multiplicity values vary so little, large variations of positive peak currents must be expected. Therefore, assuming that environmental conditions conducive to high negative peak currents also support high positive peak currents, the positive peak current map should correlate well to the negative multiplicity map.

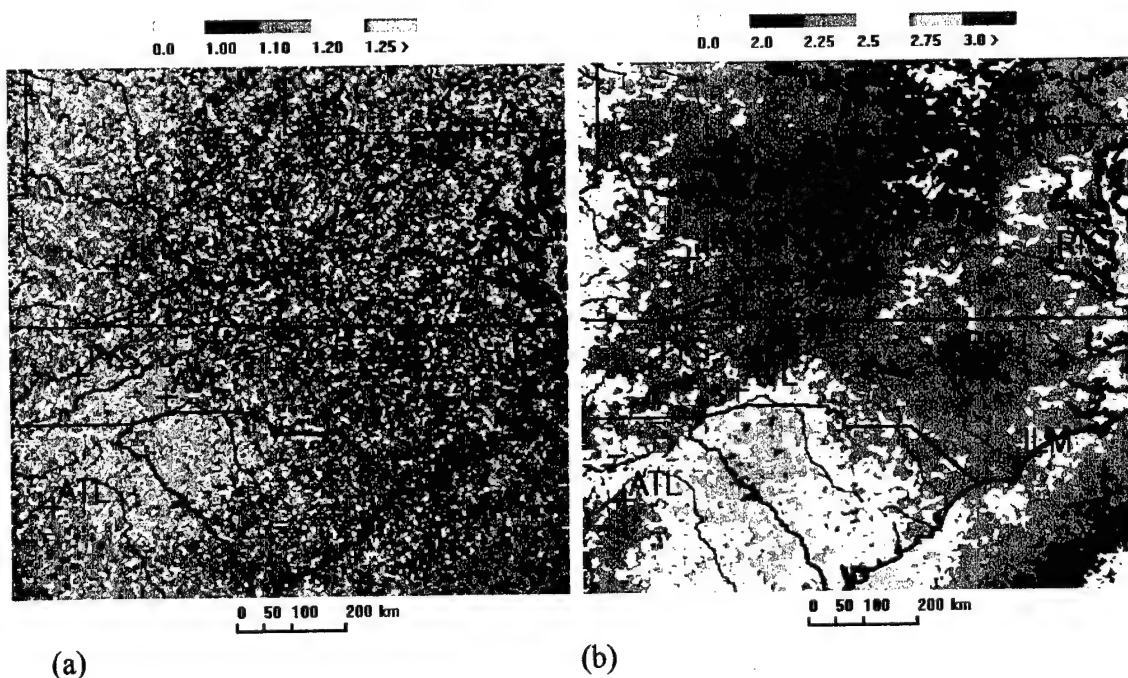


Fig. 14. SE Multiplicities (All Seasons / All Times). (a) Positive Polarity (b) Negative Polarity

### 3.1.2. All Seasons / By-Times

Results from breaking the flash density data into three-hourly increments show the diurnal evolution trends of lightning activity for each region. The following sections discuss, in detail, the patterns revealed by this method.

#### Southwest Region

Figures 15a-15d span a twelve-hour period from 1200 UTC through 0000 UTC (0500-1700 Mountain Standard Time, MST). These figures show the transition from the climatological minimum to the maximum of lightning activity.

In figure 15a (0500-0800 MST), lightning flash density values of less than 0.05 flashes  $\text{km}^{-2} \text{ yr}^{-1}$  dominate the map. Higher flash densities can be seen in the Colorado River Valley, as well as in the low deserts of south-central AZ, and the high plains in the CVS vicinity. Overall, there were 436,835 lightning flashes detected during this time period (table 1), making it the least active of all three-hourly increments.

During the period from 0800-1100 MST (fig. 15b), lightning climatologically favors the mountain peaks and ridges. The most noticeable enhancement during this time occurs over the Sacramento Mountains, with a flash density between 0.3 and 0.5 flashes  $\text{km}^{-2} \text{ yr}^{-1}$ . Other favored areas include the Sangre de Cristo, San Juan, and White Mountains, as well as the Mogollon Rim. Also, since this is the time period for which the number of lightning strikes begins to increase (28.5 percent, table 1) and discernable patterns begin to develop, this will be considered the convective initiation period for the SW region. By the third interval (1100-1400 MST), shown in figure 15c, the mountain

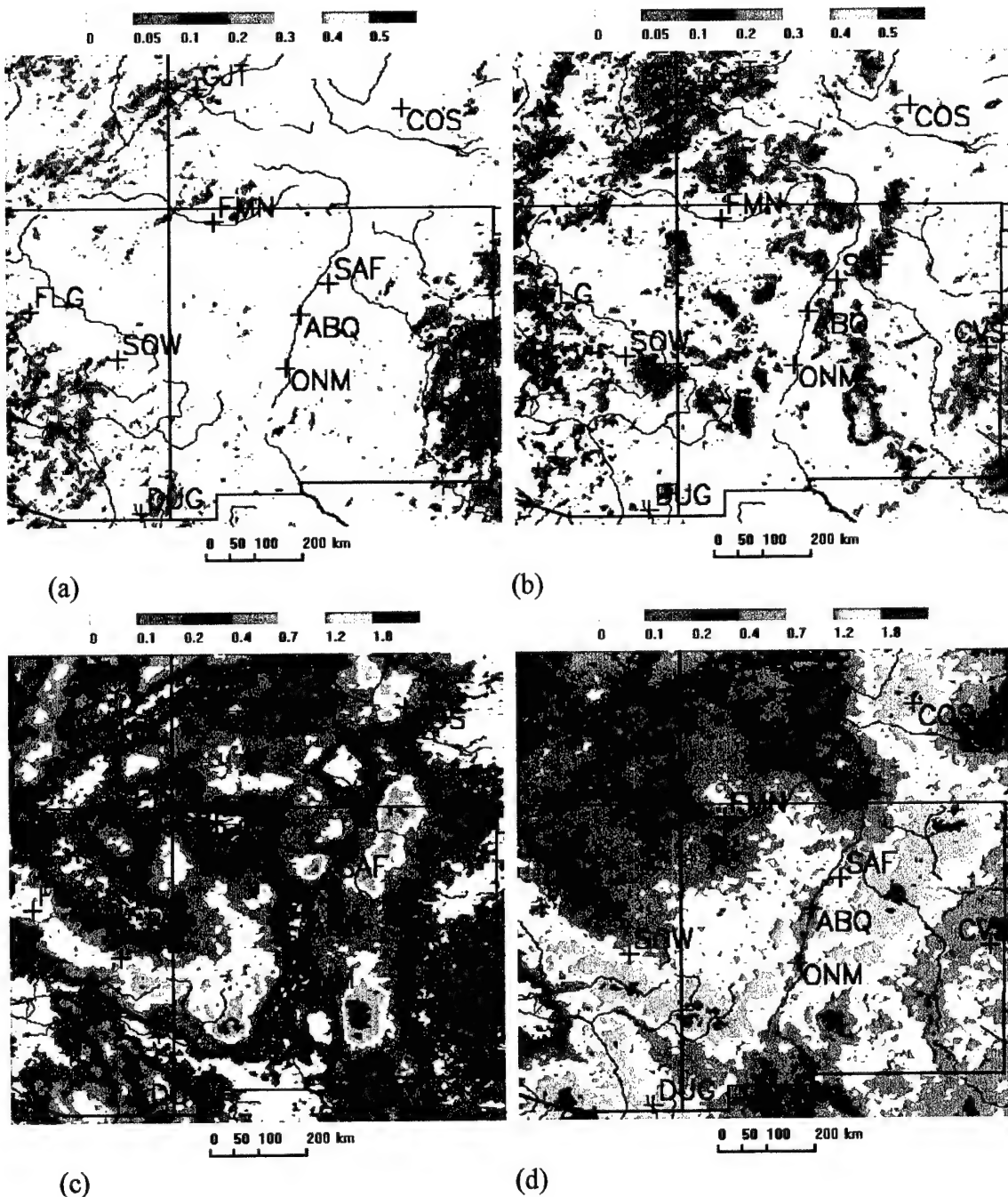


Fig. 15. SW Region By-Times Analysis: Increasing Periods. (a) 0500-0800 MST (b) 0800-1100 MST (c) 1100-1400 MST (d) 1400-1700 MST

and river effects are very clear. The “hot spot” over the Sacramento Mountains increases in spatial coverage and in flash density values (now greater than  $1.8 \text{ flashes km}^{-2} \text{ yr}^{-1}$ ).

Other definitive hot spots also arise during this time period. These include enhancements over the Sangre de Cristo Mountains, the isolated peak west of SAF, the Mogollon Rim, and the White Mountains (all with flash densities  $> 1.8 \text{ flashes km}^{-2} \text{ yr}^{-1}$ ). Other lesser enhancements ( $1.2 - 1.8 \text{ flashes km}^{-2} \text{ yr}^{-1}$ ) are seen over the San Juan Mountains, west of COS, and in southern AZ. Only the southern AZ enhancement is located in an area of predominately low terrain, but even that region contains isolated mountain peaks. The scales for figures 15c, 15d, 16a, and 16b differ from that of the other time periods, because of the much higher flash counts during the afternoon hours. During the 1100-1400 MST period, almost 5 million flashes were detected; this is an increase of 767 percent. Table 1 shows the flash counts and percent change for each time period.

**Table 1.** Southwest Region Flash Counts. The flash count is the number of flashes detected for each time period. The change is the percent increase (+) or decrease (-) in number of lightning flashes from the previous time period.

Time Period (MST)	Flash Count (Flashes)	Change (Percent)
0500-0800	436,835	-31.8
0800-1100	561,194	+28.5
1100-1400	4,863,348	+767
1400-1700	9,382,462	+93
1700-2000	6,973,711	-25.6
2000-2300	3,106,763	-55.5
2300-0200	1,308,200	-57.9
0200-0500	640,645	-51.0

Figure 15d (1400-1700 MST) shows continued evolution in the spatial lightning pattern, and a 93 percent increase in flashes detected. During this time period, we see a rapid decrease in the amount of lightning activity over the Sacramento Mountains. Flash

density values in that region dropped from greater 1.8 to less than 0.7 flashes  $\text{km}^{-2} \text{ yr}^{-1}$ . A similar decrease is noted over the peak just west of SAF, but to a lesser degree. Other interesting results from this map arise from an apparent shift in the location of lightning maxima. The maximum located over the Sangre de Cristo Mountains in figure 15c has become more diffuse, and propagated eastward away from the mountains. This propagation towards lower terrain is also seen in several other locations on the map. The maxima over the San Juan Mountain and the Mogollon Rim have both shifted southward, and moderate lightning activity ( $> 0.7$  flashes  $\text{km}^{-2} \text{ yr}^{-1}$ ) has become more widespread over the southern portions of AZ and NM. This large area of moderate activity appears to be the reason for the increase in total number of flashes.

Figures 16a-16d show the declining period in the diurnal lightning climatology for the southwest region. It is important to note that the decline of lightning activity took place more gradually than the increase did. This supports the findings of Watson et al. (1994) that lightning activity in the southwest monsoon increases rapidly, progressing from a minimum to maximum in just six hours, but decreases back to the minimum over a ten-hour period. Also, the timing of the maximum and minimum periods is also in agreement with that study's diagnosis of 1600 and 1000 MST, respectively.

Figure 16a (1700-2000 MST) continues to exhibit a migration of lightning activity towards lower terrain. The lightning maximum previously located just east of the Sangre de Cristo Mountains has propagated eastward, almost reaching CVS. The activity originating over the Mogollon Rim has moved southward by this period. That local maximum is now located well south of the rim, into the low deserts near DUG. One region

of higher values (0.6-1.0 flashes  $\text{km}^{-2} \text{ yr}^{-1}$ ) remains in a band from ABQ to FMN. This appears to be the remnants of activity that originated over the San Juan Mountains.

During the fifth time period (2000-2300 MST), the steady decrease in lightning activity and the propagation toward lower terrain continues. Flash density values of less than 0.2 flashes  $\text{km}^{-2} \text{ yr}^{-1}$  dominate the northwest half of figure 16b. The few remaining areas still experiencing an enhancement are confined to the southwest one-third of the map (ONM to CVS), the low deserts around DUG, and a small region extending northeastward from COS. With the enhancements now in the valleys, the spatial pattern for this time period appears opposite of the pattern for the early afternoon period (fig. 15c). Two examples of this are the flash density minima over the White Mountains, and along the Mogollon Rim (from FLG to SOW). Both of these regions displayed clear local maxima in figure 15c, but showed distinct local minimums in figure 16b. Other, less pronounced examples include the Sacramento and Sangre de Cristo Mountains. Figures 16c and 16d (2300-0200 and 0200-0500 MST, respectively) continue to show the steady progression and decline of lightning activity. For both figures, the majority of activity is confined to the low deserts south of the Mogollon Rim and the high plains of CVS; however, in figure 16d, this effect is exaggerated. By these times, all mountainous regions experience flash density values of less than 0.2 flashes  $\text{km}^{-2} \text{ yr}^{-1}$ , and generally, less than 0.05 flashes  $\text{km}^{-2} \text{ yr}^{-1}$ . A possible river enhancement can be seen on both maps in the Colorado, Gunnison, and San Juan River Valleys. The Rio Grande Valley, incidentally, shows no evidence of enhanced lightning activity.

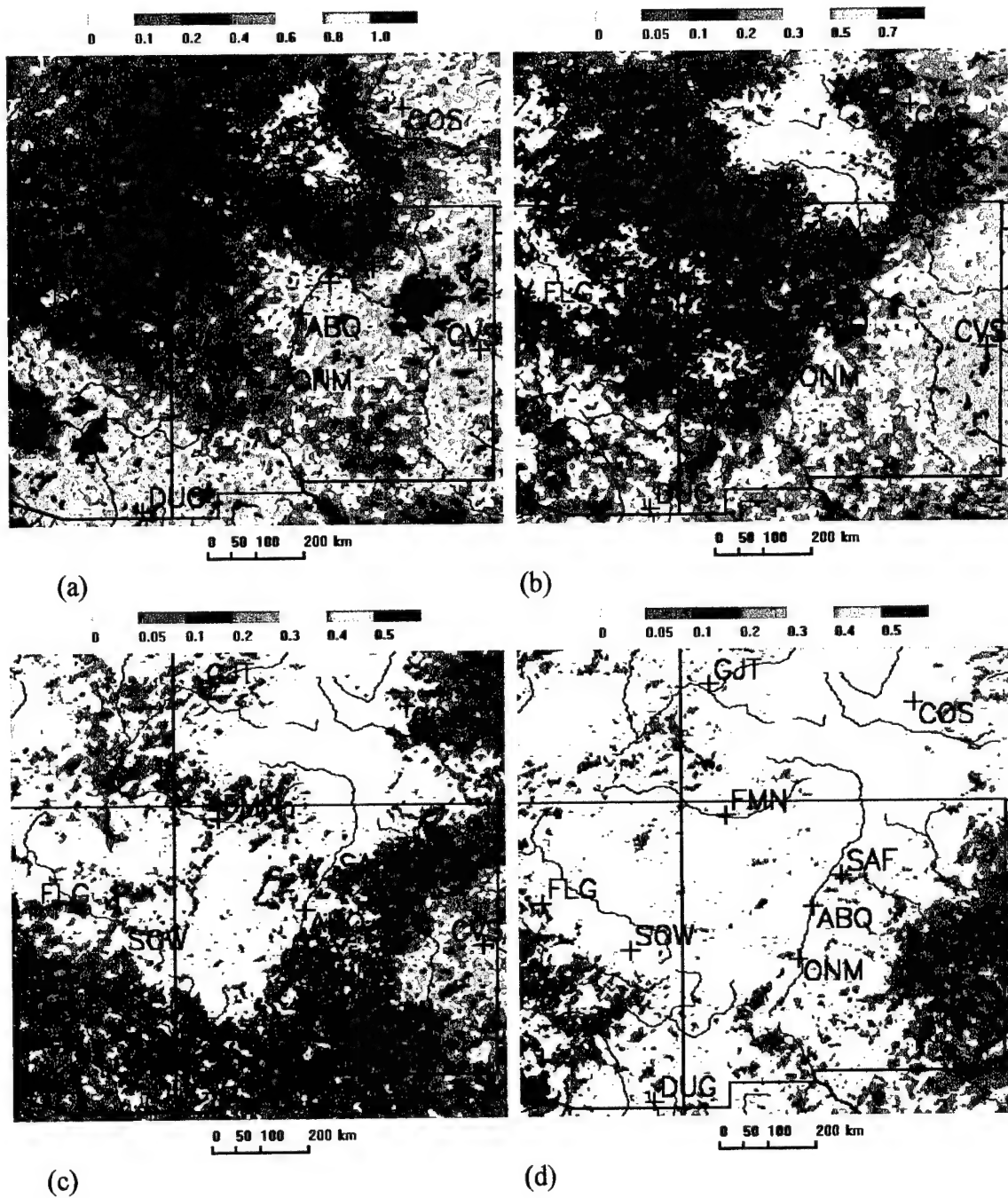


Fig. 16. SW Region By-Times Analysis: Decreasing Periods. (a) 1700-2000 MST (b) 2000-2300 MST (c) 2300-0200 MST (d) 0200-0500 MST

### Southeast Region

The southeast region was analyzed in the same manner as the southwest region. The all-seasons data file was split into eight three-hourly time intervals, which displayed the climatological trends for diurnal lightning activity. Figures 17a-17d each cover three hours of the twelve-hour period from 0700 through 1900 Eastern Standard Time (EST).

Figures 18a-18d cover the twelve-hour period from 1900-0700 EST. In chapter IV, similarities and differences between the southwestern and southeastern results will be discussed, and their implications analyzed.

Figure 17a (0700-1000 EST) demonstrates the early morning lightning patterns for the SE region. During this period, the largest enhancement ( $>0.5$  flashes  $\text{km}^{-2} \text{ yr}^{-1}$ ) is located over the Gulf Stream. A secondary maximum (0.3-0.4 flashes  $\text{km}^{-2} \text{ yr}^{-1}$ ) is located in the northwestern portions of the map, in a region west of the Appalachian chain. This enhancement appears to stop abruptly at the western edge of the mountains. During the period from 1000-1300 EST (fig. 17b), evidence of sea breeze-induced and mountain-induced thunderstorms emerge. Along the coast of NC and SC, flash densities of greater than 0.4 flashes  $\text{km}^{-2} \text{ yr}^{-1}$  extend inland approximately 100 km. Since sea breeze thunderstorms are not the focus of this study, however, only their possible interaction with mountain thunderstorms will be discussed further. Two areas of enhanced flash density that are important to this study are the elongated area west of TYS (over the Cumberland Plateau), and the narrow band ( $<50$  km wide) beginning just west of AVL (over the Blue Ridge Mountains). Both regions depict flash density of 0.4 to 0.8 flashes  $\text{km}^{-2} \text{ yr}^{-1}$ . These hot spots may represent thunderstorm genesis zones in the Appalachian Mountains that behave (at least initially) much like those in the SW region, and are triggered by the leeside

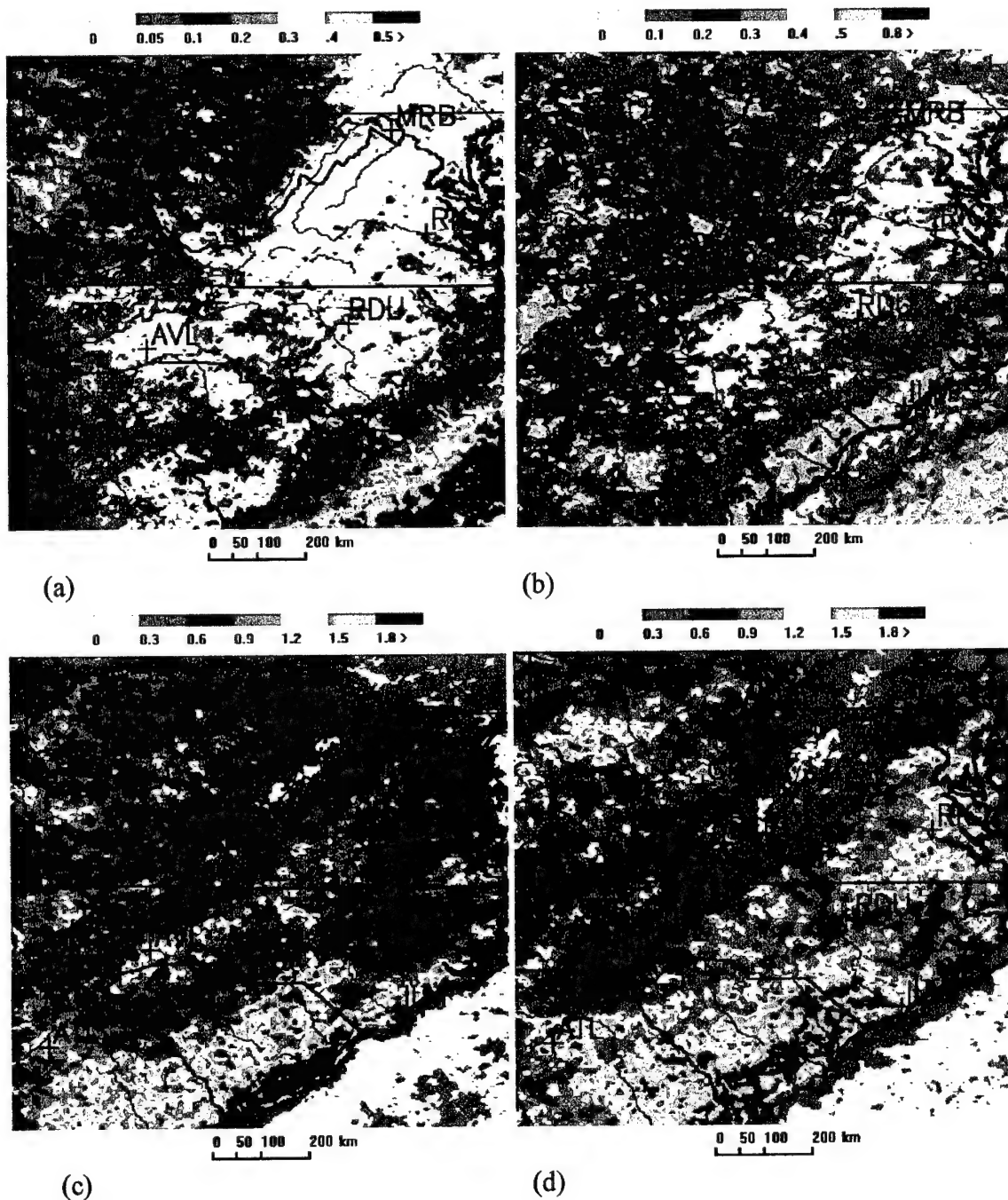


Fig. 17. SE Region By-Times Analysis: Increasing Periods. (a) 0700-1000 EST (b) 1000-1300 EST (c) 1300-1600 EST (d) 1600-1900 EST

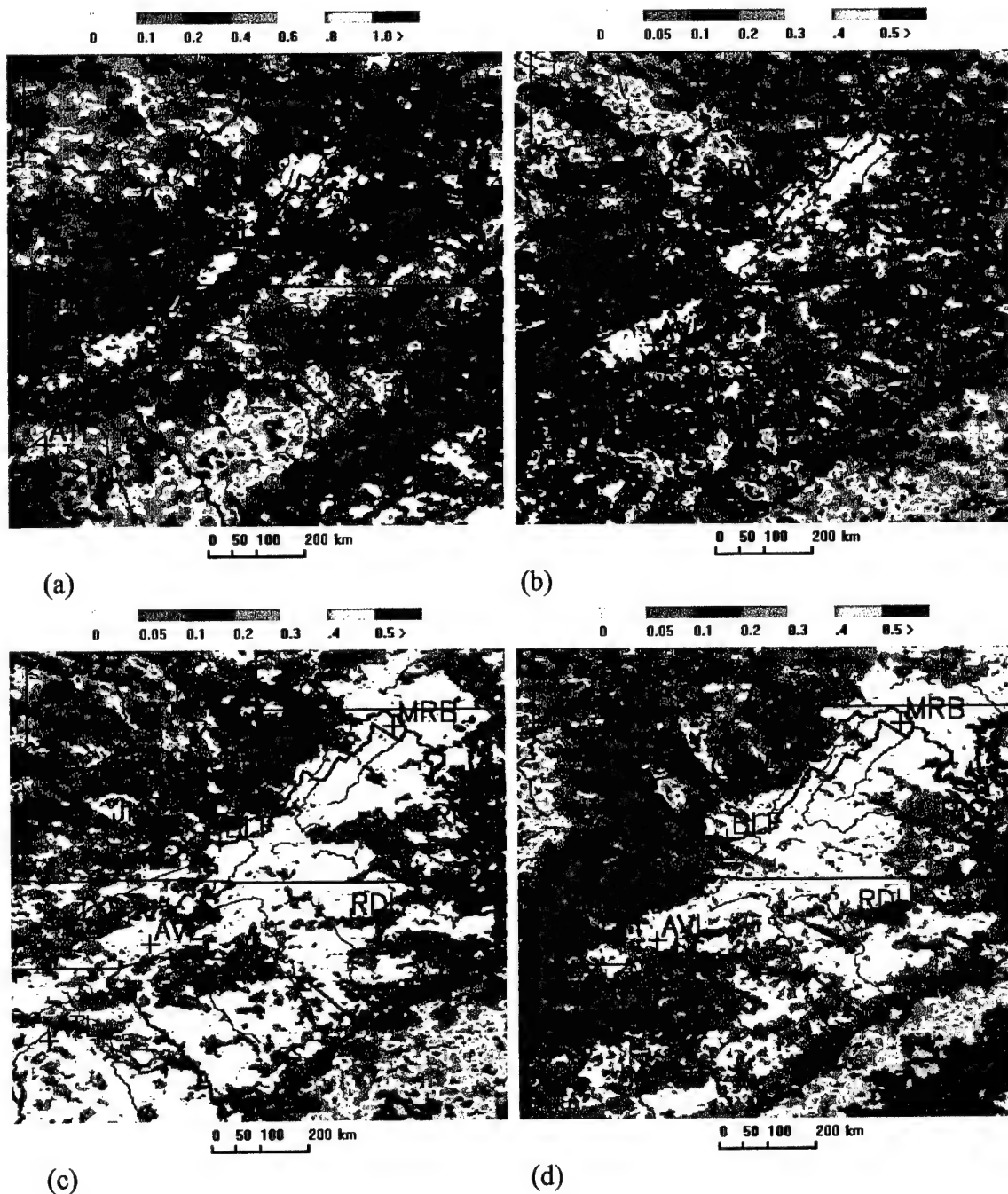


Fig. 18. SE Region By-Times Analysis: Decreasing Periods. (a) 1900-2200 EST (b) 2200-0100 EST (c) 0100-0400 EST (d) 0400-0700 EST

convergence mechanism. Evidence for this will be sought for in other sections and discussed in chapter IV. The enhancement west of JKL appears to be a remnant of activity from the previous time period, but the abrupt halting of activity at the mountain range is no longer as pronounced. This period experiences a 61 percent increase in the total number of flashes detected from the previous time frame (table 2).

**Table 2.** Southeast Region Flash Counts. The flash count is the number of flashes detected for each time period. The change is the percent increase (+) or decrease (-) in number of lightning flashes from the previous time period.

Time Period (EST)	Flash Count (Flashes)	Change (Percent)
0700-1000	2,085,142	-17.6
1000-1300	3,359,297	+61.1
1300-1600	10,746,156	+220
1600-1900	12,019,018	+11.8
1900-2200	5,098,593	-57.6
2200-0100	2,533,662	-50.3
0100-0400	1,701,065	-32.9
0400-0700	2,531,557	+48.8

The third time period, as was true with the SW region, revealed the largest increase in total flash counts. The pattern in figure 17c represents a 220 percent increase in CG lightning. The activity that initiated over the Blue Ridge Mountains has now increased in intensity ( $1.2\text{-}1.5 \text{ flashes km}^{-2} \text{ yr}^{-1}$ ) and spatial coverage (50-100 km wide). This line, now entirely east of AVL and the Yadkin River, has propagated quickly to the east. It was previously confined to west of the AVL to Yadkin River line. Also, this line has expanded further northeastward, now extending along the entire eastern edge of the Blue Ridge Mountains. Furthermore, the activity in the north is located closer to the mountain range,

than that in the south, signifying later convective initiation along the northern slopes of the Blue Ridge Mountains. The hot spot west of TYS is still located over the Cumberland Plateau, but has also extended eastward to the Tennessee River Valley. The weak gradient of lightning flash density west of the Allegheny Mountains also continues during this time period. The activity west of CRW remains confined to that area, with enhancements predominately in the river valleys west of JKL and CRW. The sea breeze activity has progressed inland about 200 km in SC and GA, but remains confined to within 75 km of the NC coast. A region of lower flash density exists between the AVL enhancement and the sea breeze activity. This time period is also the first period to display a lightning suppression over the length of the Appalachian chain. Figure 17c clearly shows lower flash density values over the western two-thirds of the mountains, along the entire length of the chain.

Figure 17d (1600-1900 EST) continues to depict a strong suppression of lightning activity over the Appalachian mountain chain. This paucity of lightning extends from the southern tip of the Appalachians to southern PA. This is the first period for which the suppression includes the higher terrain of the Cumberland Plateau and the Blue Ridge Mountains. Around this area of suppressed lightning, several areas of enhancement continue to exist. The activity west of the Allegheny Mountains has increased in intensity, but remains confined to that area west of the CRW to JKL line. A flash density gradient of  $0.012 \text{ flashes km}^{-2} \text{ yr}^{-1} \text{ km}^{-1}$  can be seen at the western mountain slopes near CRW. The Cumberland Plateau activity has moved entirely into the Tennessee River Valley. The hot spot that originated over the Blue Ridge Mountains has propagated into the Piedmont Region, and expanded in width to about 150 km. Along the Chesapeake Bay, lightning

activity increased rapidly during this time period; however, it cannot be seen from this study if this is due to convective initiation or interaction with the Blue Ridge activity. In the southern portions of the map, the progression of the sea breeze activity has slowed dramatically, extending only about 200 km inland from the coast. As with the last time period, a lull of activity exists between the sea breeze-induced lightning and the mountain-induced lightning. Finally, an enhancement occurs over ATL during this time period.

The time period from 1900-2100 EST (fig. 18a) continues to display a significant suppression of lightning over the entire extent of the Appalachian Mountains, with flash densities of less than  $0.1 \text{ flashes km}^{-2} \text{ yr}^{-1}$  dominating that region. It is during this period that the lightning activity climatologically begins to taper off. The northwest enhancement remains confined to the region west of CRW and the Allegheny Mountains. A narrow band of activity remains from the Piedmont Region, along the VA/NC border, to the Chesapeake Bay. East of this line, the area of lower activity has become more pronounced, resulting in two distinct enhancements from lightning of apparently two different convective initiation sources. The Tennessee River enhancement has disappeared by this time period, but that over ATL continues to exist.

Figure 18b represents the time period of 2100-2400 EST. During this period, the organized lightning patterns begin to disappear. The only remaining enhancement is that west of CRW. Although slightly farther east, that area still does not extend past the western foothills of the Allegheny Mountains. Lightning activity off the Carolina coastline is beginning to increase, but flash density values greater than  $0.5 \text{ flashes km}^{-2} \text{ yr}^{-1}$  are rare in that region. The lightning suppression over the Appalachians continues to strengthen, with flash density values  $< 0.05 \text{ flashes km}^{-2} \text{ yr}^{-1}$  dominating the high terrain.

The interval of 0100-0400 EST is the period of the climatological minimum of lightning activity for the SE. Figure 18c depicts values less than  $0.05 \text{ flashes km}^{-2} \text{ yr}^{-1}$  dominating all land regions over and east of the Appalachian Mountains. The activity west of CRW again remains confined to west of the Allegheny Mountains.

The final map, figure 18d, shows little pattern evolution by 0400-0700 EST, but indicates a resurgence of lightning activity during this period just before dawn. This flash count increase of 49 percent can most likely be contributed to decreased stability due to strong radiational cooling at storm tops. Other than an increase of activity (as high as  $0.2 \text{ flashes km}^{-2} \text{ yr}^{-1}$ ) eastward from ATL, the pattern remains highly active west of CRW and over the Gulf Stream, and inactive everywhere east of the Appalachians.

### *3.1.3. MAM (By-Times)*

To determine seasonal fluctuation of climatological lightning patterns, the NLDN data were analyzed for all times, and were separated into files for each of the four seasons and plotted for the same three-hourly intervals used above. The maps for all times revealed nearly identical patterns to the annual flash density maps for MAM, JJA, and SON, but with lower flash density values. Only the DJF map showed a different spatial pattern. Since the three-hourly maps also revealed that pattern, the all-times maps will not be discussed in further detail. The results are discussed briefly in the following sections.

#### Southwest Region

During the MAM season, the SW region displays climatological lightning patterns similar to those for the all-season data, except with flash density values of almost one order

of magnitude smaller (fig. 19a). The greatest increase in activity occurs during the times of 1100-1400 MST, and lightning predominately initiates over the Sacramento, White, and Sangre de Cristo Mountains, and over the Mogollon Rim. The greatest difference between the MAM season, and the annual maps is the rapid cessation of activity after 2000 MST (fig. 19b) during MAM. By this time period, flash density values of less than 0.01 flashes  $\text{km}^{-2} \text{ yr}^{-1}$  dominate mountains regions of the SW.

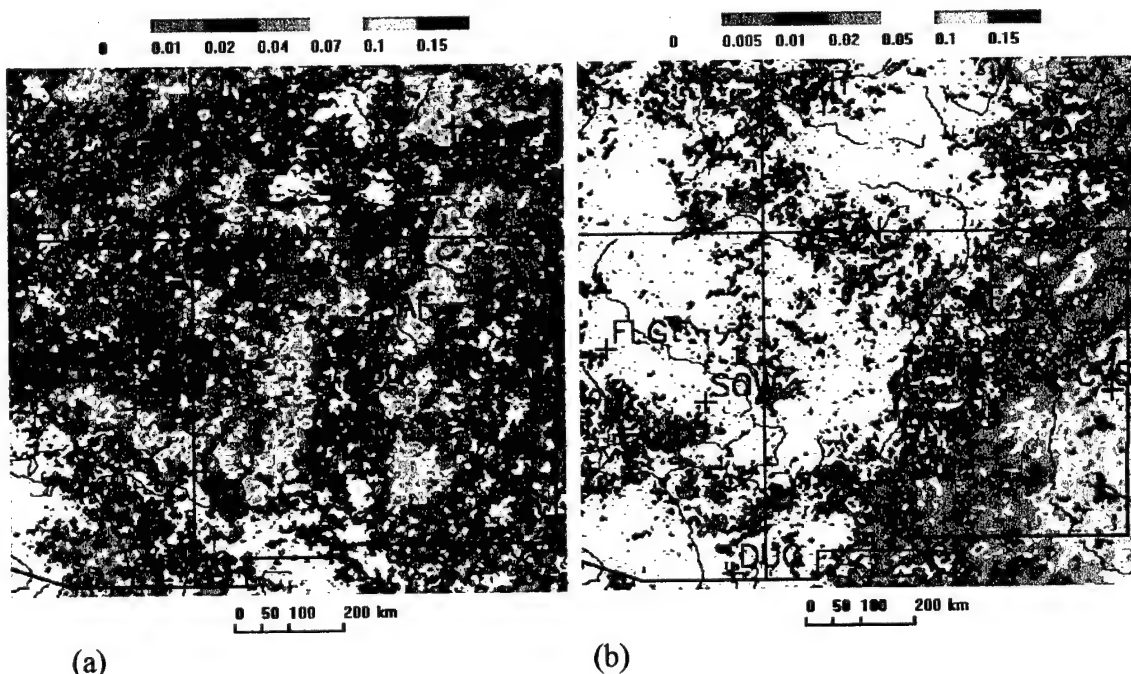


Fig. 19. MAM SW Region Three-Hourly Flash Densities. (a) 1100-1400 MST (b) 2000-2300 MST

#### Southeast Region

The MAM plots for the SE region display flash density values almost one order of magnitude smaller than the all-season plots for the same region. Furthermore, the clear patterns of the all-season plots are not easily identified during the MAM season (fig. 20).

In particular, the lightning suppression over the Appalachian Mountains is much weaker during this season, becoming evident only between the hours of 2200 and 0100 EST (fig. 20a). Late morning initiation of lightning activity takes place predominately over the Cumberland Plateau and the eastern slopes of the Blue Ridge Mountains (fig. 20b), and then propagates into the Piedmont region as the day progresses. The area lee of the Appalachians, from RIC to ATL is site of the largest lightning enhancement during the late afternoon period. Other than this enhancement, and a weak trend of decreasing lightning activity from west to east, no patterns of enhancement or suppression emerge.

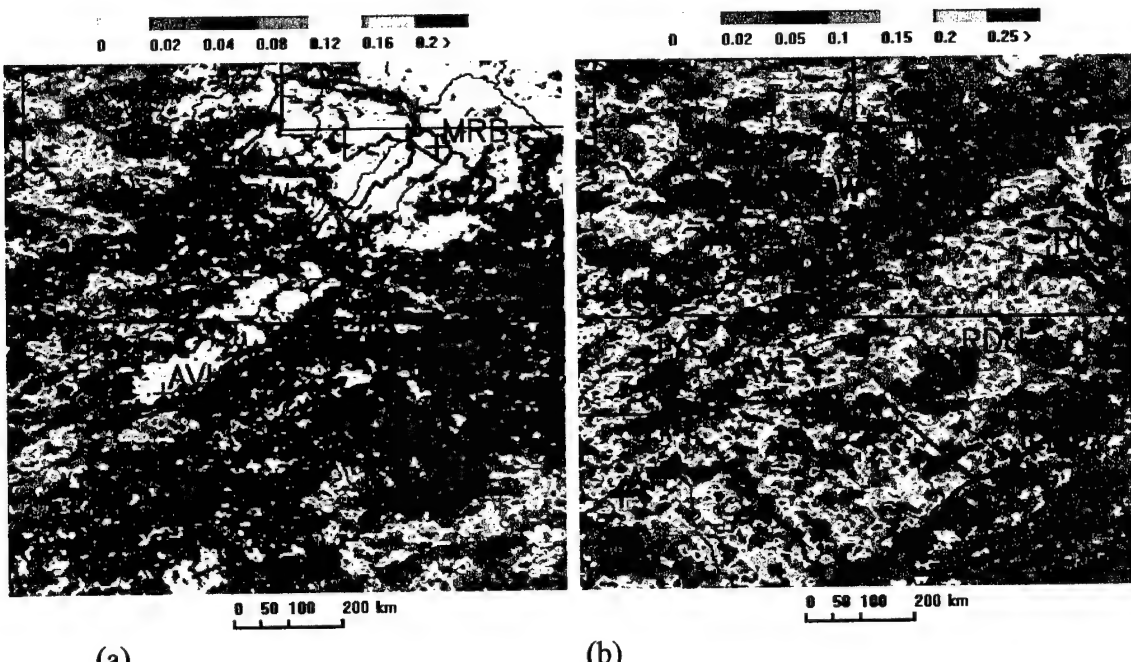


Fig. 20. MAM SE Region Three-Hourly Flash Densities. (a) 2200-0100 MST (b) 1600-1900 MST

### 3.1.4 JJA (All Times and By-Times)

#### Southwest Region

JJA is the season for which the flash density pattern is most similar to that of the annual pattern. Lightning activity initiates over the mountain peaks and ridges (starting with the Sacramento Mountains) during the 0800-1100 MST period (fig. 21a), and increases rapidly through the mid-afternoon hours. As the day progresses, the flash density enhancements propagate away from the higher terrain, reaching the low desert valleys of AZ by the 1700-2000 MST period (fig. 21b). Flash densities over  $1.5 \text{ flashes km}^{-2} \text{ yr}^{-1}$  are common over the higher terrain from 1100 to 1700 MST.

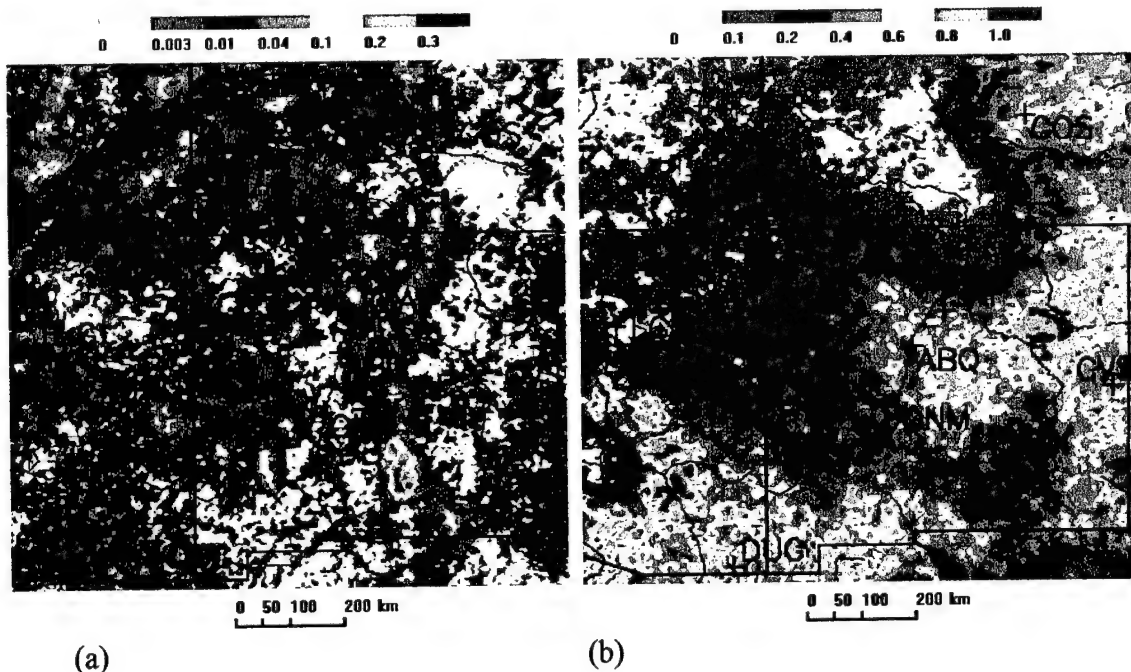


Fig. 21. JJA SW Region Three-Hourly Flash Densities. (a) 0800-1100 MST (b) 1700-2000 MST

### Southeast Region

The pattern for JJA in the SE also resembles the annual patterns. Most important during this season is the tendency for lightning activity to develop during the late morning over the Cumberland Plateau, the Blue Ridge Mountains, and along the coast (fig. 22a). The enhancements originating over high terrain propagate eastward, while the coastal activity expands westward about 200 km. The Appalachian lightning suppression is strongest in this season during the afternoon and evening hours (fig. 22b). The Allegheny Mountains appear to block the northwestern enhancements from expanding or propagating eastward. The enhancement over ATL is noticeable during the late evening hours. Flash density values greater than  $1.0 \text{ flashes km}^{-2} \text{ yr}^{-1}$  are common in the Tennessee River valley, east of the Blue Ridge Mountains, west of the Allegheny Mountains, and along the coast.

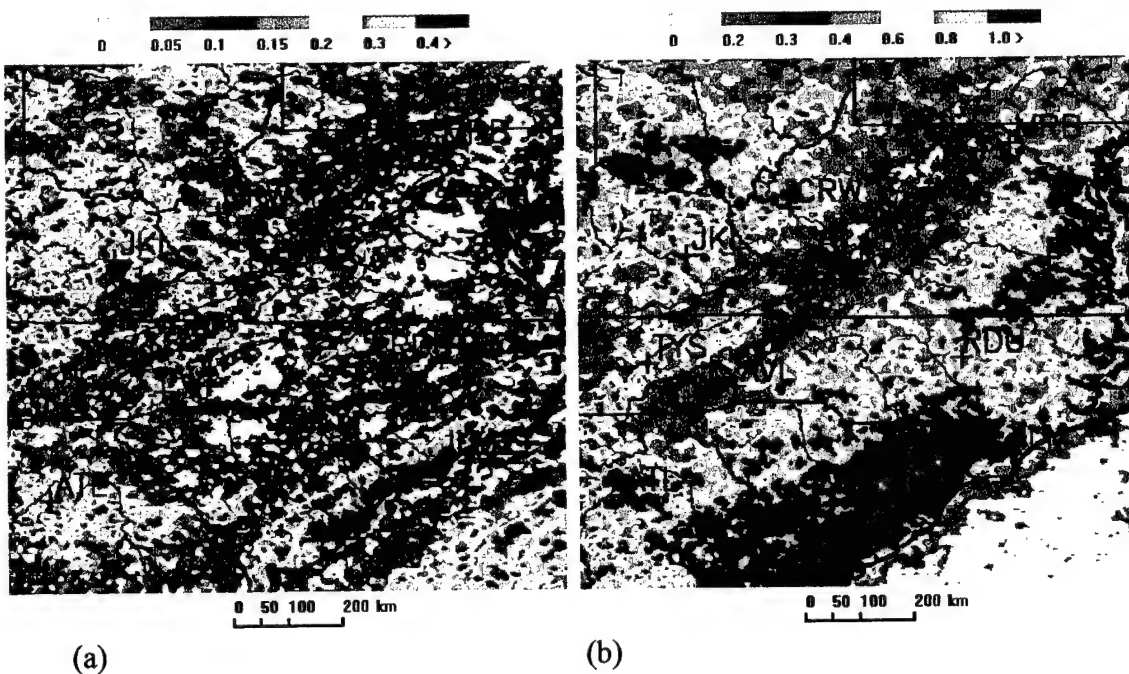


Fig. 22. JJA SE Region Three-Hourly Flash Densities. (a) 1000-1300 EST (b) 1600-1900 EST.

### 3.1.5. SON (All Times and By-Times)

#### Southwest Region

During the SON season, lightning in this region is rare. Flash density values exceeding  $0.2 \text{ flashes km}^{-2} \text{ yr}^{-1}$  are generally confined to the late morning through afternoon periods, and are found over and near the mountainous terrain. As with other seasons, high flash density values are first noted over the highest terrain, and initiates between 1100 and 1400 MST (fig 23a). The lightning enhancements propagate towards lower terrain, as the day progresses, and weaken quickly in the late afternoon. Values greater than  $0.1 \text{ flashes km}^{-2} \text{ yr}^{-1}$  are rare after 1700 MST (fig. 23b).

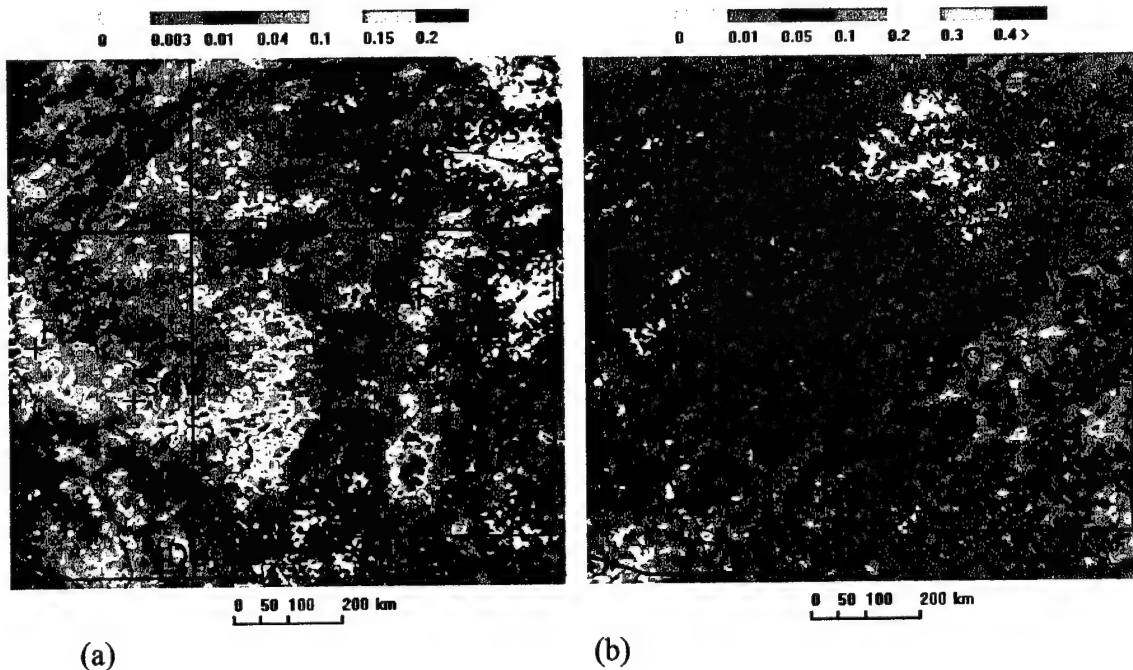


Fig. 23. SON SW Region Three-Hourly Flash Densities. (a) 1100-1400 MST (b) 1700-2000 MST

### Southeast Region

In the SE region, lightning activity in this season is also rare. Flash density values greater than  $0.05 \text{ flashes km}^{-2} \text{ yr}^{-1}$  dominate the map only for the two intervals of 1100-1400 EST and 1400-1700 EST (fig 24a). Although no evidence of lightning suppression can be retrieved from the SON maps, there were no enhancements of lightning activity during this season over the Appalachian Mountains, either. Since lightning activity is so sparse during the overnight hours (fig. 24b), the only resolvable pattern during those intervals is the trend of increased lightning in the western edge of the maps.

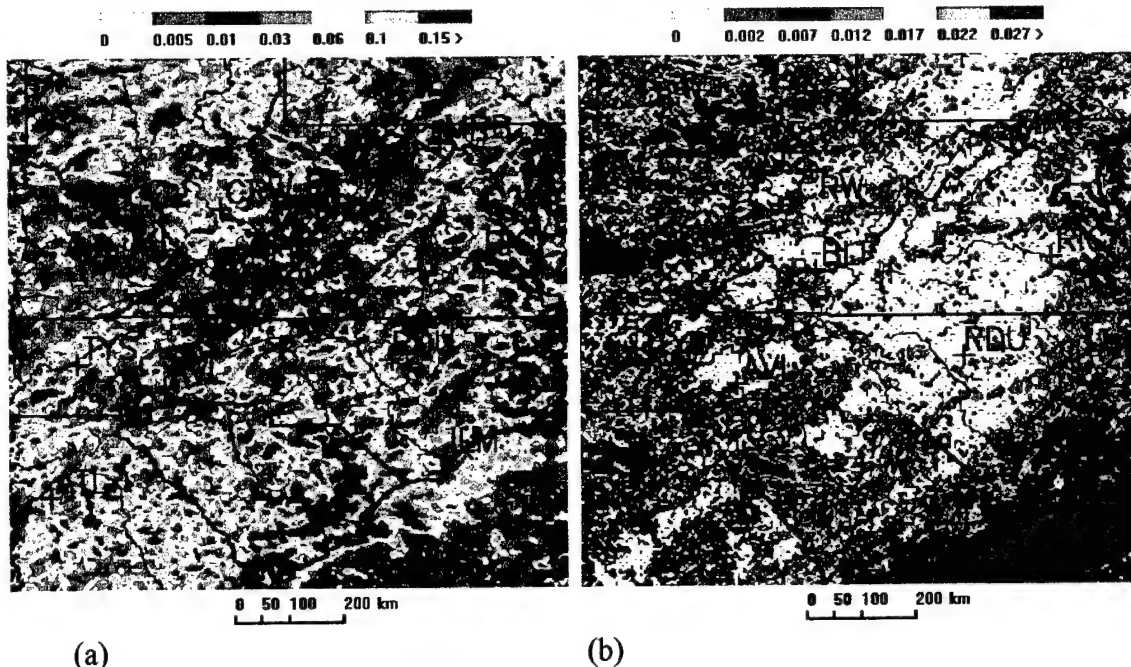


Fig. 24. SON SE Region Three-Hourly Flash Densities. (a) 1600-1900 EST (b) 0400-0700 EST

### 3.1.6. DJF (All Times and By-Times)

#### Southwest Region

DJF is the only season for which lightning activity shows no preference for higher terrain. The pattern for this season, however, is not particularly meaningful, since CG lightning is extremely limited. Flash densities  $> 0.01$  flashes  $\text{km}^{-2} \text{ yr}^{-1}$  seldom occur over areas larger than  $2500 \text{ km}^2$ , but when they do, it is generally in the valleys. Figure 25 shows the flash density map for the period of peak activity during the DJF season. Locations showing values less than  $0.003$  flashes  $\text{km}^{-2} \text{ yr}^{-1}$  reported no CG lightning flashes within 5km of that location during the entire twelve-year period.

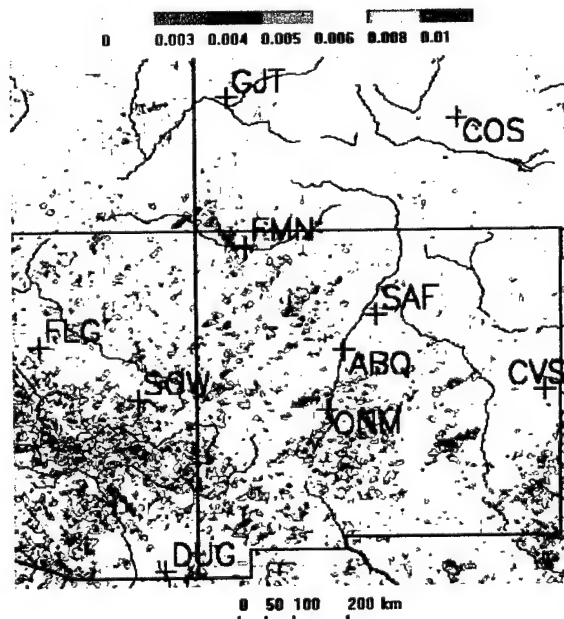


Fig. 25. DJF SW Region Three-Hourly Flash Density. 1400-1700 MST

### Southeast Region

The SE region also shows no terrain preference for lightning activity during the DJF season. The most significant feature during this season is the banding pattern of lightning enhancements. These bands are typically oriented in a west-to-east or southwest-to-northeast line. The western portion of figure 26a and the eastern portion of figure 26b, which display the peak periods of lightning activity for the SE, depict this banding pattern well. During no period of the DJF season did the SE maps show any of these bands crossing a mountain range. One or fewer CG lightning flashes were detected during the entire twelve-year period over those locations with flash density values less than 0.005 flashes  $\text{km}^{-2} \text{ yr}^{-1}$ .

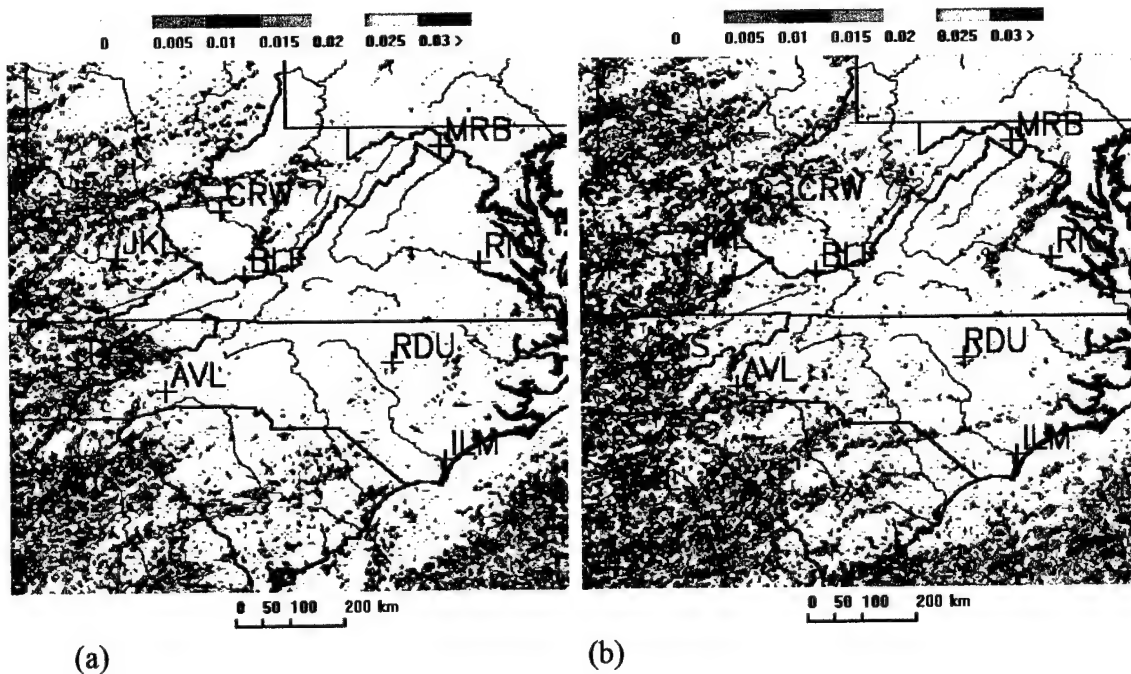


Fig. 26. DJF SE Region Three-Hourly Flash Densities. (a) 1600-1900 MST (b) 1900-2200 MST

### 3.1.7. Daily Summaries

To better understand the behavior of lightning on a daily basis, the data were stratified as described in section 2.4, into regions of high and low terrain. Summaries were generated to display the total number of flashes for every day that lightning occurred over high or low terrain. From these lists, the average flash count per lightning day was computed for both terrain classifications. Next, the top 5 percent of lightning producing days (active days) and the bottom 50 percent of lightning producing days (inactive days) were analyzed to determine the average daily flash count, and the percent of the total lightning flashes that were produced on the active and inactive days. The average number of flashes per day for the SW region's high terrain was  $2820 \text{ fl day}^{-1}$ , and the active days produced 29 percent of all lightning strikes. In the SE, the average flash count for high terrain was only  $590 \text{ fl day}^{-1}$ , but the active days produced 57 percent of all lightning flashes.

## 3.2. Precipitation Patterns

The analysis of mean annual precipitation from 1961-1990 showed a clear pattern in the SW region, but in the SE, a less consistent pattern arose. In the SW region, localized precipitation maxima are collocated with mountain ridges and peaks (fig 27a). Annual precipitation averages more than  $101.6 \text{ cm yr}^{-1}$  in the San Juan Mountains, and over  $50.8 \text{ cm yr}^{-1}$  for most of the high terrain of AZ and NM. Lower annual rainfall amounts ( $<25.4 \text{ cm yr}^{-1}$ ) dominate the major valleys, including the Rio Grande Valley, the Colorado River Valley, and the area just east of the San Juan Mountains.

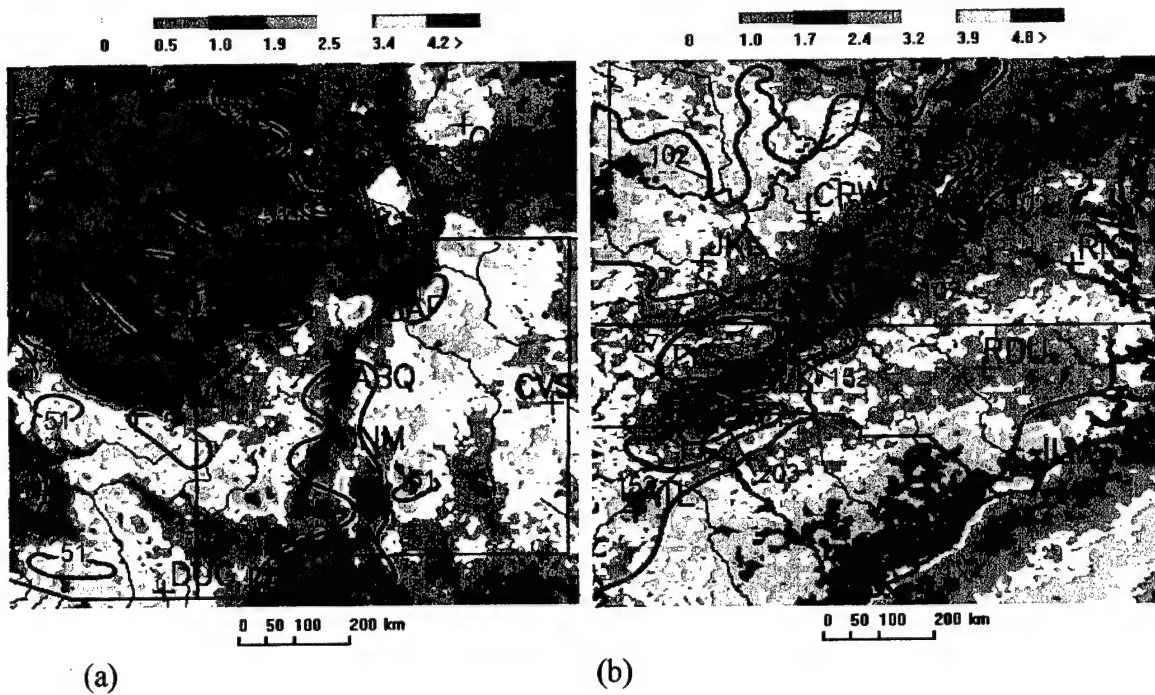


Fig. 27. Annual Average Precipitation Overlaid On Annual Flash Density. Precipitation contours (black) are overlaid upon annual flash density maps. Labels are average precipitation for the normal period 1961-1990, in cm. (a) SW Region (b) SE Region

In the SE, the southern half of the figure 27b (south of VA) depicts a pattern of lower precipitation totals ( $<127.0 \text{ cm yr}^{-1}$ ) on the western slopes and valleys of the Blue Ridge Mountains, while the eastern slopes' totals reach over  $203.2 \text{ cm yr}^{-1}$ . The northern half, however, reveals an enhancement of precipitation ( $>152.4 \text{ cm yr}^{-1}$ ) on the western slopes of the Allegheny Mountains, while a reduction of precipitation ( $<101.6 \text{ cm yr}^{-1}$ ) occurs on the eastern slopes.

### 3.3. Statistical Analysis

Before we can postulate on the causes of the apparent differences in the two patterns of flash density in the SW and the SE, we must first determine that the differences

can be quantified, and are statistically significant. To accomplish this, a t-test was performed to statistically compare the means of different populations, and conclude that the means are or are not different at a P-value of 0.01. The first t-test compared the mean flash density ( $\mu_{fd}$ ) of those boxes in the SW region with average elevation in the top 25 percent (SW high terrain) to that of those boxes in the bottom 40 percent (SW low terrain). The calculated  $\mu_{fd}$  of all boxes in the SW was 1.74 flashes  $\text{km}^{-2} \text{ yr}^{-1}$  with a standard deviation ( $\sigma$ ) of 0.66. The  $\mu_{fd}$  for the SW high terrain was 1.99 flashes  $\text{km}^{-2} \text{ yr}^{-1}$  with  $\sigma = 0.61$ , while the  $\mu_{fd}$  for SW low terrain was 1.54 flashes  $\text{km}^{-2} \text{ yr}^{-1}$  with  $\sigma = 0.66$ . These values suggest that the flash density in the high terrain is higher, and less variable than that in the lower terrain. The t-test comparing the  $\mu_{fd}$  for high versus low terrain in the SW region resulted in a t-statistic = 2.70 and a P-value of less than 0.01. These results show that the means are different, and that the  $\mu_{fd}$  for high terrain is higher than that of the low terrain, at a 99 percent confidence level.

The second t-test compared the mean flash density ( $\mu_{fd}$ ) of those boxes in the SE region with average elevation in the top 25 percent (SE high terrain) to that of those boxes in the bottom 40 percent (SE low terrain). The calculated  $\mu_{fd}$  of all boxes in the SE was 2.77 flashes  $\text{km}^{-2} \text{ yr}^{-1}$  with a standard deviation ( $\sigma$ ) of 0.68. The  $\mu_{fd}$  for the SE high terrain was 2.26 flashes  $\text{km}^{-2} \text{ yr}^{-1}$  with  $\sigma = 0.61$ , while the  $\mu_{fd}$  for SE low terrain was 3.40 flashes  $\text{km}^{-2} \text{ yr}^{-1}$  with  $\sigma = 0.52$ . These values suggest that the flash density in the high terrain is lower, and more variable than that in the lower terrain. The t-test comparing the  $\mu_{fd}$  for high versus low terrain in the SE region resulted in a t-statistic = -7.60 and a P-value of less than 0.01. This result shows that the means are in fact different, and that the  $\mu_{fd}$  for high terrain is lower than that of the low terrain, at a 99 percent confidence level.

The final t-test compared the  $\mu_{fd}$  for the highest 25 percent of elevation anomalies versus the lowest 40 percent of elevation anomalies for both regions. The resulting t-statistic in the SW was 8.7, with a P-value of less than 0.01. In the SE, the t-statistic was calculated to be 3.6, again with a P-value less than 0.01. Therefore the mean of the flash density anomalies for terrain with high elevation anomalies was significantly different than that for terrain with low elevation anomalies for both regions studied.

Polynomial and multiple regression analyses were performed on subsets of the lightning data. For the polynomial regressions, first elevation (ELEV), then elevation gradient (GRAD), and finally elevation anomaly (ELANOM) were used to predict the logarithm of flash density (DENSLOG) (flash density anomaly, DEANOM, was used for ELANOM) for both the SW and SE regions. For both predictors, and for both regions, the quadratic regression provided the best combination of simplicity and usefulness; however, neither quadratic curve could be considered a very good fit. The adjusted  $R^2$  value was chosen to quantify the quality of a model since it rewards for goodness of fit and penalizes for complexity. In the SW region, the best quadratic regression resulted from using GRAD and  $GRAD^2$  as predictors. The resulting adjusted  $R^2$  was 0.156. In the SE region, ELEV and  $ELEV^2$  produced the best results with an adjusted  $R^2$  value of 0.363. The results of predicting DEANOM from ELANOM also produced  $R^2$  values less than 0.37 for both regions, despite showing a very strong relationship when displayed graphically (figure 27). It is believed that the large data spread produces the low  $R^2$  values. Since slightly better results arose from multiple regression analysis, only those results will be discussed in more detail.

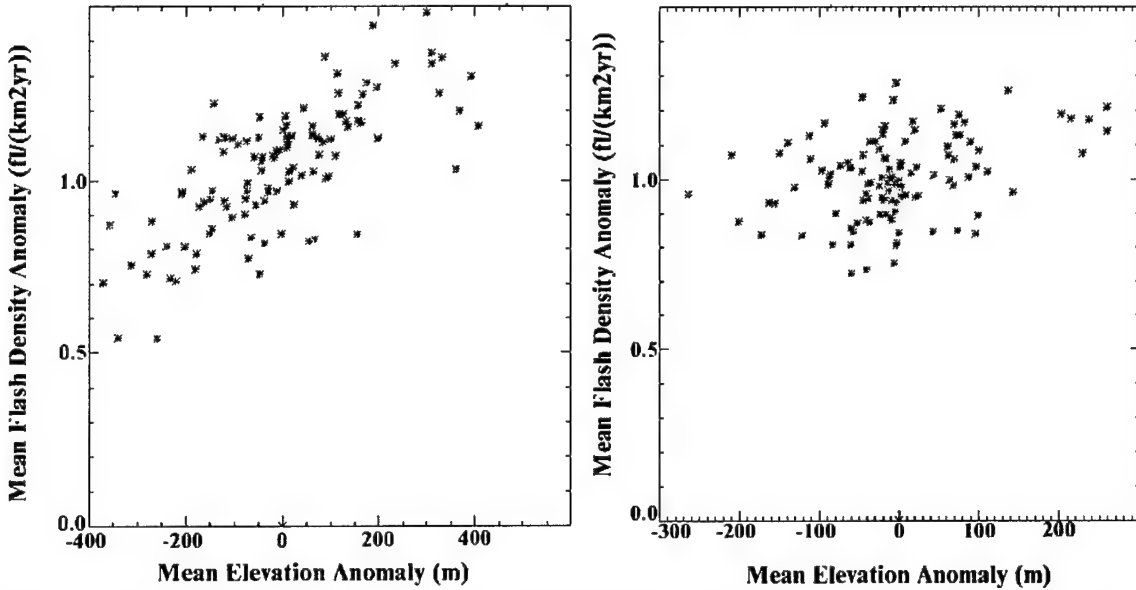


Fig. 28. Flash Density Anomalies Versus Elevation Anomalies. (a) SW Region (b) SE Region

The multiple regressions used ELEV, ELEV<sup>2</sup>, GRAD, and GRAD<sup>2</sup> to predict DENSLOG. For both regions, the regression using all four predictors resulted in the highest R<sup>2</sup>, but in the SW it was the three-predictor regression involving ELEV, GRAD, and GRAD<sup>2</sup> that provided the most efficient fit, and the highest adjusted R<sup>2</sup>. In the SW, the R<sup>2</sup> of 0.204 for the three-predictor model was only slightly lower than the R<sup>2</sup> for the four-predictor model, but the adjusted R<sup>2</sup> for the reduced model was higher. Another indicator of the value versus complexity of a model is the Mallow's C(p). This parameter represents a good model when its value is less than 2\*P+1 (where P is the number of parameters in the model), and the lower the Mallow's C(p) for a model, the better the combination of usefulness and simplicity. This model resulted in a Mallow's C(p) of 3.942, compared to 5.000 for the four-predictor model. For the SE region, the R<sup>2</sup> (0.419) and the adjusted R<sup>2</sup> (0.400) were both higher for the full four-predictor model. The Mallow's C(p) of 5.000 for the full model was exactly on the threshold of the 2\*P+1 mark,

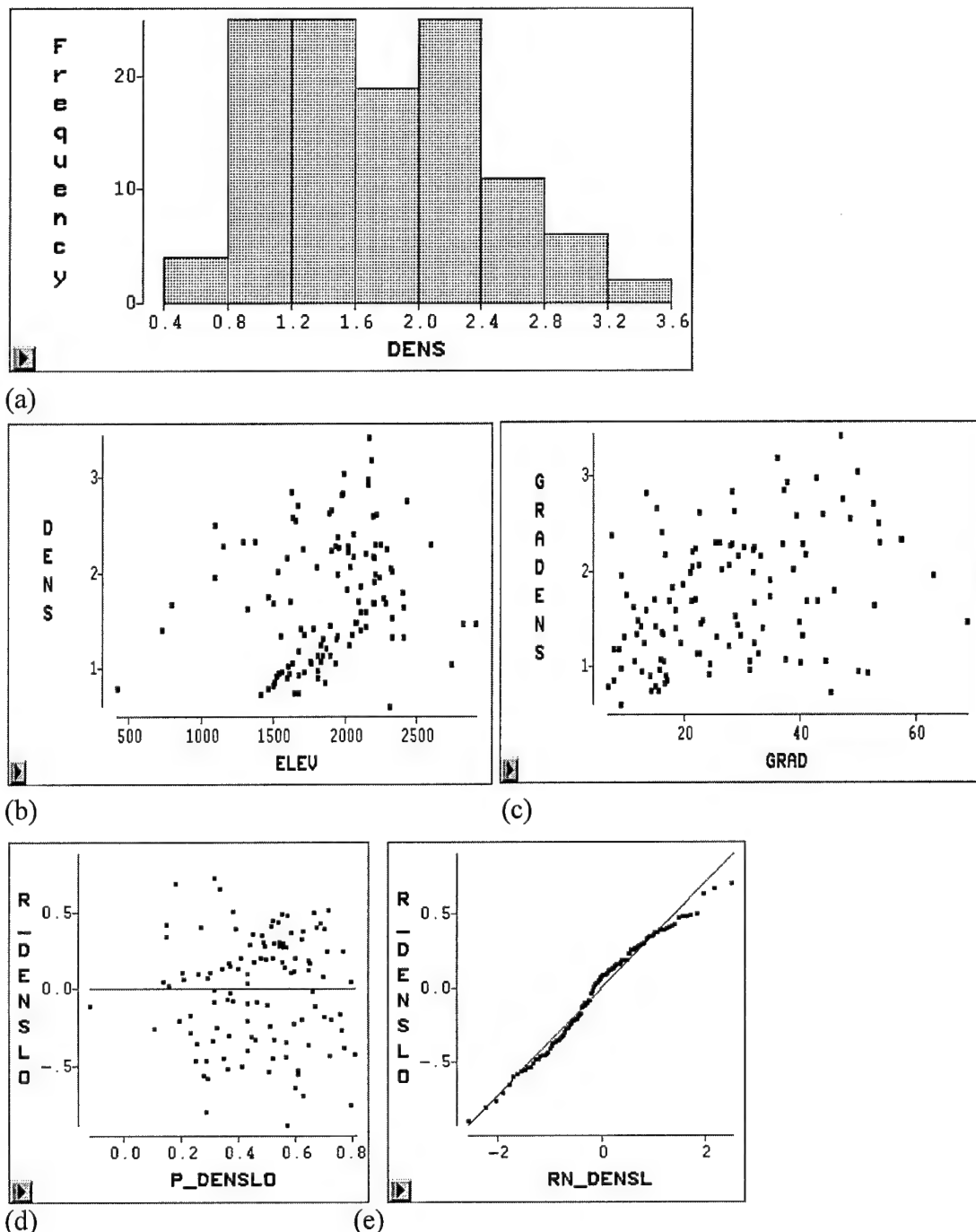


Fig. 29. SW Multiple Regression Output. (a) Histogram of average flash density for statistical boxes. (b) Scatter plot of Flash Density versus Elevation. (c) Scatter plot of Flash Density versus Elevation Gradient. (d) Scatter plot of model residuals (e) Residual Normal Quantiles Plot

but was better than the 4.333 scored by the reduced model (P=3). This showed that the improved efficiency of the reduced model outweighed the slight improvement of fit in the SW, but in the SE, the full model provides significant improvement and should be used.

The multiple regression model chosen to represent the distribution of average flash density among the statistical boxes in the SW region was the following:

$$\text{DENSLOG} = -0.3635 + 0.0002*\text{ELEV} + 0.0269*\text{GRAD} - 0.0003*\text{GRAD}^2$$

The graphs in figure 28 display the histogram of average flash density (fig. 28a), scatter plots of flash density versus elevation (fig. 28b) and flash density versus elevation gradient (fig. 28c), and plots of the residuals (fig. 28d) and the residual normal quantiles (fig. 28e) for the above model (SW Region). The flash density histogram revealed a nearly even distribution of average flash density between 0.8 and 2.4 flashes  $\text{km}^{-2} \text{ yr}^{-1}$ . The residuals plot demonstrated a spread of over 1.5 units. The residual normal quantiles plot was initially linear, with a very steep center region, and a very flat right region. The scatter plots for flash density versus elevation gradient and flash density versus elevation both revealed a positive slope, but the data was widely spread. It was this wide distribution that lead to the large residuals and low  $R^2$  value.

The multiple regression model chosen to represent the SE region follows:

$$\text{DENSLOG}=1.5727-0.0015*\text{ELEV}+6.91\text{E-}07*\text{ELEV}^2-0.0158*\text{GRAD}+0.0003*\text{GRAD}^2$$

The graphs in figure 29 display the histogram of flash density (fig. 29a), scatter plots of flash density versus elevation (fig. 29b) and flash density versus elevation gradient (fig. 29c), and plots of the residuals (fig. 29d) and the residual normal quantiles (fig. 29e) for the above model (SE Region). The flash density histogram revealed a distribution with a mode in the range of 2.6 to 3.0 flashes  $\text{km}^{-2} \text{ yr}^{-1}$ , a heavy left tail, and a light right tail.

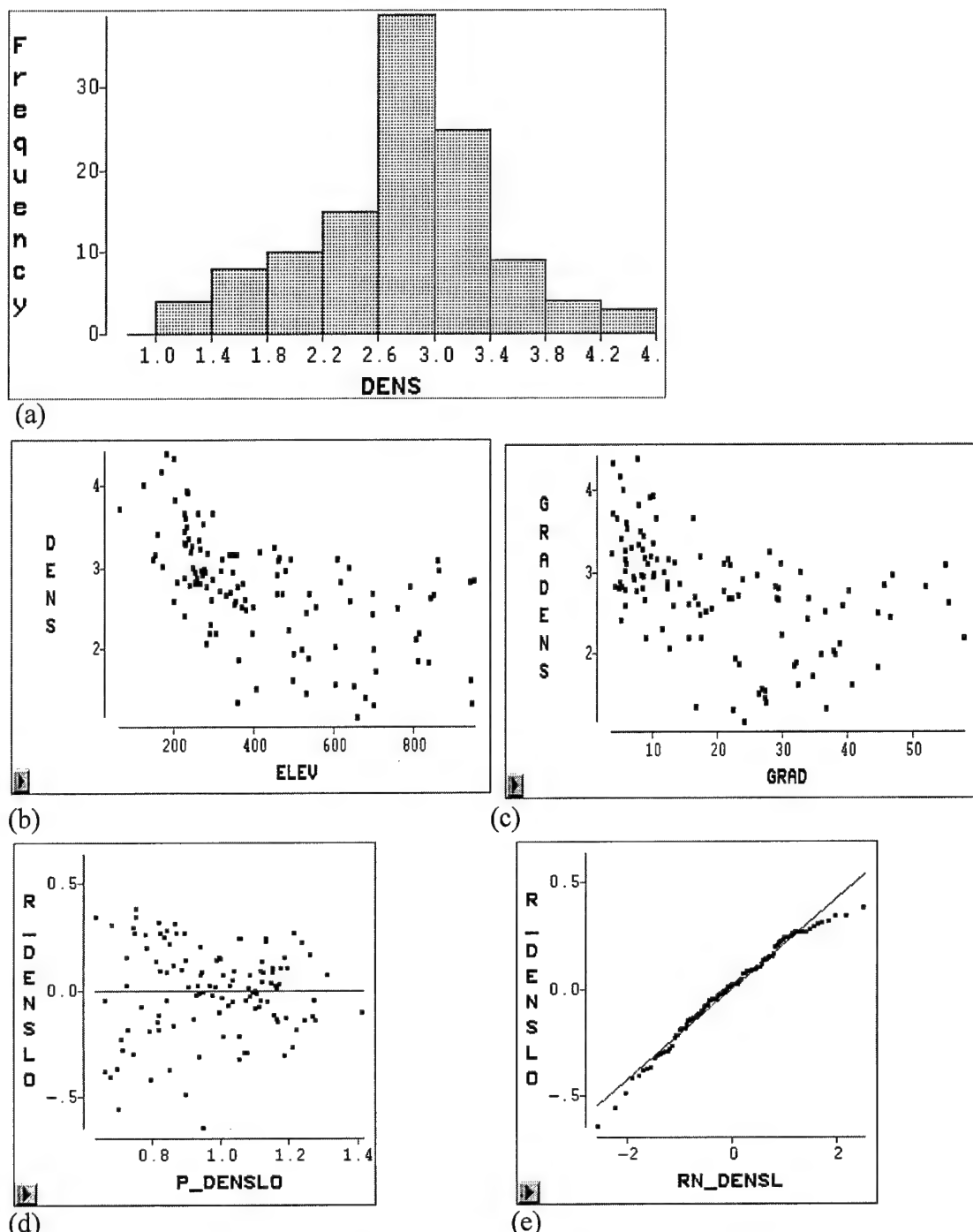


Fig. 30. SE Multiple Regression Output. (a) Histogram of average flash density for statistical boxes. (b) Scatter plot of Flash Density versus Elevation. (c) Scatter plot of Flash Density versus Elevation Gradient. (d) Scatter plot of model residuals (e) Residual Normal Quantiles Plot

The residuals plot demonstrated a spread of about 1.0 unit. The residual normal quantiles plot was initially steep (again depicting a heavy left tail), linear in the center region, and flat at the right region. The scatter plots for flash density versus elevation gradient and flash density versus elevation both revealed a negative exponential slope with less spread than for the SW region.

### **3.4. Upper Air Analysis**

Upper air analysis consisted of two parts. First was the computation of surface, ridge-top, and upper level winds, averaged over four upper air observation sites in the SE, for each day that was identified as a member of one of the four classes of the daily summaries. The upper air sites that were chosen included Wilmington, OH (ILN), Greensboro, SC (GSO), Nashville, TN (BNA), and Peach Tree, GA (FFC). From these results, the average synoptic flow for all three levels, and for each class, was calculated. The second part of the upper air analysis determined the difference in equivalent potential temperature ( $\Theta_e$ ) between the valley floor and the mountain ridges. This was accomplished by computing  $\Theta_e$  for the surface, 850mb, and 700mb for specified upper air sites. In the SW, upper air data from Grand Junction, CO (GJT), Flagstaff, AZ (FLG), Tucson, AZ (TUS), and Albuquerque, NM (ABQ) were averaged to produce a representative upper air profile. The average  $\Theta_e$  from ILN, GSO, and Roanoke, VA (RNK) was chosen to represent the Allegheny Mountain area's thermodynamic profile, while  $\Theta_e$  calculations from BNA and FFC were averaged to produce a thermodynamic profile for the Blue Ridge Mountain area.

The upper air wind analysis consisted of computing the average wind speed and direction for the surface, ridge top (850 mb), and the upper levels (500 mb), in the SE region, for active (top 5 percent lightning producing) and inactive (bottom 50 percent lightning producing) days. All wind speeds are reported as “ddd°/ff ms<sup>-1</sup>”; where “ddd” is the direction (measured clockwise in degrees from due north) that the wind is blowing from, and “ff” is the speed in meters per second. The resulting wind profiles are displayed in figure 30. Beginning with the low-elevation region’s inactive days, analysis showed that the typical flow pattern consisted of surface winds of 152°/0.6 ms<sup>-1</sup>, ridge top winds of 266°/2.1 ms<sup>-1</sup>, and upper level winds of 266°/10.7 ms<sup>-1</sup>. The average pattern for the surface, ridge top, and upper levels, respectively, on high-elevation inactive days was 240°/1.0 ms<sup>-1</sup>, 257°/4.4 ms<sup>-1</sup>, and 090°/10.7 ms<sup>-1</sup>. For active days, the patterns were considerably different. In the low-elevation terrain, the average active day produced surface winds at 214°/1.3 ms<sup>-1</sup>, ridge top winds at 253°/4.2 ms<sup>-1</sup>, and upper level winds at 095°/6.0 ms<sup>-1</sup>. The high-elevation’s average active day pattern was 212°/1.3 ms<sup>-1</sup> at the surface, 248°/4.2 ms<sup>-1</sup> at the ridge top, and 267°/6.4 ms<sup>-1</sup> at the upper levels. The low-active and the high-inactive profiles showed strong similarities, in that both were southwesterly at the surface, then veered with height to an easterly wind at the upper levels. The upper level wind speed for the high-inactive, however, was nearly twice that of the low-active, while the surface and ridge-top winds were more southerly for the low-active days. Several differences are revealed when comparing the active and inactive days for the high terrain. First, the average surface wind for the active days was more southerly (212°), while that of the inactive days was southwesterly. Also, the vertical wind profile for the active days showed much less veering than that of the inactive days, resulting in a wind

profile entirely southwesterly. Finally, the average ridge-top wind for the active days was slightly slower than for the inactive days ( $4.1 \text{ ms}^{-1}$  versus  $4.4 \text{ ms}^{-1}$ ). The apparent differences between high-active and high inactive-days were the easterly component in the upper level winds for the inactive days and the more southerly component to the surface winds for the active days.

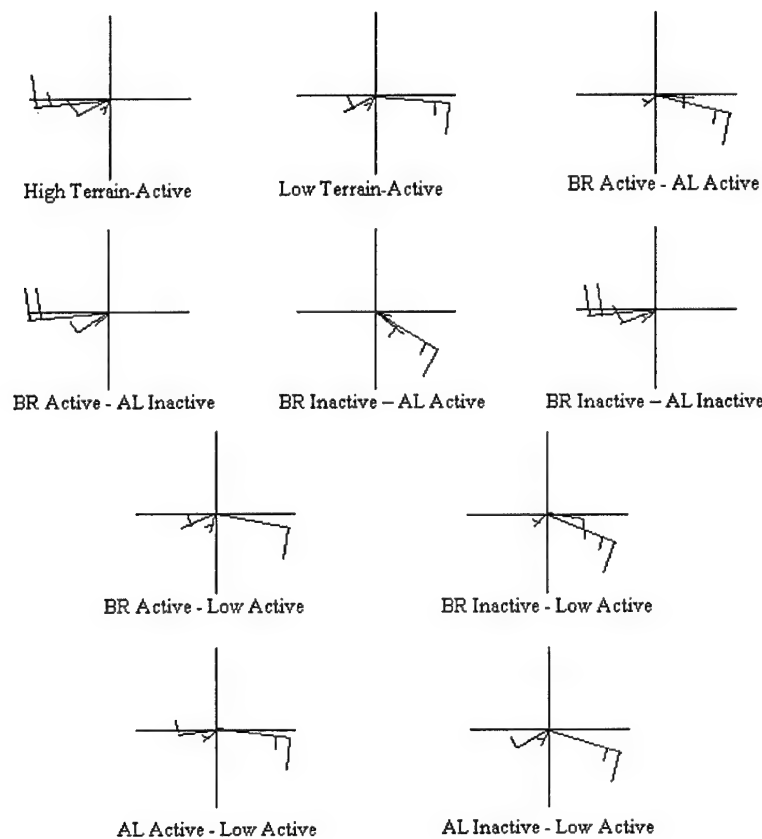


Fig. 31. Wind Profiles. Small barbs represent surface winds, medium barbs represent ridge top winds, and large barbs represent upper level winds.

Several comparisons were made possible by splitting the high-elevation regions into the Allegheny and Blue Ridge regions. Comparisons included all possible combinations of low-elevation active and inactive days, Allegheny (AL) active and

inactive days, and Blue Ridge (BR) active and inactive days. The surface, ridge-top, and upper level wind averages for each of these classes were carefully studied, and some patterns did emerge. First, for all combinations involving low elevation active days, the average upper flow was easterly. Second every combination with AL-active shows easterly upper level flow, as well. Furthermore, averages for days with both AL and BR active resulted in easterly ridge-top and upper level winds, while the days with only the AL active resulted in easterly wind averages at all three levels. All cases with an active BR region displayed southwesterly surface winds. The case with BR-active and AL- inactive was the only case (besides the all high terrain active case) that showed a southwesterly wind profile for all three levels.

The thermodynamic analysis produced a unique profile in the SW, but two similar profiles in the SE, with only subtle differences between the Blue Ridge and Allegheny regions. In the SW, the average  $\Theta_e$  (surface) was 327.3 K. When compared to the average ridge top observation ( $\Theta_e$  (700) = 342.9 K), this gives a difference of 15.6 K between the average surface and ridge top equivalent potential temperatures. Considering an average altitude change of 1800 m between the surface and ridge top, this gives a vertical  $\Theta_e$  gradient of 8.6E-3 K m<sup>-1</sup>. In the Blue Ridge region, the  $\Theta_e$  (surface) was 330.0 K, while the  $\Theta_e$  (850) was calculated at 342.7 K, resulting in a difference of 12.7 K. With an average altitude change of 1287 m, a vertical  $\Theta_e$  gradient of 9.9E-3 K m<sup>-1</sup> resulted. Finally, the  $\Theta_e$  (surface) in the Allegheny region was calculated at 329.0 K, while the  $\Theta_e$  (850) was 340.4. This produced a difference of 11.4 K, and, given an average altitude change of 1086 m, a vertical gradient of 1.0E-2 K m<sup>-1</sup>. Table 3 summarizes the thermodynamic profiles for each region.

One other item to note is that the standard deviation of the SW  $\Theta_e$  (surface) was 12.00, but in the Blue Ridge and Allegheny regions, the standard deviation of the  $\Theta_e$  (surface) was only 7.93 and 8.32, respectively. This shows a much more variable surface temperature and moisture content in the SW for the top 5 percent lightning producing days, than in the SE.

**Table 3.** Thermodynamic Data. Columns represent the region, the difference between the surface and ridge top equivalent potential temperatures (K), and the vertical gradient of equivalent potential temperature ( $\text{K km}^{-1}$ ).

Region	Surface $\Theta_e$ – Ridge Top $\Theta_e$ (K)	Vertical $\Theta_e$ Gradient ( $\text{K km}^{-1}$ )
SW	15.6	8.6
BR	12.7	9.9
AL	11.4	10.0

The variation of the horizontal temperature difference ( $\Delta T_H$ ) between the summits and ambient environments at summit level was very large when comparing Mount Lemmon (in the SW) to Grandfather Mountain (SE). The average  $\Delta T_H$  between Mount Lemmon and the 700 mb level was 25.7 K, and the average  $\Delta T_H$  between Grandfather Mountain and the 850 mb level was 17.6 K. This indicates that the heating on the mountain slope, relative to the free atmosphere at the same elevation, is much stronger in the SW region. This stronger horizontal temperature difference drives stronger horizontal pressure gradients at the ridge-top, and therefore a stronger diurnal mountain breeze.

## CHAPTER IV

### SUMMARY AND CONCLUSION

#### 4.1. Discussion

The following sections explain the results described in Chapter III and discuss their implications.

##### *4.1.1. Lightning Characteristics*

###### Annual Maps

From the annual lightning characteristics maps, several patterns were observed. The most notable of these was the appearance of two distinct and opposite mountain and river effects (figs. 1 and 2). In the SW region, the maps revealed an enhancement of flash density over mountain peaks and ridges and suppression over the river valleys. In the SE, a pattern of minimum flash density over the mountains and enhancements over the rivers emerged.

In both the SW and SE regions, patterns of high percent positive lightning became evident in areas of minimum flash density. These areas did not reveal an increase in positive flash density comparable to the increase in percent positive. This suggested that spatial variations in percentage of positive flashes depends more on the total number of flashes recorded than on the number of positive flashes recorded. Another possible explanation for the high percent positive in the Allegheny Mountains rises from meteorological reasoning, rather than from the mathematical definition of a percentage.

An organized mesoscale convective system (MCS), with an anvil to the east of the main updraft would place the anvil over higher terrain than it typically would be if there were no mountains east of the MCS. This would place the upper positive charge region (Krehbiel, 1986) closer to the ground, thus resulting in a stronger electric potential and higher likelihood of positive discharges over the mountains. The by-times analysis showed that the area east of CRW is commonly subjected to nocturnal lightning activity that resembles the above situation. Because the positive flash density did not increase in this region, however, this explanation can only be a contributing factor, not a full description of the phenomenon.

The SE positive flash density map (fig. 11a) displayed a significant pattern. Northward from the AVL latitude, a strong zonal gradient appeared at the western edge of the Appalachian Mountains, with lower positive flash densities persisting across the 500 km east of the gradient. South of AVL, however, the positive flash density remained zonally constant, with only weak local fluctuations. This could be a result of the mountains disrupting the organization of thunderstorm complexes; however, a more detailed investigation would be required to fully understand the phenomenon.

The peak current and multiplicity maps for the SW and SE regions (figs. 9,10,12, and 14) revealed two very different tendencies. First, in the SE (excluding the bulls-eye of low peak currents southwest of AVL, as discussed in section 3.1.1), high negative peak currents coincide almost perfectly with low negative multiplicity observations, and patterns of high positive peak currents very closely match the patterns of low positive flash density (the positive multiplicity plot revealed no discernable patterns). Second, in the SW, high peak currents were observed on the eastern mountain slopes, and were often co-located

with flash density enhancements. Cummins et al. (1999) showed that for a portion of the central United States, mean peak current and mean multiplicity are positively correlated. This study shows that those results are probably not valid over larger spatial scales. The SE observations suggest that a balance exists between the magnitude of the discharged current and the number of discharges (through variations in either multiplicity or flash density), such that the total charge transferred remains spatially constant in an environment with a spatially constant average electric potential. In an environment of steady-state charge separation within a single storm, a change in peak current must be countered by an opposite change in multiplicity or flash density, in order to maintain a steady state electric potential. Climatologically, if the average electric potential is spatially constant, areas of high peak currents must display lower multiplicities or lower flash densities. Furthermore, since a threshold electric potential is only necessary to initiate an electric discharge, rather than to maintain a current once a channel is established, consistently high peak current values could deplete the average electric potential in an environment at a higher rate than charge separation process can replace it. If this occurs consistently, the resulting downstream environment would necessarily experience a suppression of discharges, unless the charge separation rate is increased.

According to the above theory, the area of very high median negative peak currents around CRW would predict the observed decreases in negative multiplicity and flash density in the same location. In western VA, however, low multiplicity, peak current, and flash density all coexist, thus requiring a rapid reduction in the average available electric potential. This could be due to reduced climatological charge separation in the area, or due to consistent advection of air whose electric potential has been drained, as described above,

by very high peak currents upstream. In the case of the Allegheny Mountains, the wind profile data does support at least some decrease in charge separation rates, since all combinations of AL active days displayed southwesterly surface winds. This wind component would produce a descending inflow for storms to the north and northwest of the mountain chains. Since it is this region where the strongest lightning suppression was observed, both mechanisms should be examined in detail before one particular hypothesis is chosen. Case studies measuring equivalent potential temperature in the surface inflow would be helpful in determining if the diminished lightning activity is directly related to a lack of surface moisture in the mountainous regions and a corresponding decrease in updraft intensities and charge separation rates. Measurements of electric fields and peak currents would be required to determine if the lightning suppression can be attributed to a depletion of electric potential by large peak current flashes. From the data in this study, it appears that the western edge of the northern Appalachians lightning suppression is caused by a combination of the two effects.

In the same region where decreased negative peak currents, decreased multiplicity, and decreased flash density were collocated, an area of strong median positive peak currents is observed. This increase was more dramatic than that of the negative peak current ( $0.1 \text{ kA km}^{-1}$  versus  $0.02 \text{ kA km}^{-1}$ ) and was displaced just to the east of the negative peak current maximum. Since the region was collocated with low positive flash density, and no significant change in multiplicity was noted, these observations suggested that either the jump in positive median peak current acted to deplete the environment of its positive polarity electric potential and contribute to the suppression of total lightning, or that the charge separation process weakened dramatically in that area. The positive peak

current enhancement extended southwestward all the way to the GA border, despite the contamination due to sensor configuration (which would bias the observations toward lower peak currents). To accurately quantify the magnitude of the peak current increase west of AVL, the sensor configuration error must first be filtered out; however, from this study, it is certain that the feature does exist.

In the SW region, the high median negative peak currents follow along eastern slopes of mountain ridges, and are co-located with high flash density and high negative multiplicity. The enhancements over the San Juan and Sangre de Cristo Mountains were located just east of the thunderstorm genesis zones identified by Banta and Schaaf (1987) and Schaaf, et al. (1988). Also, the regions of enhanced median negative peak currents in AZ were located just south of the area of initial convection, as noted by Watson, et al. (1994). These observations support the peak current versus multiplicity-flash density balance theory discussed above, since thunderstorms in their initial development stages must have an increasing charge gradient over time, and therefore can exhibit high flash density, multiplicity, and median peak currents, without depleting the electric potential.

By measuring the mean peak current of each return stroke, the multiplicity of each flash, and the annual flash density, an estimation of the average total charge transferred annually in a region can be achieved. However, since the median peak current measurements consider only the initial return stroke, these measurements alone cannot be used to calculate the total charge transferred for flashes with multiplicities greater than one. Also, since the SE median negative peak current maximum is collocated with a decrease in multiplicity and flash density, these data cannot determine whether the electric potential between the main negative charge center and the ground would increase or decrease.

However, the median positive peak current was collocated with low positive flash density and a constant positive multiplicity, resulting in a relative increase of charge transferred from the main positive charge center and the ground, thus decreasing the electric potential between those regions. If future studies with more detailed measurements could show that increased median negative peak currents dominate the decreased negative multiplicities, the total charge transferred to ground could be shown to increase. If future studies could determine that the average charge separation rate does not increase in the region where higher peak currents dominate, it could be shown that the electric potential in that region would decrease over time. If the two conditions above could be verified in western WV, the subsequent decrease in flash density in eastern WV would be explained by the decreased electric potential due to increased peak currents upstream. If the charge separation rate were found to be lower over the area that shows a lightning suppression, the theory of high peak currents depleting the electric potential of the storm environment would still apply if that depletion were found to occur more quickly than the decreased charge separation rate would explain.

#### By Times / By Season Maps

When the data were split by times and by season, more key observations were unveiled. First, the SW analysis supported the work of Reap (1986) and Watson et al. (1994) in that the lightning enhancements appeared over the mountain peaks and ridges between 0800 and 1100 MST, then propagated towards lower terrain. The result was a late morning maximum of activity over the higher elevations and a nocturnal maximum over the low terrain. Because this study was performed at a 5 km resolution, the mountain and

valley effects were very evident. Figure 15(c) showed flash density increases of more than an order of magnitude over distances of 50 km or less, and a visual inspection of the figure suggests that the 1100-1400 MST flash density can be used directly as a proxy for terrain elevation. The second key result was the evolution of the Appalachian lightning suppression noted by Huffines and Orville (1999). During the late night and early morning hours, lightning was scarce from the Appalachians, eastward. West of the mountains, however, flash densities greater than 0.3 flashes  $\text{km}^{-2} \text{ yr}^{-1}$  persisted. During the 1000-1300 EST interval (fig 17b), patterns of lightning enhancements representing climatologically favored areas of convective initiation, developed over the Blue Ridge Mountains and the Cumberland Plateau. Signs of a lightning suppression did not appear until after 1300 EST, and disappeared after 0100 EST. Although the annual flash density in the Appalachians is inversely proportional to the elevation, the area of suppression did not follow individual terrain features as well as the lightning enhancements of the SW did.

One question that arose from the by-times maps of the SW region concerned the Sacramento Mountains. This was the only region to develop flash densities over 0.3 flashes  $\text{km}^{-2} \text{ yr}^{-1}$  during the convective initiation period of 0800-1100 MST. This region also displayed the largest area enclosed by the 1.8 flashes  $\text{km}^{-2} \text{ yr}^{-1}$  contour during the 1100-1400 MST period, but showed a rapid decline in activity immediately thereafter. This earlier development and decay suggested that the southern location, the access to Gulf of Mexico moisture, and the elevation, slope, and orientation of the terrain provided an optimal situation for earlier convective initiation, and a rapid propagation of storms towards lower terrain. This phenomenon may be useful in describing the behavior of mountain-initiated convection in the southern Blue Ridge region, because of the rapid

propagation of lightning enhancements there. The two mountain ranges share similar slope characteristics and latitude, but the Blue Ridge are oriented about 60 degrees clockwise from the north-south orientation of the Sacramento Range. This displacement from the north-south orientation delayed the diurnal heating of the Blue Ridge slopes by reducing the rate of heating from early morning solar radiation. The result was the two-hour local delay of convective initiation over the Blue Ridge Mountains when compared to the local timing of the Sacramento Mountains. Another key observation from the SW that was repeated in the SE was the distance over which the lightning enhancements propagated. For the Sacramento, San Juan, Sangre de Cristo, and White Mountains, as well as for the Mogollon Rim, the lightning maxima propagated about 100 km away from the ridges, and in the direction of the lowest terrain. This same result is shown along the length of the Blue Ridge Mountains, where the enhancement also propagates about 100 km before stalling and dissipating slowly. The narrow region of higher flash density values extending southwestward from RDU (in figure 2) can be largely explained by the inability of the mountain convection to propagate more than 100 km away from the mountain range. The fact that the mountain convection resulted in a climatological maximum 50 to 100 km east of the mountains, rather than over the mountains (as seen in the SW) requires more insight.

In the SW (figs. 15 and 16), the flash densities over the mountains quickly increased from less than 0.05 flashes  $\text{km}^{-2} \text{ yr}^{-1}$  to approximately 1.0 flashes  $\text{km}^{-2} \text{ yr}^{-1}$  in just six hours, and remained over the ridges and peaks for the duration of that six-hour period. Over the following nine hours, the enhancements progressed steadily away from the mountain ridges, and dissipated to about 0.8 flashes  $\text{km}^{-2} \text{ yr}^{-1}$  in the lowlands. In the SE (figs. 17 and 18), however, the initial band of lightning enhancements produced flash

densities of only about 0.5 flashes  $\text{km}^{-2} \text{ yr}^{-1}$ , and persisted over the ridges for only three hours. After the initial three hours, the enhancement strengthened to over 1.0, and persisted for nine hours at or near that strength, in the region 50 to 100 km away from the ridges. It was this increase in activity as the enhancements moved quickly away from the Blue Ridge Mountains that drove the eastern edge of the Appalachian Mountain lightning suppression pattern. The evolution of the lightning pattern in the Cumberland Plateau region was similar, except the initial flash density values in that area approached 0.8 flashes  $\text{km}^{-2} \text{ yr}^{-1}$ , resulting in a weaker pattern of suppression in that region.

The western edge of the Appalachian suppression developed because of a weak, but very consistent flash density gradient at the western edge of the Appalachians. Since it was shown that the precipitation maximum existed on the western edge of the Appalachians in the north, it was only the lightning that was suppressed in that region, not necessarily convection.

Analyzing the flash density data by seasons offered little more insight to the Appalachian suppression problem. Lightning activity was rare in both regions for all non-summer seasons, but was most sparse in the DJF season. During DJF, flash density patterns showed no preference for high or low terrain in either the SE or SW, likely because of the much weaker solar insolation on the eastward-facing slopes. In the SE, DJF maps revealed a banding effect, indicative of a few strong storms dominating the lightning patterns over the twelve-year period. This effect should fade as more many years of data are added to the analysis. During the spring and fall seasons, the Appalachian suppression was much less apparent. This suggests that the suppression cannot be attributed to weather

patterns typical of transition seasons, such as an increase of dynamically induced lift versus thermodynamic instability, or an increase in ridge top wind speeds.

#### *4.1.2. Upper Air Analysis*

Analysis of surface and upper air wind and potential temperature ( $\Theta_e$ ) characteristics provided additional insight into the causes of the Appalachian lightning suppression patterns. When the high elevation regions (in the SE) were active, the average winds at all three levels (surface, 850 mb, 500 mb) were all southwesterly; however, when the low elevation regions were active, the 500 mb average flow was easterly. For cases of active low elevation regions, a more complicated pattern resulting in easterly flow would be necessary. Also, when the AL region was active, the average upper winds were easterly for any combination with active or inactive BR or low terrain. When the BR region was active, the average surface wind was southwesterly for all combinations, thus promoting channeling and upslope flow. None of the above results were definitive in describing consistent meteorological patterns, which could be deemed responsible for lightning activity favoring one region over another. Furthermore, the standard deviations of the winds components were very high. A typical wind speed of 2 to 5  $ms^{-1}$  came with a standard deviation of 3 to 6. Because of the large variations, these patterns were not assumed to be indicative of any true synoptic situations.

The results of the potential temperature analysis showed that the region showing the strongest mountain lightning enhancement (SW) showed the weakest average vertical gradient of  $\Theta_e$ , (Table 3) while the region with a lightning suppression over the mountains (AL) displayed the strongest gradient. The weaker gradient in the SW represents a less

stable environment which could potentially support stronger updrafts and convection with greater vertical extent. These results would allow the initial updrafts to dominate longer, delaying the propagation of surface cold pools. Braham (1958) and Hales (1977) showed that about 90% of Arizona thunderstorms move less than 3 km during their lifetime. Watson et al. (1994) supported those findings by noting that CG lightning flashes sit over the higher topography for several hours before propagating towards lower terrain, and theorized that the propagation was due to interactions between cool downdrafts and warm, moist surface air. Applying this theory to the Appalachian Mountains requires the assumption that the SE region's summer thunderstorms advect at nearly the same rate as AZ thunderstorms. A summary of several case studies would be needed to verify this assumption, but because the diurnal evolution of the BR lightning pattern was so similar to that of AZ, that assumption is made for the purpose of this discussion. In SE, the increased stability would allow for weaker updrafts and thunderstorms of shorter duration. This shorter duration would hasten the propagation of thunderstorm, and therefore, lightning activity by allowing new convection to develop along the cold pools.

This hastened evolution would explain the shorter duration of the mountain-initiated lightning enhancements on the eastern slopes of the Blue Ridge Mountains. Once the thunderstorms move far enough away from the mountain (flash density data suggests that "far enough" is about 100 km), the cold pool is free to disperse in more directions, becomes shallower, and is less likely to initiate further convection. This would explain the paucity of CG lightning in the Piedmont region.

The horizontal temperature difference between mountain summits and the ambient environment at summit level gives an indication of the strength of the horizontal pressure

gradients that drive diurnal mountain breeze circulations. The results from comparing Mount Lemmon and Grandfather Mountain showed that in the SW, this horizontal temperature difference is typically much greater. The stronger mountain breeze that develops would enhance the leeside convergence mechanism, giving a greater chance for convective initiation. The factor most responsible for the annual average lightning pattern, however, appears to be the propagation characteristics of the convection, once initiated. The mountain breeze, which flows up the mountain, directly opposes the movement of the cold pool, which flows down the mountain. Therefore, a stronger mountain breeze would impede the motion of the cold pool, and thereby the propagation of convective activity. Combining the two theories above would explain the propagation properties of mountain-initiated lightning in the Southern Appalachians, and therefore the eastern edge of the lightning suppression pattern.

Figure 31 presents a conceptual model of effects the above theories. In that figure, the SW is depicted in the upper two rows, while the SE is represented by the two lower rows. Panels (a) demonstrate the state of convection during the period approximately 3-6 hours after convective initiation. The mountain breeze circulation is stronger for the SW than the SE. By panels (b), downdrafts from the mountain-initiated convection have created organized cold pools. In the SE, the cold pools have traveled further and have spawned new thunderstorms significantly further from than mountains than in the SW. By panels (c), the more quickly evolving storms of the SE are producing organized cold pools from the second-generation storms, while the second-generation storms in the SW are still inflow-dominated. Third-generation storms are possible in the SW by this time period. In panels (d) both regions are likely to contain third-generation storms; however, these storms

are most likely outflow-dominated. By panels (e), convection is weakening in both regions. The third-generation storms in both regions are located about 100 km away from the mountains.

Cold pools generated from these storms' outflow are no longer blocked by the mountains on one side, and are therefore free to travel in any direction. As a result, cold pools are shallower at this distance, and less likely to initiate new convection. Another factor that aids in the cessation of widespread convection by the 12-15 hour period is the weakened surface flow. Because convection vertically mixes the atmosphere, and cold pools disrupt the surface temperature fields, the diurnal circulation weakens over time. The weaker surface flow, in conjunction with the shallower cold pools, produces weaker convergence and a reduction of convective initiation.

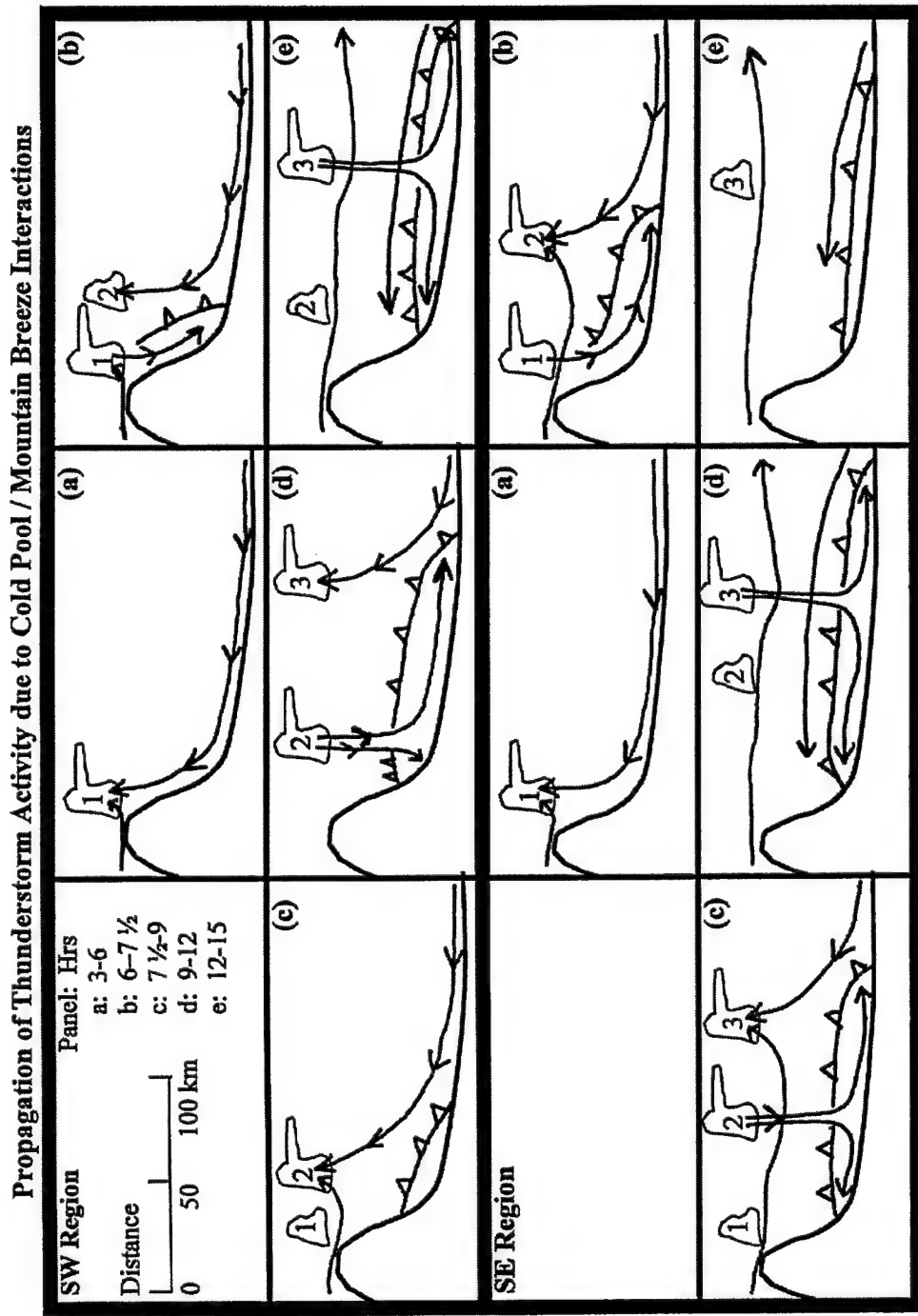


Figure 31. Propagation of Thunderstorm Activity due to Cold Pool / Mountain Breeze Interactions. Each panel represents a period of time as defined in figure keys (upper left panel). "Hrs" indicates the number of hours past convective initiation. Arrows indicate streamlines for mountain breezes and downdrafts; the number of arrowheads indicates relative intensity of flow. Numbers indicate storms initiated during the same time period. The cold front indicates the cold pool boundary.

#### 4.2. Conclusion

Despite the opposite appearance between annual flash density patterns of the Southern Rocky Mountains and the Southern Appalachian Mountains, the diurnal progression of lightning activity in the two regions are remarkably similar. The SW region exhibits late morning lightning initiation, followed by about six hours with very little movement and rapid intensification, then a steady progression of lightning activity towards lower terrain and a decrease in activity. On the eastern edge of the Appalachian chain are the Blue Ridge Mountains, which display the diurnal pattern most like the southern Rockies. In the Blue Ridge Mountains, the same late morning lightning initiation was noted, followed by only about three hours with very little movement and only moderate intensification. A period of continued intensification and rapid movement, followed by twelve hours of very little movement and a steady decrease in activity finished the evolution in the Blue Ridge. Evidence of a similar pattern was also seen over the Cumberland Plateau, where late morning convective initiation over the highlands was followed by a rapid propagation of lightning activity into the Tennessee River Valley. The distance to which mountain-initiated enhancements propagated away from their points of origin was about 50-100 km in both the Rocky and Blue Ridge Mountains.

The major differences between the patterns of the SW and SE were the persistent nocturnal activity in the northwest portions of the SE Region and the sea breeze activity along the SE coastline. Flash density values in the northwest portions of the SE remained consistently higher than  $0.1 \text{ flashes km}^{-2} \text{ yr}^{-1}$  and often greater than  $0.3 \text{ flashes km}^{-2} \text{ yr}^{-1}$ . In the SW region, only the extreme eastern portions of New Mexico experienced consistent nocturnal flash density values greater than  $0.1 \text{ flashes km}^{-2} \text{ yr}^{-1}$ . From the by-times

analysis, it was clear that the SW lightning pattern was driven by mountain-initiated convective activity, which remained stationary for about six hours, then diminished and moved towards lower terrain. The result was flash density enhancements over and near the mountain peaks and ridges. Also present were areas of broad, but weaker enhancements in the southern and eastern extremes, where moisture was more common.

The pattern in the SE resulted from two main factors. First, mountain-initiated lightning activity developed on the eastern slopes of the Blue Ridge Mountains from south of AVL, up to MRB. This activity propagated away from the mountains much more quickly than did similar activity in the SW. This rapid propagation caused the enhancements to reach peak intensity about 50 to 100 km east of the mountains that initiated them. The activity then stalled in that same location, resulting in an overall lightning enhancement that was broader than the SW enhancements, and displaced eastward from the mountain ridges. This enhancement, being east of the mountains, marked the eastern edge of the Appalachian Mountain lightning suppression. The second major factor that drove the overall SE pattern was the persistent nocturnal lightning activity in the northwestern portions of the SE region. This steady lightning enhancement maintained a weak, but consistent flash density gradient at the western edge of the mountains. Maintaining this weak, but constant pattern over the entire day produced a very strong flash density gradient on the overall annual flash density map. That strong gradient marked the abrupt western edge of the Appalachian lightning suppression.

Another apparent difference that stands out from the above discussion is the opposite river effects. In the SW, the major river valleys all displayed a sharp reduction in lightning flash densities, despite very close proximity to mountains. In contrast, the

Tennessee River Valley of the SE revealed a flash density enhancement. This contrasting effect appears to be a manifestation of the same propagation speed differences discussed above. In the SW, lightning activity remained close enough to their initiation points for a long enough period, that the cumulative effect masked the lightning activity that did reach the river valleys. In the SE, the lightning propagated into the Tennessee River Valley as it was still intensifying. This produced the apparently opposite patterns.

Another important observation was the strong relationship noted between elevation anomalies and flash density anomalies. This was shown to be a direct relationship in both the SW and the SE regions, thereby supporting the theory that convection in both regions is initiated by the same mechanism (leeside convergence).

Identifying the factors that led to the observed lightning pattern prompted the following two questions. What meteorological factors caused the more rapid propagation of the lightning enhancements in the SE? What meteorological theories could explain the consistent flash density gradient at the western edge of the Appalachian Mountains? Reviewing wind profiles for several combinations of highly active and inactive lightning days in the low and high terrain revealed very subtle difference between days for which very intense lightning activity and very weak lightning activity occurred over the Appalachian Mountains. These differences were statistically varied, and did not reveal any significant meteorological patterns. Also, it was noted during the by-season analysis that the lightning suppression was less evident in the transitional fall and spring seasons, when the ridge top winds were typically greater. This discounts the hypothesis that higher ridge top wind speeds in the SE inhibited the leeside convergence mechanism, thus suppressing convection. The above arguments support the reasoning that the lightning suppression

over the Appalachian Mountains was a result of the cumulative effect of subtle differences in the propagation of convective activity, not a lack of convective initiation. Therefore, answering the two questions stated above would be sufficient to describe the Appalachian lightning suppression.

The first question, "what meteorological factors caused the more rapid propagation of the lightning enhancements in the SE?" was answered by the differences in the thermodynamic profiles of the SE and SW regions. In the SE, a stronger vertical gradient of equivalent potential temperature would allow for weaker updrafts and faster evolution of individual thunderstorm cells. This process would result in faster propagation of new convective cells, as they develop along the gust fronts of old downdrafts. Furthermore, the enhanced mountain breeze in the SW provides stronger opposition to the progress of gust fronts, as they move down the mountain slopes. It has been shown in the SW that the propagation of the lightning pattern is due to new storm formation on the cold pool, rather than advection of old storms (Watson et al., 1994). By the very similar evolution of lightning patterns, it appears that the SE lightning pattern is also a result of new storms propagating along outflow boundaries; only in the SE, these boundaries propagate more quickly.

The second question, "what meteorological theories could explain the consistent flash density gradient at the western edge of the Appalachian Mountains?" was not completely answered, but two theories were put forth to provide insight, and set up future studies which could potentially solve the problem. Since precipitation was not over the western edge of the Appalachians, the lightning suppression must be caused by a lack of electric potential over the region, not necessarily a lack of convection. This study put forth

two hypotheses for describing this lack of electric potential. The first hypothesis was that the increased peak currents just west of the suppression area drained the environment of its electric potential to the point that even a steady charge separation rate would require time to re-charge the environment enough to support large-scale lightning activity downstream. The second hypothesis was that the south to southwesterly surface flow that was shown to be dominant during active lightning episodes in the low elevations would be descending from the mountains, and thus moisture-starved. This drier inflow would tend to weaken the updrafts, and therefore the charge separation process. Both hypotheses would require field studies for a complete answer.

This study has identified the lightning characteristics of both the Southern Rocky Mountains and the Southern Appalachian Mountains, and verified at a resolution of 5 km, the observations of Reap (1986) and Huffines and Orville, (1999). It has also described, in detail, the diurnal evolution of the annual lightning patterns, and documented the lightning suppression pattern over the Appalachian Mountains. Although several hypotheses are presented here, case studies must be performed, which would involve detailed observations of wind and potential temperature profiles and electric field properties, before a definitive theory can be made.

## REFERENCES

Banta, R. M., 1984: Daytime boundary-layer evolution over mountainous terrain. Part I: Observations of the dry circulations. *Mon. Wea. Rev.*, **112**, 340-356.

\_\_\_\_\_, 1986: Daytime boundary-layer evolution over mountainous terrain. Part II: Numerical studies of upslope flow duration. *Mon. Wea. Rev.*, **114**, 1112-1130.

\_\_\_\_\_, and C. B. Schaaf, 1987: Thunderstorm genesis zones in the Colorado Rocky Mountains as determined by traceback of geosynchronous satellite images. *Mon. Wea. Rev.*, **115**, 463-476.

Benjamin, T. B., 1968: Gravity currents and related phenomena. *J. Fluid Mech.*, **31**, 209-248.

Braham, R. R., Jr., 1958: Cumulus cloud precipitation as revealed by radar-Arizona 1955. *J. Atmos. Sci.*, **15**, 75-83.

Cummins, K. L., R. O. Burnett, W. L. Hiscox, and A. E. Pifer, 1993: Line reliability and fault analysis using the National Lightning Detection Network, paper presented at the Precise Measurements in Power Conference, National Science Foundation and Center for Power Engineering at Virginia Tech., Arlington, Va.

\_\_\_\_\_, E. A. Bardo, W. L. Hiscox, R. B. Pyle, and A. E. Pifer, 1995: NLDN '95: A combined TOA/MDF technology upgrade of the U. S. National Lightning Detection Network, paper presented at the International Aerospace and Ground Conference on Lightning and Static Electricity, Natl. Interagency Coord. Group, Williamsburg, Va.

\_\_\_\_\_, M. J. Murphy, E. A. Bardo, W. L. Hiscox, R. B. Pyle, and A. E. Pifer, 1998: A combined TOA/MDF technology upgrade of the U.S. national lightning detection network. *J. Geophys. Res.*, **103**, 9035-9044.

\_\_\_\_\_, R. B. Pyle, and G. Fournier, 1999: An integrated North American lightning detection network, paper presented at the 11<sup>th</sup> International Conference on Atmospheric Electricity, Guntersville, Al. 218-225.

Droegemeier, K. K., and R. B. Wilhelmson, 1987: Numerical Simulation of thunderstorm outflow dynamics. Part I: Outflow sensitivity experiments and turbulence dynamics. *J. Atmos. Sci.*, **44**, 1180-1210.

Hales, J. E., Jr., 1977: On the relationship of convective cooling to nocturnal thunderstorms at Phoenix. *Mon. Wea. Rev.*, **105**, 1609-1613.

Huffines, G. R., and R. E. Orville, 1999: Lightning ground flash density and thunderstorm duration in the continental United States: 1989-96. *J. Appl. Meteor.*, **38**, 1013-1019.

Klitch, M. A., J. F. Weaver, F. P. Kelly, and T. H. Voder Haar, 1985: Convective cloud climatologies constructed from satellite imagery. *Mon. Wea. Rev.*, **113**, 326-337.

Krehbiel, P.R., 1986: The electrification of storms, in *The Earth's Electrical Environment*. E. P. Krider and R. G. Roble, eds., Natl. Acad. Press, Washington, D.C., 90-113..

Krider, E. P., R. C. Noggle, A. E. Pifer and D. L. Vance, 1980: Lightning direction finding systems for forest fire detection. *Bull. Amer. Meteorol. Soc.* **61**, 980-986.

\_\_\_\_\_, 1996: 75 years of research on the physics of a lightning discharge, in *Historical Essays on Meteorology*. J. R. Fleming, ed., Am. Meteorol. Soc., Boston, Ma. 321-350.

Linder, W., W. Schmid, H. H. Schiesser, 1999: Surface winds and development of thunderstorms along southwest-northeast oriented mountain chains. *Weather and Forecasting*, **14**, 758-770.

Lopez, R. E., and R. L. Holle, 1986: Diurnal and spatial variability of lightning activity in northeastern Colorado during the summer. *Mon. Wea. Rev.*, **114**, 1288-1312.

O'Handley, C., and L. F. Bosart, 1996: The impact of the Appalachian Mountains on cyclonic weather systems. Part I: A climatology. *Mon. Wea. Rev.*, **124**, 1353-1372.

Orville, R. E., R. W. Henderson, and L. F. Bosart, 1983: An East Coast lightning detection network, *Bull. Am. Meteorol. Soc.*, **64**, 1029-1037.

\_\_\_\_\_, and G. R. Huffines, 1999: Annual summary: Lightning ground flash measurements over the contiguous United States: 1995-97. *Mon. Wea. Rev.*, **127**, 2693-2703.

\_\_\_\_\_, G. R. Huffines, J. Nielsen-Gammon, R. Zhang, B. Ely, S. Steiger, S. Phillips, S. Allen, and W. Read: 2001. Enhancement of cloud-to-ground lightning over Houston, Texas, *Geophys. Res. Lett.*, **28**, 2597-2600.

\_\_\_\_\_, and G. R. Huffines, 2001: Cloud-to-ground lightning in the United States: NLDN results in the first decade, 1989-1998. *Mon. Wea. Rev.*, **129**, 1179-1193.

Reap, R. M., 1986: Evaluation of cloud-to-ground lightning data from the Western United States for the 1983-84 summer seasons. *J. Clim. and Appl. Meteor.*, **25**, 785-799.

Schaaf, C. B., J. Wurman, and R. M. Banta, 1988: Thunderstorm-producing terrain features. *Bull. Amer. Meteorol. Soc.*, **69**, 272-277.

Uman, M. A., 1987: *The Lightning Discharge*, Academic Press, Orlando, Fl.

Wacker, R. S., and R. E. Orville, 1999a: Changes in measured lightning flash count and return stroke peak current after the 1994 U. S. National Lightning Detection Network upgrade: 1. Observations. *J. Geophys. Res.*, **104**, 2151-2157.

\_\_\_\_\_, and R. E. Orville, 1999b: Changes in measured lightning flash count and return stroke peak current after the 1994 U. S. National Lightning Detection Network upgrade: 2. Theory. *J. Geophys. Res.*, **104**, 2159-2162.

Watson, A. I., R. E. Lopez, R. L. Holle, 1994: Diurnal cloud-to-ground lightning patterns in Arizona during the southwest monsoon. *Mon. Wea. Rev.*, **122**, 1716-1725.

\_\_\_\_\_, R. L. Holle, and R. E. López, 1994: Cloud-to-ground lightning and upper-air patterns during bursts and breaks in the southwest monsoon. *Mon. Wea. Rev.*, **122**, 1726-1739.

Weaver, J. F., and F. P. Kelly, 1982: A mesoscale, climatologically-based forecast technique for Colorado. *Preprints, Ninth Conf. on Weather Forecasting and Analysis*, Seattle, Wa. Amer. Meteor. Soc., 277-280.

Williams, E. R., 1989: The tripole structure of thunderstorm. *J. Geophys. Res.*, **94**, 13 151-13 167.

## APPENDIX

The following pages are a collection of many of the computer programs required to perform the data analysis for this study. These programs are all written in the Interactive Data Language (IDL). While attending Texas A&M University, Major Gary Huffines, PhD. (now affiliated with Air Force Institute of Technology, Wright-Patterson Air Force Base, OH), created the programs that analyzed the NLDN data. Other programs were written by Brandon Ely and Captain Stephen Phillips, both of Texas A&M University. Each program in this section states the programmer's name and the purpose of the program. A list of these programs follows.

PROGRAM	Page
any_anal_years .....	89
ams_conf_gif .....	100
daily_summary .....	105
box_maker .....	109
elev_anal .....	112
t_test.....	118
search_days.....	120
thetae_anal .....	123
ua_anal .....	132

```

pro any_anal_years, dates, region, outpath = outpath, res = res, $
  suffix = suffix, curr_res = curr_res, time_res = time_res, $
  times = times, months = months

; Performs the analysis of CG lightning data for any time of day
; and any region. Saves the gridded values for these conditions to the
; outpath provided. If resolution (res) is not provided, then a
; resolution of 0.2 degrees is selected. The time resolution (time_res),
; in minutes, allows for
; the calculation of the time of day with the maximum flashes. The
; keyword times refers to an array of times during the day (UTC) for
; which the data will be used in the analysis. The months keyword allows
; the user to select months of the year to perform analysis upon.
;
; Output included the following:
;
; flash density: dens?????.txt
; positive flash density: pos_?????.txt
; percent positive flashes: ppos?????.txt
; flash counts (all): cnt_?????.txt
; positive flash counts: pcnt?????.txt
; mean negative multiplicity: nmul?????.txt
; mean positive multiplicity: pmul?????.txt
; median negative peak currents: nmed?????.txt
; median positive peak currents: npos?????.txt
; all CG flashes maximum time: tall?????.txt
; positive flashes maximum time: tpos?????.txt
; negative flashes maximum time: tneg?????.txt
;
; Here, the ???? indicates the suffix provided by the user. If no
; suffix is provided, then today's date (MMDD) is used. This avoids
; overwriting files by using a default filename. If the outpath is
; not provided, then the current working directory is used. The suffix
; can be longer than 4 characters, if desired.
;
; Dates includes the time as well. An example follows in the sample
; run command. The region has the format of [minlat, maxlat, minlon,
; maxlon]. All longitudes are negative values.
;
; The median peak currents are determined to a resolution of curr_res.
; This value defaults to 0.1 kA unless provided.
;
; Output from the file is as follows in ASCII files.
; region
; # of latitude elements, # of longitude elements, resolution, # of
; flashes used
; results in default IDL output (row ordered array)
;
; Note: All positive flashes less than 10 kA are ignored in the
; calculations. This is based on Cummins et al. 1998 recommendation on
; the
; NLDN upgrade.
;
; Sample run command:
; any_anal, ['01/25/95 02:13:00', '02/03/98 03:00:00'], $
;   region = [25.0, 50.0, -125.0, -67.0], outpath = '\lightning_study\' ,
$
```

```

;      res = 0.05, suffix = 'leaps', time_res = 15, $
;      times = [3,4,5,6,7,20,21,22,23], months = ['apr','may','jun']
;
; Steiger sample:
; any_anal_years, ['01/01/89 00:00:00', '12/31/00 23:59:59'],
region=[25.0, 35.0, -100.0, -90.0], res=0.05, suffix='sum2', time_res=15,
times=[0, 1, 2, 3, 4, 5, 6, 7, 8, 9, 10, 11, 12, 13, 14],
months=['jun','jul','aug']
; or any_anal_years, ['01/01/89 00:00:00', '12/31/00 23:59:59'],
region=[29.8, 30.3, -95.5, -95.0], res=0.05, suffix='allboxb0221',
time_res=15
; Programmer: Gary Huffines
; Last Update: 30 August 2000
;any_anal_years, ['01/01/89 00:00:00', '12/31/00 23:59:59'],
region=[25.00, 50.00, -135.00, -67.00], res=0.05, suffix='01',
time_res=15, times=[0, 1]
;any_anal_years2, ['01/01/89 00:00:00', '12/31/00 23:59:59'],
region=[30.2, 30.9, -94.65, -93.8], res=0.05, suffix='allboxc0409',
time_res=15

; Last update: 26 April 2001 (Gary Huffines)
; Modified code to round off numbers in determining array sizes in case
of
; region that is not a multiple of the resolution.
; Also fixed problem with status printout when only one flash is present

; start the timer
time = systime(1)

; set up some default values
if (!d.name EQ 'WIN') then $ ; PC version
  data_path = 'D:\lightning_data\' $
else $ ; Unix version
  data_path = '/stroke1/' ; parent directory for lgh directories
if (n_elements(months) EQ 0) then $
  months = ['jan','feb','mar','apr','may','jun','jul','$'
            'aug','sep','oct','nov','dec']
nmonths = n_elements(months)
month_names = ['jan','feb','mar','apr','may','jun','jul','$'
               'aug','sep','oct','nov','dec']

; determine the cutoff for positive flashes, if any
cutoff = 10.0

; set up the maximum number of flashes per pass
nf = 50000L

; determine if the region is provided
if (n_elements(region) EQ 0) then region = [18.0, 55.0, -135.0, -58.0]

; determine if the outpath is provided
if (n_elements(outpath) EQ 0) then outpath = 'C:\My
Documents\bely\text\'

; determine if resolution is provided
if (n_elements(res) EQ 0) then res = 0.2

```

```

; determine if the current resolution is provided
if (n_elements(curr_res) EQ 0) then curr_res = 0.1

; determine if the time resolution is provided
if (n_elements(time_res) EQ 0) then time_res = 60.0 ; minutes

; determine if the suffix is provided
if (n_elements(suffix) EQ 0) then begin
  d = systime()
  mon = strlcase(strmid(d, 4, 3))
  day = strmid(d, 8, 2)
  suffix = mon+day
endif

; determine if the time of day is provided
if (n_elements(times) EQ 0) then $ ; default to all
  times = indgen(24)
n_times = n_elements(times)

; set up an array of strings for 2 digit numbers
num = strcompress(sindgen(100), /remove_all)
num[0:9] = '0'+num[0:9]

; check the region for correct order of values
lon = where(abs(region) GT 57.0, count)
if (count EQ 0) then return ; invalid region
lat = where(abs(region) LE 57.0, count)
if (count EQ 0) then return ; invalid region
region = [min(region[lat]), max(region[lat]), min(-
1.0*abs(region[lon])), $
  max(-1.0*abs(region[lon]))]

; determine the size of the arrays needed and set them up
nx = long(round((region(3)-region(2))/res))
ny = long(round((region(1)-region(0))/res))
nmed = fltarr(nx,ny) ; median peak negative current
pmed = fltarr(nx,ny) ; median peak positive current
cnt = fltarr(nx,ny) ; all flash counts
pcnt = fltarr(nx,ny) ; positive flash counts
nmul = fltarr(nx,ny) ; negative multiplicity
pmul = fltarr(nx,ny) ; positive multiplicity
time_all = fltarr(nx,ny) ; time of max flashes
time_pos = fltarr(nx,ny) ; time of max positive flashes
time_neg = fltarr(nx,ny) ; time of max negative flashes

; the array for the "cumulative histograms" for the small region
nbins = long(200.0/curr_res)+1L ; peak current bins
nt_bins = long(24.0 * 60.0 / time_res) ; number of time bins
ngrids = double(nx)*double(ny)*double(nbins) ; total size if all used
nsections = ceil(ngrids / 5.0E7) ; number of sections needed to make it
run
  nx_section = ceil(float(nx) / float(nsections)) ; size of longitude
  section

; set up starting longitude bins for each section
xstart = indgen(nsections)*nx_section
nx_section = replicate(nx_section, nsections)

```

```

if (nsections GT 1) then begin $ ; allow for portion of a section
  xstart[nsections-1] = nx - nx_section[nsections-1] - 1
  nx_section[nsections-2] = xstart[nsections-1]-xstart[nsections-2]
endif

nn = 0L ; number of negative flashes
np = 0L ; number of positive flashes
tt = 0L ; total number of flashes
cneg = nbins/2-1-indgen(nbins/2) ; indicates the negative current bins
cpos = indgen(nbins/2)+nbins/2 ; indicates the positive bins

; determine the data files available on the computer (if all under
data_path)
  filepaths = findfile(data_path+'lgh????', count = nyears) ; list of
paths
  okay = where(strlen(filepaths) EQ strlen(data_path)+8, nyears)
  if (nyears EQ 0) then begin
    print, 'No files found'
    return
  endif
  filepaths = filepaths(okay)
  if (!d.name NE 'WIN') then $ ; unix version
    filepaths = strmid(filepaths, 0, strlen(data_path)+7) + '/' $
  else $ ; PC version
    filepaths = strmid(filepaths, 0, strlen(data_path)+7) + '\'
  filepaths = filepaths(sort(filepaths)) ; sort by year
  years_full = strmid(filepaths, strlen(filepaths[0])-5, 4) ; 4 digit
year
  years = strmid(years_full,2,2) ; 2 digit year
  keep = where(fix(years_full) GE 1989, nyears) ; only keep those after
1989
  filepaths = filepaths(keep) ; limit filepaths
  years_full = years_full(keep) ; limit the 4 digit years to after 1989
  years = years(keep) ; limit 2 digit years to after 1989
  files = strarr(nyears*nmonths) ; set up an array to hold the files
  for y = 0, nyears-1 do $
    for m = 0, nmonths-1 do $
      files(y*nmonths+m) =
  filepaths[y]+strlowlcase(months(m))+years(y)+'.lgh'
  ; check to see if the files are there
  okay = intarr(n_elements(files)) ; check to be sure there are no
missing files
  for i = 0, n_elements(files)-1 do begin
    temp = findfile(files(i), count = c)
    okay[i]=c
  endfor
  keep = where(okay EQ 1, nfiles) ; only keep the list of files that are
there
  files = files(keep) ; limit the files to those there

; find the actual first and last flash in the times provided (for dens
calculations)
  given_years = fix(strmid(dates,6,2))
  given_years = given_years + 100*(given_years LT 89)
  given_months = fix(strmid(dates,3,2))
  nyears = given_years[1] - given_years[0] + (given_months[1] GT
given_months[0])

```

```

; find the locations of the first and last flash in the files
findtime, dates, startind, startpos, lastind, lastpos, files, 11L

; reformat the variables (except current) to make this run faster
cnt = reform(cnt, nx*ny)
pcnt = reform(pcnt, nx*ny)
pmul = reform(pmul, nx*ny)
nmul = reform(nmul, nx*ny)

; start pass through each section
for sect = 0, nsections-1 do begin
    curr = lonarr(nx_section[sect], ny, nbins) ; peak current counts for
each section
    t_all = lonarr(nx_section[sect], ny, nt_bins); time counts for each
section (all)
    t_pos = t_all ; time counts for each section (positive)
    t_neg = t_all ; time counts for each section (negative)
    ; define region for this pass
    subregion = [region[0], region[1], region[2]+xstart[sect]*res, $
                 region[2]+(xstart[sect]+nx_section[sect])*res]
    ; zero out the peak current histogram for each section
    curr = curr*0L
    ; zero out the time arrays for each section
    t_all = t_all * 0L
    t_pos = t_pos * 0L
    t_neg = t_neg * 0L

    ; reformat the arrays to make the calculations faster
    curr = reform(curr, long(nx_section[sect])*long(ny)*long(nbins))
    t_all = reform(t_all, long(nx_section[sect])*long(ny)*long(nt_bins))
    t_pos = reform(t_pos, long(nx_section[sect])*long(ny)*long(nt_bins))
    t_neg = reform(t_neg, long(nx_section[sect])*long(ny)*long(nt_bins))

    ; set up the current (this pass) indices in the data files
    currpos = startpos
    currind = startind
    ; determine if the data is done
    done = (currpos EQ lastpos) AND (currind EQ lastind)
    ; pass through data until done
    while not(done) do begin
        ; get the data for this pass in this section
        f = getchunk(files, startind, startpos, lastind, lastpos,
subregion, $
                     currind, currpos, 11L, nf)
        ; check to see if any data was returned
        if (n_elements(f) GE 11) then begin ; any flashes returned
            ; convert flash data to structures
            f = exp_lgh(f)
            ; find flashes with hours equal to one of the times
            keep = -1L
            for i = 0, n_times-1 do $
                keep = [keep, where(f.hour EQ times[i])]
            okay = where(keep GE 0L, count)
            if (count GT 0) then begin
                keep = keep[okay]
                keep = keep[sort(keep)]

```

```

f = f[keep]
keep = 0B
okay = 0B
; find flashes with peak current magnitude GT cutoff
above = where((f.peak LT 0.0) OR (f.peak GE cutoff), count)
if (count GT 1) then begin ; necessary for histogram
  f = f(above)
  ; find the positive flashes
  pos = where(f.peak GE 0.0, pcount)
  ; find the negative flashes
  neg = where(f.peak LT 0.0, ncount)
  ; increment the flash counts
  np = np + pcount
  nn = nn + ncount
  tt = tt + count ; increment flash counter
  ; limit the peak current to within -100 and 100 kA fo median
calculations
  f.peak = (f.peak > (-100.0))
  f.peak = (f.peak < 100.0)
  ; find the peak current indices for the histogram
  pind = long((f.lon - subregion[2])/res) + $
    long((f.lat - subregion[0])/res)*nx_section[sect] + $
    ((long(floor(f.peak + nbins/2*curr_res)/curr_res) <
  (nbins-1)) > 0)*$
    nx_section[sect]*ny
  ; calculate the peak currents
  curr = histogram(pind, min=0L,
max=nx_section[sect]*ny*nbins-1, binsize=1, $
  input = curr)
  ; find the time indices for the histogram
  pind = long((f.lon - subregion[2])/res) + $
    long((f.lat - subregion[0])/res)*nx_section[sect] + $
    long(floor((float(f.hour)*60.0+float(f.minute))/time_res))*$
    nx_section[sect]*ny
  ; calculate the number of all flashes in each time bin
  t_all = histogram(pind, min=0L,
max=nx_section[sect]*ny*nt_bins-1, binsize=1, $
  input = t_all)
  ; calculate the number of all flashes in each time bin
  if (pcount GT 1) then $
    t_pos = histogram(pind[pos], min=0L,
max=nx_section[sect]*ny*nt_bins-1, binsize=1, $
  input = t_pos)
  ; calculate the number of all flashes in each time bin
  if (ncount GT 1) then $
    t_neg = histogram(pind[neg], min=0L,
max=nx_section[sect]*ny*nt_bins-1, binsize=1, $
  input = t_neg)

  ; find the counting indices for each flash
  pind = long((f.lon - region[2])/res) + $
    long((f.lat - region[0])/res)*nx
  ; count the number of flashes
  cnt = histogram(pind, min = 0, max = nx*ny-1, binsize = 1,
input = cnt)
  ; count the positive flashes

```

```

        if (pcount GT 1) then $
            pcnt = histogram(pind[pos], min = 0, max = nx*ny-1,
binsize = 1, $
                input = pcnt)
            ; find the total multiplicities for positive flashes
            for i = 0L, pcount-1 do $
                pmul(pind(pos(i))) = pmul(pind(pos(i))) + f(pos(i)).mult
            ; find the total multiplicities for negative flashes
            for i = 0L, ncount-1 do $
                nmul(pind(neg(i))) = nmul(pind(neg(i))) + f(neg(i)).mult

            endif ; more than 1 flash for histograms
            endif ; flashes matching time constraints
            print, 'Just finished flashes from ', num[f[0].day], ' ',
strupcase(month_names[f[0].month-1]), $
            strcompress(string(f[0].year)), ' to ', num[f[count-1>0].day], ' ',
$                strupcase(month_names[f[count-1>0].month-1]),
            strcompress(string(f[count-1>0].year)), $
                ' (section ', strcompress(string(sect+1)), ' of ',
            strcompress(string(nsections)), ')'
            endif ; any flashes at all
            ; check to see if done
            done = (currind EQ lastind) AND (currpos EQ lastpos)
        endwhile

        ; print a spacer for the status reports
        print, ' '

        ; calculate the median from the histogram
        ; pass through the grid for positive and negative values
        nprint = fix(ny/30) ; intervals to print status report
        cum = lonarr(nbins/2)

        ; reset the peak current array to allow the median calculations
        curr = reform(curr, nx_section[sect], ny, nbins)

        ; reset the time arrays to find the max time
        t_all = reform(t_all, nx_section[sect], ny, nt_bins)
        t_pos = reform(t_pos, nx_section[sect], ny, nt_bins)
        t_neg = reform(t_neg, nx_section[sect], ny, nt_bins)

        ; find the median peak current in each bin
        for y = 0, ny-1 do begin ; each latitude band
            for x = 0, nx_section[sect]-1 do begin ; each longitude increment
                ; check for sufficient flashes (need at least 3)
                ptot = total(curr(x, y, cpos))
                ntot = total(curr(x, y, cneg))
                if (ptot GE 2L) then begin ; find median positive value
                    cum[0] = curr[x, y, cpos[0]]
                    for i = 1, nbins/2-1 do $
                        cum[i] = cum[i-1] + curr[x, y, cpos[i]]
                    pmed(xstart[sect]+x, y) = float(min(where(cum GT
ptot/2))*curr_res
                endif else pmed(xstart[sect]+x, y) = 0.0
                if (ntot GE 2L) then begin ; find median negative value
                    cum[0] = curr[x, y, cneg[0]]

```

```

        for i = 1, nbins/2-1 do $
            cum[i] = cum[i-1] + curr[x, y, cneg[i]]
            nmed(xstart[sect]+x, y) = -1.0*float(min(where(cum GT
ntot/2)))*curr_res
        endif else nmed(xstart[sect]+x, y) = 0.0
    endfor ; longitude

    ; print a status report
    if (((y+1) mod nprint) EQ 0) then $
        print, 'Finished median peak currents for ',
        strcompress(string(y+1)), ' of ', $
            strcompress(string(ny)), ' latitudes (section ',
        strcompress(string(sect+1)), '$
            ' of ', strcompress(string(nsections)), ')'
    endfor ; latitude
    print, ' '

    ; print a status report for the time variables
    print, 'Finding the times of the maximum flash count for section ', $
        strcompress(string(sect+1)), ' of ',
        strcompress(string(nsections))
    print, ' '

    ; find the time bin with the maximum flashes in each bin
    for y = 0, ny-1 do begin ; each latitude band
        for x = 0, nx_section[sect]-1 do begin ; each longitude increment
            ; find the maximum for each type of array
            time_all[xstart[sect]+x,y] = min(where(t_all[x,y,*] EQ
max(t_all[x,y,*])))*(time_res/60.0)
            time_pos[xstart[sect]+x,y] = min(where(t_pos[x,y,*] EQ
max(t_pos[x,y,*])))*(time_res/60.0)
            time_neg[xstart[sect]+x,y] = min(where(t_neg[x,y,*] EQ
max(t_neg[x,y,*])))*(time_res/60.0)
        endfor ; longitude
    endfor ; latitude

    endfor ; sections

    ; reformat the count and multiplicity variables
    cnt = float(reform(cnt, nx, ny))
    pcnt = float(reform(pcnt, nx, ny))
    pmul = float(reform(pmul, nx, ny))
    nmul = float(reform(nmul, nx, ny))

    ; calculate the mean positive multiplicity
    non_zero = where(pcnt GT 0, count)
    if (count GT 0) then $
        pmul(non_zero) = pmul(non_zero) / pcnt(non_zero)

    ; calculate the mean negative multiplicity
    non_zero = where((cnt - pcnt) GT 0, count)
    if (count GT 0) then $
        nmul(non_zero) = nmul(non_zero) / (cnt(non_zero) - pcnt(non_zero))

    ; calculate the percentage of positive flashes
    ppos = fltarr(nx, ny)
    non_zero = where(cnt GT 0, count)

```

```

if (count GT 0) then $
  ppos(non_zero) = 100.0 * pcnt(non_zero) / cnt(non_zero)

; find the area of each grid element based on latitude
lat = findgen(ny)*res+region(0)
b1 = 6370.0*cos(lat*!dtor)*(res*!dtor)
b2 = 6370.0*cos((lat+res)*!dtor)*(res*!dtor)
h = 6370.0*(res*!dtor)
area = h*(b1+b2)/2.0

; find the flash densities
dens = fltarr(nx, ny)
pdens = fltarr(nx, ny)
for y = 0, ny-1 do begin
  dens(*,y) = cnt(*,y) / area(y)
  pdens(*,y) = pcnt(*,y) / area(y)
endfor

; convert the time to local time for the maximum flashes
lon = findgen(nx)*res+region[2]+res/2.0
offset = lon*24.0/360.0
for x = 0, nx-1 do begin
  time_all[x,*] = (time_all[x,*]+offset[x]+24.0) mod 24.0
  time_pos[x,*] = (time_pos[x,*]+offset[x]+24.0) mod 24.0
  time_neg[x,*] = (time_neg[x,*]+offset[x]+24.0) mod 24.0
endfor

; set the times where there were no flashes to -99.9
zero = where(cnt EQ 0, count)
if (count GT 0) then time_all[zero] = -99.0
zero = where(pcnt EQ 0, count)
if(count GT 0) then time_pos[zero] = -99.0
zero = where((cnt-pcnt) EQ 0, count)
if (count GT 0) then time_neg[zero] = -99.0

; save the flash counts
openw, 2, outpath+'cnt_'+suffix+'.txt'
printf, 2, region
printf, 2, ny, nx, res, tt
printf, 2, cnt / nyyears
close, 2

; save the positive flash counts
openw, 2, outpath+'pcnt'+suffix+'.txt'
printf, 2, region
printf, 2, ny, nx, res, np
printf, 2, pcnt / nyyears
close, 2

; save the flash density
openw, 2, outpath+'dens'+suffix+'.txt'
printf, 2, region
printf, 2, ny, nx, res, tt
printf, 2, dens / float(nyears)
close, 2

; save the positive flash density

```

```
openw, 2, outpath+'pos_'+suffix+'.txt'
printf, 2, region
printf, 2, ny, nx, res, np
printf, 2, pdens / float(nyears)
close, 2

; save the percentage of positive flashes
openw, 2, outpath+'ppos'+suffix+'.txt'
printf, 2, region
printf, 2, ny, nx, res, tt
printf, 2, ppos
close, 2

; save the mean negative multiplicity
openw, 2, outpath+'nmul'+suffix+'.txt'
printf, 2, region
printf, 2, ny, nx, res, nn
printf, 2, nmul
close, 2

; save the mean positive multiplicity
openw, 2, outpath+'pmul'+suffix+'.txt'
printf, 2, region
printf, 2, ny, nx, res, np
printf, 2, pmul
close, 2

; save the median negative peak current
openw, 2, outpath+'nmed'+suffix+'.txt'
printf, 2, region
printf, 2, ny, nx, res, nn
printf, 2, nmed
close, 2

; save the positive median peak current
openw, 2, outpath+'pmed'+suffix+'.txt'
printf, 2, region
printf, 2, ny, nx, res, np
printf, 2, pmed
close, 2

; save the time of max flash counts (all)
openw, 2, outpath+'tall'+suffix+'.txt'
printf, 2, region
printf, 2, ny, nx, res, tt
printf, 2, time_all
close, 2

; save the time of max flash counts (positive)
openw, 2, outpath+'tpos'+suffix+'.txt'
printf, 2, region
printf, 2, ny, nx, res, np
printf, 2, time_pos
close, 2

; save the time of max flash counts (negative)
openw, 2, outpath+'tneg'+suffix+'.txt'
```

```
printf, 2, region
printf, 2, ny, nx, res, nn
printf, 2, time_neg
close, 2

; end the timer and print elapsed run time
time = systime(1) - time
num = strcompress(sindgen(100), /remove_all)
num(0:9) = '0'+num(0:9)
hr = fix(time/3600.0)
time = time - hr * 3600.0
minut = fix(time / 60.0)
time = fix(time - minut * 60.0)
print, 'Congratulations! The program finished without a problem!
print, ' '
print, 'Required run time was '+num(hr)+':'+num(minut)+':'+num(time)

end
```

```
pro ams_conf_gif, dens = dens, positive = positive, ppos = all_ppos, $  
    pmed = pmed, nmed = nmed, pmult = all_pmul, nmult = all_nmul, $  
    post = post  
  
cty='TSSN Event'  
dens='dens'  
;positive='pos_'  
;ppos='ppos'  
;nmult='nmul'  
;pmult='pmul'  
;nmed='nmed'  
;pmed='pmed'  
  
; Plots ten years worth of data on one sheet using data  
; from files found in inpath. The keywords determine the  
; type of data to be plotted and post is the filename of  
; the postscript image, if that is desired. Assumes the  
; colors have already been determined.  
  
; Programmer: Gary Huffines  
; Last Update: 6 Jan 99  
; Modified by: Brandon Ely 08/18/2000  
  
!p.color = 256  
device, decomposed = 0  
tvlct, 255, 255, 255, 0  
tvlct, 0, 0, 0, 1  
tvlct, 255, 0, 255, 2  
tvlct, 186, 55, 211, 3  
tvlct, 66, 134, 255, 4  
tvlct, 0, 255, 255, 5  
tvlct, 0, 15, 255, 6  
tvlct, 204, 255, 51, 7  
tvlct, 0, 255, 0, 8  
tvlct, 0, 187, 0, 9  
tvlct, 255, 255, 0, 10  
tvlct, 255, 120, 0, 11  
tvlct, 204, 83, 0, 12  
tvlct, 132, 0, 0, 13  
tvlct, 255, 0, 0, 14  
tvlct, 210, 210, 210, 15  
tvlct, 190, 190, 190, 16  
tvlct, 160, 160, 160, 17  
tvlct, 135, 135, 135, 18  
tvlct, 110, 110, 110, 19  
;tvlct, 255, 0, 0, 1  
;tvlct, 255, 255, 0, 2  
;tvlct, 255, 180, 0, 3  
;tvlct, 0, 0, 170, 4  
;tvlct, 0, 138, 0, 5  
;tvlct, 0, 255, 0, 6  
;tvlct, 0, 255, 162, 7  
;tvlct, 0, 255, 255, 8  
;tvlct, 0, 138, 255, 9  
;tvlct, 0, 0, 255, 10  
;tvlct, 138, 0, 138, 11  
;tvlct, 210, 0, 255, 12
```

```

;tvlct, 255, 0, 120, 13
;tvlct, 205, 205, 205, 14
;tvlct, 156, 156, 156, 15
;tvlct, 105, 105, 105, 16
;tvlct, 55, 55, 55, 17
;tvlct, 0, 0, 0, 18
;tvlct, 255, 255, 255, 19
tvlct, r, g, b, /get
;end

; set file information
;inpath = 'd:\lightning text files\5k_res\' 
;outpath = 'c:\My Documents\sphill\maps\' 
inpath = 'c:\My Documents\Stuart\' 
outpath = 'c:\My Documents\Stuart\' 

; determine type of plot
case 1 of
  (n_elements(dens) GT 0): begin ; flash density
    type = 'dens'
    lev = [0,.001,.002,.003,.004,.005,.006]
    slev =
    ['0','.001','.002','.003','.004','.005','.006 >']
    col = [15, 4, 6, 9, 10, 11, 14]
    ;col = [15, 3, 4, 6, 9, 10, 11, 14]
    title = 'Mean Annual Flash Density (Flashes
km!u-2!n yr!u-1!n)'
    ;title = 'Flash Density (Flashes km!u-2!n
yr!u-1!n)'
    end
  (n_elements(positive) GT 0): begin ; positive flash density
    type = 'pos_'
    lev = [0,0.01,0.03,0.06,0.1,0.15,0.3]
    slev =
    ['0','0.01','0.03','0.06','0.1','0.15','0.3 >']
    col = [15, 4, 6, 9, 10, 11, 14]
    title = 'Mean Annual Positive Flash
Density (Flashes km!u-2!n yr!u-1!n)'
    ;title = 'Positive Flash Density (Flashes
km!u-2!n yr!u-1!n)'
    end
  (n_elements(ppos) GT 0): begin ; percentage of positive flashes
    type = 'ppos'
    lev = [0,2,3,4,6,7,8]
    slev = ['0','2','3','4','6','7','8 >']
    col = [15, 4, 6, 9, 10, 11, 14]
    title = 'Percent Positive Flashes'
    end
  (n_elements(pmed) GT 0): begin ; median peak positive current
    type = 'pmed'
    lev = [0, 15, 25, 35, 45, 50]
    slev = ['0','15','25','35','45','50 >']
    ;col = [14, 8, 10, 4, 11, 12, 1, 3, 2]
    col = [15, 6, 9, 10, 11, 14]
    title = 'Median Peak Positive Current
(kA)'
    end

```

```

(n_elements(nmed) GT 0): begin ; median peak negative current
    type = 'nmed'
    lev = [0, 16, 18, 20, 22, 24, 26]
    slev = ['0','16','18','20','22','24','26'
    >]
    ;col = [14, 8, 9, 10, 4, 11, 12, 1, 3, 2]
    col = [15, 4, 6, 9, 10, 11, 14]
    title = 'Median Peak Negative Current
    (kA)'
    end
(n_elements(pmull) GT 0): begin ; positive multiplicity
    type = 'pmul'
    lev = [0, 1.00, 1.10, 1.20, 1.25]
    slev = ['0.0','1.00','1.10','1.20','1.25
    >]
    ;col = [14, 8, 9, 10, 4, 11, 12]
    col = [15, 6, 9, 10, 11]
    title = 'Mean Positive Multiplicity'
    end
(n_elements(nmult) GT 0): begin ; negative multiplicity
    type = 'nmul'
    lev = [0.0, 1.8, 2.0, 2.2, 2.4, 2.6]
    slev = ['0.0','1.8','2.0','2.2','2.4','2.6
    >]
    ;col = [14, 8, 9, 10, 11, 1]
    col = [15, 6, 9, 10, 11, 14]
    title = 'Mean Negative Multiplicity'
    end
else: begin
    print, 'Invalid or missing plot type.'
    return
end
endcase

; set up files
;files = inpath+type+'8900.txt'
files = inpath+type+'30dec_03to18Z.txt'

; set up graphics
!p.font = -1
window, xsize = 600, ysize = 600

; set up region
region = [34.00, 42.00, -76, -69]

; get data from file
openr, 2, files
reg = fltarr(4)
info = fltarr(4)
readf, 2, reg, info
data = fltarr(info(1), info(0))
readf, 2, data
close, 2
data = abs(data)

; set up lat and lon values
lat = findgen(info(0))*info(2)+reg(0)+info(2)/2.0

```

```

lon = findgen(info(1))*info(2)+reg(2)+info(2)/2.0

; crop the data for filled contours
lo = -20.0
lat1 = min(where(lat GT region(0)))
lat2 = max(where(lat LT region(1)))
lon1 = min(where(lon GT region(2)))
lon2 = max(where(lon LT region(3)))
data(*,0:lat1) = lo
data(*,lat2:*) = lo
data(lon2:*,*) = lo
data(0:lon1,*) = lo

; draw a map
map_set, 0, -95, 0, limit = region([0,2,1,3]), /cylindrical,
/isotropic, /noborder, /noerase, $
      xmargin = [0,0], ymargin = [0,0]

; contour the data
contour, data, lon, lat, levels = lev, c_colors = col, /fill, /close,
/overplot

; mask off region outside US borders
;us_mask, region+[-1,1,-1,1], 0
;nldnmask, data, reg, 0, distance = 400

; put map on top of plot
map_continents, /continents, color=1, mlinethick=1.0, /HiRes,
/Rivers, /usa

;These lines give a clean border:
plots, region[2], region[0]
plots, region[[2, 3, 3, 2, 2]], region[[0, 0, 1, 1, 0]], color=0,
thick = 150, /continue

;Plot a city
xyouts, -82.43, 35.53, 'AVL', color=1, charsize=2.5, charthick=1.5
plots, -82.53, 35.43, Psym=1, color=1, SymSize=2.5

;Plot a second city
;xyouts, -109.93, 34.35, 'SOW', color=1, charsize=2.5, charthick=1.5
;plots, -110.03, 34.25, Psym=1, color=1, SymSize=2.5

;Plot a third city
;xyouts, -103.9, 34.47, 'CVS', color=1, charsize=2.5, charthick=1.5
;plots, -103.3, 34.37, Psym=1, color=1, SymSize=2.5

;Plot a fourth city
;xyouts, -108.43, 39.27, 'GJT', color=1, charsize=2.5, charthick=1.5
;plots, -108.53, 39.17, Psym=1, color=1, SymSize=2.5

;Plot a fifth city
;xyouts, -108.13, 36.85, 'FMN', color=1, charsize=2.5, charthick=1.5
;plots, -108.23, 36.75, Psym=1, color=1, SymSize=2.5

;Plot a sixth city

```

```

;xyouts, -104.62, 38.42, 'COS', color=1, charsize=2.5, charthick=1.5
;plots, -104.72, 38.82, Psym=1, color=1, SymSize=2.5

;Plot a seventh city
;xyouts, -105.98, 35.72, 'SAF', color=1, charsize=2.5, charthick=1.5
;plots, -106.08, 35.62, Psym=1, color=1, SymSize=2.5

;Plot a seventh city
;xyouts, -109.5, 31.55, 'DUG', color=1, charsize=2.5, charthick=1.5
;plots, -109.6, 31.45, Psym=1, color=1, SymSize=2.5

;Plot a seventh city
;xyouts, -111.57, 35.23, 'FLG', color=1, charsize=2.5, charthick=1.5
;plots, -111.67, 35.13, Psym=1, color=1, SymSize=2.5

; put a title on the chart
polyfill, [0.0, 0.0, 1.0, 1.0], [1.0, 0.87, 0.87, 1.0], 0, /normal,
color=0
;xyouts, 0.5, 0.96, 'May - July '+title, $
;xyouts, 0.5, 0.96, '1989 - 00 '+title, $
xyouts, 0.5, 0.96, '03Z to 18Z '+title, $
color=1, charsize = 1.5, /normal, alignment = 0.5

; put the colorbar on the chart
dx = 0.08
dy = 0.02
xbox = dx*[0,0,1,1]
ybox = dy*[0,1,1,0]
xref = 0.5-float(n_elements(lev))/2.0*dx
yref = 0.92
for i = 0, n_elements(lev)-1 do begin
  polyfill, xref+dx*i+xbox, yref+ybox, color = col(i), /normal
  xyouts, xref+dx*i, yref-1.5*dy, slev(i), color=1, /normal, charsize =
1.0
endfor

;Copyright info
xyouts, 0.5, 0.04, 'Courtesy of the Lightning Project at Texas A&M
University', color=1, $
  charsize=1.5, charthick=1.0, /normal, alignment = 0.5

; save image to gif file
image24 = tvrd(True=1)
image = color_quan(image24, 1, r, g, b)
;Write_GIF, outpath+type+'mjj.gif', image, r, g, b
;Write_GIF, outpath+type+'8900'+cty+'.gif', image, r, g, b
Write_GIF, outpath+type+'03to18Z.gif', image, r, g, b

;wdelete, !d.window
end

```

```

pro daily_summary, dates = dates, region = region, center = center, $
  radius = radius, outfile = outfile

; Finds the daily summary of lightning data given a rectangular region
; or uses a circle given the center latitude and longitude.
;
; Explanation of inputs:
;   dates: 2 element array of strings with date in format MM/DD/YYYY
;           First and last date of concern.  REQUIRED
;   region: 4 element array of latitudes and longitudes for the
;           rectangular region of concern.  This is not required
;           if using a circle.
;           Format is [min lat, max lat, min lon, max lon]
;   center: 2 element array [lat, lon] for the center of a circle
;           Not required if using a rectangular region.
;   radius: A scalar number which indicates the radius of a circle
;           for data isolation.  Units are kilometers.
;           Not used for rectangular cases.
;   outfile: Where you want the output stored.  This is a text
;           or ASCII file that has columns of results.  The default
;           filename is 'daily_summary.txt' in the working directory.
;           The input is a scalar string quantity.
;
; Other files needed for the program to run
;   You must also have the programs, findtime.pro, and getchunk.pro
;
; How to run the program:
;   To run this program, you can either operate on a rectangular or
;   circular area.  Both examples are shown.
;   Rectangular area:
;     daily_summary, dates = ['05/03/1998', '01/10/1999'], $
;     region = [30.0, 45.0, -120.0, -90.0], outfile = 'case1.txt'
;   Circular area:
;     daily_summary, dates = ['05/03/1998', '05/02/1999'], $
;     center = [35.0, -100.4], radius = 150.0, outfile = 'case2.txt'
; Known limitations:
;   1. The circle option uses a straight line distance from the
; lightning
;       flash to the center of the circle.  The earth's curvature is not
;       taken into account.  This is not normally significant unless
;       a large area (more than 1000 km or so in radius) is used.
;   2. The time frame for each 24 hour period begins at 00 UTC.
;
; Programmer: Gary R. Huffines
; Last Update: 27 June 2000

; check the options to see if they are viable
; must have either circle or rectangle selected
if ((n_elements(region) + n_elements(center) + n_elements(radius)) EQ
0) $
  then begin
    print, 'You must select a region.'
    return
  endif
; must have a start and stop date
if (n_elements(dates) EQ 0) then begin
  print, 'You must designate the start and stop dates.'

```

```

        return
    endif
    ; if no outfile designated, assign one
    if (n_elements(outfile) EQ 0) then outfile = 'C:\My
Documents\sphill\cluster_input.txt'

    ; set up the directory with the lightning data files
    if (!d.name EQ 'WIN') then begin
        inpath = 'D:\lightning_data\'  

        slash = '\'
    endif else begin
        inpath = '/home/fujital2/flash/'
        slash = '/'
    endelse

    ; search for files with lightning data (*.lgh files)
    filepaths = findfile(inpath+'lgh*', count = nyears)
    filepaths = filepaths(where(strpos(filepaths, slash) GE 0, nyears))
    filepaths = filepaths[sort(filepaths)]

    ; Unix adds a colon to end of directory.  Delete it.
    if (!d.name NE 'WIN') then $
        filepaths = strmid(filepaths, 0, strlen(filepaths[0])-1)+slash

    ; add the rest of the file information
    months = ['jan','feb','mar','apr','may','jun','jul','aug','sep',  

              'oct','nov','dec']
    years = strmid(filepaths, strlen(filepaths[0])-3, 2)
    nmonths = n_elements(months)
    files = strarr(nyears*nmonths)
    for y = 0, nyears-1 do $
        for m = 0, nmonths-1 do $
            files[y*nmonths+m] = filepaths[y]+months[m]+years[y]+'.lgh'
    ; check to make sure each file is there
    okay = intarr(n_elements(files)) ; check to be sure there are no
missing files
    for i = 0, n_elements(files)-1 do begin
        temp = findfile(files(i), count = c)
        okay[i]=c
    endfor
    keep = where(okay EQ 1, nfiles) ; only keep the list of files that are
there
    files = files(keep) ; limit the files to those there

    ; find the number of days
    d1 = dates[0]
    d2 = dates[1]
    d1 = fix(str_sep(d1,'/'))
    d2 = fix(str_sep(d2,'/'))
    day1 = julday(d1[0],d1[1],d1[2])
    day2 = julday(d2[0],d2[1],d2[2])
    ndays = day2 - day1

    ; set up structure to hold summary data
    output = {output, date: ' ', flashes: 0L, positive: 0.0, ppos: 0.0, $  

              nmult: 0.0, pmult: 0.0, nmed: 0.0, pmed: 0.0}
    data = replicate(output, ndays)

```

```

; set up string array for 2 digit numbers
num = strcompress(sindgen(100), /remove_all)
num[0:9] = '0'+num[0:9]

; if circle is selected, define region to limit data retrieval
;if (n_elements(center) GT 0) then begin
;  dist = radius / 6370.0
;  loc = reverse(center)
;  west = ll_arc_distance(loc, dist, 270, /degrees)
;  east = ll_arc_distance(loc, dist, 90, /degrees)
;  north = ll_arc_distance(loc, dist, 0, /degrees)
;  south = ll_arc_distance(loc, dist, 180, /degrees)
;  region = [south[1], north[1], west[0], east[0]]
;  circle = 1B
;endif else circle = 0B

; open output file for results
;openw, 2, outfile
;printf, 2, 'Date', 'N-All', format = "(a4,6x)"
printf, 2, 'Date', 'N-All', 'N-Pos', '% Pos', 'Mul-N', 'Mul-P', 'Peak-
N', 'Peak-P', $
      format = "(a4,6x,a6,2x,a6,2x,a5,2x,a5,2x,a6,2x,a6)"
close, 2

; loop through each day and find results
for day = 0L, ndays-1 do begin
  ; set up dates for this time period
  caldat, day1+day, m1, d1, y1
  caldat, day1+day+1L, m2, d2, y2
  period = [num[m1]+'/'+num[d1]+'/'+num[y1 mod 100], $
             num[m2]+'/'+num[d2]+'/'+num[y2 mod 100]]
  ; store the date
  data[day].date = period[0]
  ; find the first and last position and index in files for daily data
  findtime, period+' 00:00:00', si, sp, li, lp, files, 11L
  ; get data for time period and region
  v = getchunk(files, si, sp, li, lp, region, si, sp, 11L, 250000L)
  if (n_elements(v) GT 10) then begin
    ; convert binary data to a usable structure
    f = exp_lgh(v)
    ; limit data to eliminate positive flashes less than 10 kA
    okay = where((f.peak LT 0.0) OR (f.peak GE 10.0), count)
    if (count GT 0) then begin
      v = v[okay]
      f = f[okay]
      ; if circle was selected, limit data to region of circle
      ;if circle then begin
      ;  xdist = 6370.0*cos(center[0]*!dtor)*(f.lon-center[1])*!dtor
      ;  ydist = 6370.0*(f.lat-center[0])*!dtor
      ;  dist = ((xdist^2.0)*(ydist^2.0))^.5
      ;  okay = where(dist LE radius, count)
      ;  if (count GT 0) then begin
      ;    f = f[okay]
      ;    v = v[okay]
      ;  endif
      ;endif
    endif
  endif
endfor

```

```

; process flashes to get results
if (count GT 0) then begin

    ; store the number of flashes
    data[day].flashes = count

    ; store the positive flash count
    ;pos = where(f.peak GT 0.0, pcount)
    ;data[day].positive = pcount
    ; store the percentage of positive flashes
    ;data[day].ppos = float(pcount)/float(count)*100.0

    ; store the mean negative multiplicity
    ;neg = where(f.peak lt 0.0, ncount)
    ;if (ncount GT 0) then begin
    ;    data[day].nmult = total(f[neg].mult)/float(ncount)
    ; store the median negative peak current
    ;    if (ncount GT 1) then $
    ;        data[day].nmed = median(f[neg].peak) $
    ;    else $
    ;        data[day].nmed = f[neg].peak
    ;endif
    ; store the mean positive multiplicity
    ;if (pcount GT 0) then begin
    ;    data[day].pmult = total(f[pos].mult)/float(pcount)
    ;    ; store the median positive peak current
    ;    if (pcount GT 1) then $
    ;        data[day].pmed = median(f[pos].peak) $
    ;    else $
    ;        data[day].pmed = f[pos].peak
    ;endif

    ; save results to the outfile
    openu, 2, outfile, /append
    printf, 2, data[day], $
        format =
    "(a8,2x,i6,2x,i6,2x,f5.1,2x,f5.2,2x,f5.2,2x,f6.1,2x,f6.1)"
        close, 2
    endif ; processing results
    endif ; flashes existed
    endif ; flashes in region
    print, 'Finished with ', period[0]
endfor ; end of day

close, 2

print, 'All done!'

end

```

```

pro box_maker, date1, date2, reg1, reg2, reg3, reg4, suffix, times,
months

; This program feeds/runs any_anal_years.pro for several different times
and locations

; Programmer: Brandon Ely
; Last Update: 26 Oct 01
; Modified by: Stephen Phillips

;init_suffix='high'
init_suffix='low'

loc='SW'
outfile='C:\My Documents\SPhill\Thesis Files\box_info\'

; text file outpath for any_anal_years
outpath='C:\My Documents\SPhill\text\boxes_'+loc+'\'
;outpath='C:\My Documents\SPhill\text\boxes_SE\'

times=[1,2,3,4,5,6,7,8,9,10,11,12,13,14,15,16,17,18,19,20,21,22,23]
months=['jan','feb','mar','apr','may','jun','jul','aug','sep','oct','nov',
,'dec']
res=0.05
curr_res=0.1
time_res=15

; Date1 indicates the starting date/time for each analysis
; Date2 indicates the ending date/time for each analysis
; Note: Both of these should be in the format "mm/dd/yy hr:mm:ss

date1='01/01/89 00:00:00'
date2='12/31/89 23:59:59'

; Region1 is the southern bounding latitude
; Region2 is the northern bounding latitude
; Region3 is the western bounding longitude
; Region4 is the eastern bounding longitude

;reg1=[40.75,30.25,31.25,32.25,33.25,34.25,35.25,36.25,37.25,38.25,39.25,
40.25]
;reg2=[41.25,30.75,31.75,32.75,33.75,34.75,35.75,36.75,37.75,38.75,39.75,
40.75]
reg1=[40.75]
reg2=[41.25]
reg3=[-113.0]
reg4=[-112.5]
;reg3=[-113.0,-107.5,-107.5,-107.5,-107.5,-107.5,-107.5,-107.5,-107.5,-
107.5,-107.5,-107.5]
;reg4=[-112.5,-107.0,-107.0,-107.0,-107.0,-107.0,-107.0,-107.0,-107.0,-
107.0,-107.0,-107.0]

if (strlen(date1) NE strlen(date2)) then begin
  print, 'The dates are not in the appropriate format.'

```

```

stop
endif

if ((n_elements(reg1) NE n_elements(reg2)) OR (n_elements(reg1) NE
n_elements(reg3)) $  

    OR (n_elements(reg1) NE n_elements(reg4))) then begin
    print, 'There are an unequal number of regional boundaries listed.'
    stop
endif

dates=strarr(2)
dates=[date1,date2]
regnumb=n_elements(reg1)

; determine resolution of terrain boxes
boxwidth = reg2[0] - reg1[0]
rows = 1320      ;# rows for SW
;rows = 1200      ;# rows for SE
cols = 1320
gs = 0.008333333333333 ;grid spacing in deg of elevation data
nx = round(boxwidth/gs)
ny = nx
sr = 0L
nr = 0L
wc = 0L
ec = 0L
elev = intarr(cols,rows)
elevmod = intarr(cols,rows)
region_elev = intarr(nx,ny)
elev_box = intarr(regnumb,nx,ny)

; Get terrain data and set up array
openr, 13, 'c:\my documents\sphill\thesis files\SWglobe.dat'
readf, 13, elev
;elevmod = reverse(elev,2)
for i = 0, (rows-1) do begin
    j= rows-1-i
    elevmod[*,i] = elev[*,j]
endfor
;print, elev[0:4,0:4]
;print, 'elevmod'
;print, elevmod[0:4,1316:1319]

; continue boxes for any_anal
openw,69, outfile+'box_summ_'+init_suffix+'_'+loc+'.txt'
printf, 69, 'Start Time for Analysis -> '+date1
printf, 69, 'End Time for Analysis -> '+date2
printf, 69, ' '


for num = 0, (regnumb-1) do begin

    ; compute elevation data for each box
    sr = round((reg1[0]-30.25)/gs)      ;southern most row number in
elevmod for SW region
    ;sr = long((reg1[0]-31.25)/gs)      ;southern most row number in
elevmod for SE region

```

```

nr = round(sr + ny)-1                                ;northern most "   "
"
wc = round((reg3[0]+113.0)/gs)      ;western most column number in
elevmod for SW region
;wc = long((reg3[0]+85.0.0)/gs)      ;western most column number in
elevmod for SE region
ec = round(wc + nx)-1                                ;eastern most "   "
"
"

; get dat from elevmod and assign to proper element in elev_box
j = nx-1
k = ny-1
region_elev[0:k,0:j] = elevmod[wc:ec,sr:nr]
elev_box[num,0:k,0:j] = region_elev

; continue with any_anal boxes

numb=num+1
numb=strcompress(numb, /remove_all)
region=[reg1(num),reg2(num),reg3(num),reg4(num)]
suffix=init_suffix+numb

compreg=string(reg1(num))+','+string(reg2(num))+','+string(reg3(num))+','+
string(reg4(num))
compreg=strcompress(compreg, /remove_all)

printf, 69, suffix+' -> '+compreg

any_anal_years2, dates, region, outpath, res, suffix, curr_res,
time_res, times, months

filenum=strcompress(num, /remove_all)

; open file for elevation matrix
box = fltarr(nx,ny)
box(*,*) = elev_box(num,*,*)
print, box(0:4,56:59)
openw, 29, outpath+'elev_box_'+filenum+'.txt'
printf, 29, box
close, 29
print, 'Box #' +numb+ ' was finished successfully'
endfor

close, 69
close, 13
end

```

```

pro elev_anal, regnum, nx, ny, location

; This program uses the elevation data created for statistical boxes to
; calculate terrain elevation
; averages, flash density averages, and correlation coefficients between
; terrain and flash density.

; Programmer: Stephen Phillips
; Last Update: 26 Oct 01
; Modified by: Me

; use elev_anal, 117, 60, 60, 'SW'
; set file information
close, /all

inpath = 'C:\My Documents\SPhill\text\boxes_'
;inpath = '\\\Trigger\sphill\text\boxes_'
outpath = 'c:\My Documents\sphill\text\boxes_'
graphpath = 'c:\My Documents\sphill\thesis files\maps\'

; variables
count = 0L
elevation_box = intarr(ny, nx)           ;terrain data for a statistical
box
elev_char = fltarr(regnum,4)
elev_char(*,*) = 0
avgelev = fltarr(regnum)
elev_anom = fltarr(regnum)               ;height of a box's
avg elevation above or below the average elevation
                                         ;of all surrounding
boxes
dens_anom = fltarr(regnum)              ;magnitude of difference
between mean flash density of a box and
                                         ;the mean flash
density of all surrounding boxes
num_surround = 0L                       ;the number of boxes that
surround a given box

dx = 13                                  ;number of columns
regions
dy = 9                                   ;number of rows of
regions

sorted_avgelev = fltarr(regnum)
sorted_indexed_elev = fltarr(regnum, regnum)
sorted_dens = fltarr(regnum)
avg_dens = fltarr(regnum)
Regr_curve = fltarr(regnum,1)
sorted_gradient = fltarr(regnum)
dens_sorted_grad = fltarr(regnum)
grad = fltarr(ny-5,nx-5)
gradient = fltarr(regnum)
stats = fltarr(2)
var = fltarr(regnum)
grad_dens = fltarr(regnum)

```

```

j = nx-1
k = ny-1
index = 0L
index2 = 0L

; set up files
for region = 0, regnum-1 do begin
;for region = 0,220 do begin
    num=strcompress(region, /remove_all)
    files = inpath+location+'\elev_box_'+num+'.txt'
    ;read in the elevation data for each statistical box
    openr, 7, files
    ;readf, 7, elevation_box(0:j,0:k)
    readf, 7, elevation_box
    count = count+1

    ;calculate elevation characteristics for each statistical box
    ;           elev_char(*,0) = Average Elevation
    ;           (*,1) = Maximum Elevation
    ;           (*,2) = Minimum Elevation
    ;           (*,3) = box index

    sum = 0L
    l = 0L
    m = 0L
    bad = -500L
    minimum = 15000L
    maximum = 0L

    for l = 0, j do begin
        for m = 0, k do begin
            maxcol = l+5
            maxrow = m+5
            if (elevation_box(l,m) NE bad) then begin
                sum = sum + elevation_box(l,m)
                if (elevation_box(l,m) LT minimum) then begin
                    minimum = elevation_box(l,m)
                endif
                if (maxcol LE (j)) and (maxrow LE (k)) and $
                    (elevation_box(l,m) NE bad) then begin
                    if (elevation_box(maxcol,maxrow)NE bad)
then begin
                    grad(l,m) =
sqrt(((elevation_box(maxcol,m)-elevation_box(l,m))/5)^2 $ +
                    + ((elevation_box(l,maxrow)-
elevation_box(l,m))/5)^2)
                    endif
                endif
            endif
        endfor
    endfor

    stats = moment(grad, /nan)
    ;gradient(region) = max(grad)
    gradient(region) = stats(0)
    var(region) = stats(1)
    ;gradient(region) = total(grad)/((nx-5)*(ny-5))

```

```

elev_char(region,0) = sum/(ny*nx)
elev_char(region,1) = max(elevation_box(*, *))
elev_char(region,2) = minimum
elev_char(region,3) = region
avgelev(region) = elev_char(region,0)
close, 7

;read flash densities and calc avg fl dens for each box
files = inpath+location+'\dens'+num+'.txt'
openr, 25, files
reg = fltarr(4)
info = fltarr(4)
readf, 25, reg, info
dens_size = info(0)*info(1)
dens = fltarr(dens_size)
readf, 25, dens
close, 25
dens = abs(dens)
avg_dens(region) = total(dens)/dens_size
endfor

;compute the elevation and flash density anomalies
for region = 0, regnum-1 do begin
    regionnumber = 0L
    regionnumber = region
    ;corners
    if (region EQ 0) OR (region EQ dx-1) OR (region EQ dx*(dy-1))
OR (region EQ regnum-1) then begin
        numsurround = 3
        if (region EQ 0) then begin
            elev_anom(region) = avgelev(region)-
(avgelev(0)+avgelev(1)+avgelev(dx)+avgelev(dx+1))/4
            dens_anom(region) =
avg_dens(region)/((avg_dens(0)+avg_dens(1)+avg_dens(dx)+avg_dens(dx+1))/4
)
            endif
            if (region EQ nx-1) then begin
                elev_anom(region) = avgelev(region)-
(avgelev(region)+avgelev(region-1)+avgelev(region+dx)-
+avgelev(region+dx-1))/4
                dens_anom(region) =
avg_dens(region)/((avg_dens(region)+avg_dens(region-
1)+avg_dens(region+dx)-
+avg_dens(region+dx-1))/4)
            endif
            if (region EQ dy*(dx-1)) then begin
                elev_anom(region) = $-
avgelev(region)-
(avgelev(region)+avgelev(region+1)+avgelev(region-dx)+avgelev(region-
dx+1))/4
                dens_anom(region) = $
avg_dens(region)/((avg_dens(region)+avg_dens(region+1)+avg_dens(region-
dx)+avg_dens(region-dx+1))/4)
            endif
            if (region EQ regnum-1) then begin

```

```

        elev_anom(region) = avgelev(region)-
(avgelev(region)+avgelev(region-1)+avgelev(region-dx)$
+avgelev(region-dx-1))/4
        dens_anom(region) =
avg_dens(region)/((avg_dens(region)+avg_dens(region-1)+avg_dens(region-
dx)$
+avg_dens(region-dx-1))/4)
        endif
    endif else begin
;outer rows
        if (region GT 0 AND region LT dx) OR (region GT regnum-dx AND
region LT regnum-1)$
            OR (remainder(regionnumber,dx) EQ 0) OR
(remainder(regionnumber+1,dx) EQ 0) then begin
            numsurround = 5
            if (region GT 0 AND region LT dx) then begin
                elev_anom(region) = avgelev(region)-
(avgelev(region)+avgelev(region-1)+avgelev(region+1)$
+avgelev(region+dx-1)+avgelev(region+dx)+avgelev(region+dx+1))/6
                dens_anom(region) =
avg_dens(region)/((avg_dens(region)+avg_dens(region-
1)+avg_dens(region+1)$
+avg_dens(region+dx-1)+avg_dens(region+dx)+avg_dens(region+dx+1))/6)
                endif
            if (region GT regnum-dx AND region LT regnum-1) then
begin
                elev_anom(region) = avgelev(region)-
(avgelev(region)+avgelev(region-1)+avgelev(region+1)$
+avgelev(region-dx-1)+avgelev(region-
dx)+avgelev(region-dx+1))/6
                dens_anom(region) =
avg_dens(region)/((avg_dens(region)+avg_dens(region-
1)+avg_dens(region+1)$
+avg_dens(region-dx-1)+avg_dens(region-dx)+avg_dens(region-
dx+1))/6)
                endif
            if (remainder(regionnumber,dx) EQ 0) then begin
                elev_anom(region) = avgelev(region)-
(avgelev(region)+avgelev(region-dx)+avgelev(region+dx)$
+avgelev(region-
dx+1)+avgelev(region+1)+avgelev(region+dx+1))/6
                dens_anom(region) =
avg_dens(region)/((avg_dens(region)+avg_dens(region-
dx)+avg_dens(region+dx)$
+avg_dens(region-
dx+1)+avg_dens(region+1)+avg_dens(region+dx+1))/6)
                endif
            if (remainder(regionnumber+1,dx) EQ 0) then begin
                elev_anom(region) = avgelev(region)-
(avgelev(region)+avgelev(region-dx)+avgelev(region+dx)$
+avgelev(region-dx-1)+avgelev(region-
1)+avgelev(region+dx-1))/6
                dens_anom(region) =
avg_dens(region)/((avg_dens(region)+avg_dens(region-
dx)+avg_dens(region+dx)$
+avg_dens(region+dx-1)+avg_dens(region+dx))/6)
            endif
        endif
    endif

```

```

        +avg_dens(region-dx-1)+avg_dens(region-
1)+avg_dens(region+dx-1))/6)
            endif
        endif else begin
;interior
        num_surround = 8
        elev_anom(region) = avgelev(region)-
(avgelev(region)+avgelev(region-1)+avgelev(region+1)$
+avgelev(region+dx-
1)+avgelev(region+dx)+avgelev(region+dx+1)$
+avgelev(region-dx-1)+avgelev(region-
dx)+avgelev(region-dx+1))/9
        dens_anom(region) =
avg_dens(region)/((avg_dens(region)+avg_dens(region-
1)+avg_dens(region+1)$
+avg_dens(region+dx-
1)+avg_dens(region+dx)+avg_dens(region+dx+1)$
+avg_dens(region+dx-
1)+avg_dens(region+dx)+avg_dens(region+dx+1))/9)
            endelse
        endelse

endfor
index = sort(avgelev)
sorted_avgelev = avgelev(index)
sorted_dens = avg_dens(index)
index2 = sort(gradient)
grad_dens = avg_dens(index2)
sorted_gradient = gradient(index2)
elev_sorted_grad = gradient(index)
sorted_var = var(index2)
index3 = sort(elev_anom)
sorted_elev_anom = elev_anom(index3)
sorted_dens_anom = dens_anom(index3)

; set up graphics
!p.color = 256
device, decomposed = 0
!p.font = -1
window, xsize = 600, ysize = 600
tvlct, 255, 255, 255, 0
tvlct, 0, 0, 0, 1
tvlct, 70, 70, 70, 5

;openw,79, outpath+location+'\SASmultdata'+'.txt'
;openw,70, outpath+location+'\SASElevdata'+'.txt'
openw,79, outpath+location+'\SASAnomdata'+'.txt'
;printf, 79, 'avg elev', '    avg flash dens'
printf, 79, ''
;printf, 70, ''
for i=0,regnum-1 do begin
;    printf, 70, sorted_avgelev(i), elev_sorted_grad(i), sorted_dens(i)
;    printf, 79, sorted_avgelev(i), elev_sorted_grad(i), sorted_dens(i),
sorted_gradient(i), grad_dens(i)
    printf, 79, sorted_elev_anom(i), sorted_dens_anom(i)
endfor
close, 79

```

```
;close, 70

;plot, sorted_gradient, grad_dens, PSym=2, color=1, XTitle='Mean
Elevation Gradient (m2/km2)',$
;      YTitle='Avg Flash Density (fl/km2)', Title=location+: Flash
Density versus Elevation Gradient'
;plot, sorted_gradient, grad_dens, color=1, background=0, thick=1,
XTitle='Mean Elevation Gradient (m2/km2)',$
;      YTitle='Avg Flash Density (FL/km2)', Title='Box Averaged
Correlation'
plot, sorted_elev_anom, sorted_dens_anom, PSym=2, color=1, XTitle='Mean
Elevation Anomaly (m)',$
;      YTitle='Avg Flash Density Anomaly (fl/(km2yr))',$
Title=location+: Flash Density Anomaly versus Elevation Anomaly'

; save image to gif file
image24 = tvrd(True=1)
image = color_quan(image24, 1, r, g, b)
;Write_GIF, graphpath+location+'densVSelevgrad.gif', image, r, g, b
Write_GIF, graphpath+location+'dens_anomVSelev_anom.gif', image, r, g, b
;wdelete, !d.window

;plot, sorted_avgelev, sorted_dens, PSym=2, color=1, XTitle='Mean
Elevation (m)',$
;      YTitle='Avg Flash Density (fl/km2)', Title=location+: Flash
Density versus Elevation'
;plot, sorted_avgelev, sorted_dens, color=1, background=0,
XTitle='Elevation (m)',$
;      YTitle='Avg Flash Density (FL/km2)', Title='Box Averaged
Correlation'

; save image to gif file
;image24 = tvrd(True=1)
;image = color_quan(image24, 1, r, g, b)
;Write_GIF, graphpath+location+'densVSelev.gif', image, r, g, b
;wdelete, !d.window

end
```

```

pro search_days

; this program searches the active and inactive days of specified
regions, and
; writes a list of days for which the following criteria are met for the
high terrain:
;                                A is active and B is active
;                                A is active and B is inactive
;                                A is inactive and B is active
;                                A is inactive and B is inactive

; Programmer: Stephen Phillips
; Last Update: 26 Oct 01
; Modified by: Me

close, /all

;define i/o file names

;date_file = 'C:\My Documents\sphill\text\high_active_SW.txt'
;date_file = 'C:\My Documents\sphill\text\high_inactive_SW.txt'
;date_fileA = 'C:\My Documents\sphill\text\high_active_BR.txt'
date_fileA = 'C:\My Documents\sphill\text\high_inactive_BR_50.txt'
;date_fileA = 'C:\My Documents\sphill\text\high_active_AL.txt'
;date_fileA = 'C:\My Documents\sphill\text\high_inactive_AL_50.txt'

;date_fileB = 'C:\My Documents\sphill\text\high_active_AL.txt'
;date_fileB = 'C:\My Documents\sphill\text\high_inactive_AL_50.txt'
date_fileB = 'C:\My Documents\sphill\text\low_active.txt'
;date_fileB = 'C:\My Documents\sphill\text\low_inactive_50.txt'

;outfile = 'C:\My Documents\sphill\text\Theta_E_SW.txt'
;outfile = 'C:\My Documents\sphill\text\BRact_ALinact.txt'
;outfile = 'C:\My Documents\sphill\text\BRact_ALact.txt'
;outfile = 'C:\My Documents\sphill\text\BRinact_ALact.txt'
;outfile = 'C:\My Documents\sphill\text\BRinact_ALinact.txt'
;outfile = 'C:\My Documents\sphill\text\ALact_Lowact.txt'
;outfile = 'C:\My Documents\sphill\text\ALact_Lowinact.txt'
;outfile = 'C:\My Documents\sphill\text\ALinact_Lowact.txt'
;outfile = 'C:\My Documents\sphill\text\BRact_Lowact.txt'
;outfile = 'C:\My Documents\sphill\text\BRact_Lowinact.txt'
outfile = 'C:\My Documents\sphill\text\BRinact_Lowact.txt'

;define variables
datestring = ''                                ;temp variable to read a line
of dates from data files
temparray = strarr(8)                            ;temp array containing individual
dates from splitting 1 line of data
date_arrayA = strarr(1)                          ;array of all dates from file A
date_arrayB = strarr(1)                          ;array of all dates from file B
common_dates = strarr(1)                        ;array of all dates belonging to both
A & B

```

```

;read dates from file A:           stores list of days in date_arrayA
openr, 7, date_fileA
while not eof(7) do begin
    readf, 7, datestring
    temparray = strssplit(datestring, ' ', /extract)
    if (n_elements(temparray) EQ 8) then begin
        ;a full line of 8 days
        date_arrayA = [date_arrayA, temparray(0), temparray(1),
temparray(2), temparray(3), temparray(4),$
                                         temparray(5),
temparray(6), temparray(7)]
    endif else begin
        n = n_elements(temparray)
        ; number of days on the partial line
        for i = 0,n-1 do begin
            date_arrayA = [date_arrayA, temparray(i)]
        endfor
    endelse
endwhile
close, 7

;read dates from file B:           stores list of days in date_arrayB
openr, 11, date_fileB
while not eof(11) do begin
    readf, 11, datestring
    temparray = strssplit(datestring, ' ', /extract)
    if (n_elements(temparray) EQ 8) then begin
        date_arrayB = [date_arrayB, temparray(0), temparray(1),
temparray(2), temparray(3), temparray(4),$
                                         temparray(5),
temparray(6), temparray(7)]
    endif else begin
        n = n_elements(temparray)
        for i = 0,n-1 do begin
            date_arrayB = [date_arrayB, temparray(i)]
        endfor
    endelse
endwhile
close, 11
;eliminate initial blank space
date_arrayA = date_arrayA(where(date_arrayA NE ''))
date_arrayB = date_arrayB(where(date_arrayB NE ''))

;compare the two files, store any common days to "common"

n = n_elements(date_arrayA)
m = n_elements(date_arrayB)

for i = 0,n-1 do begin
    for j = 0,m-1 do begin
        if (date_arrayA(i) EQ date_arrayB(j)) then begin
            common_dates = [common_dates, date_arrayA(i)]
        endif
    endfor
endfor

```

```
;truncate "common" array to contain only valid days
if (n_elements(common_dates) NE 1) then begin
    common_dates = common_dates(where(common_dates NE ''))
endif
;write output to outfile

openw, 17, outfile
printf, 17, common_dates
close, 17

end
```

```

pro t_test

; Programmer: Stephen Phillips
; Last Update: 26 Oct 01
; Modified by: Me

: This program reads data from files and tests whether or not the means
; are different

close, /all

path='C:\My Documents\sphill\text\boxes_'

;loc = 'SW'
loc = 'SE'
num = 117
of regions ;number

header = ''
elev_anom = fltarr(num)
sorted_elev = fltarr(num)
dens_anom = fltarr(num)
sorted_dens = fltarr(num)
low = 0.0
high = 0.0
top = 0L ;top
index of bottom 40%
bottom = 0L ;bottom
index of top 25%

OpenR, 20, path+loc+'\SASanomdata.txt' ;input file
ReadF, 20, header ;read blank
line

for region = 0, num-1 do begin
    ReadF, 20, tempelev, tempdens
    elev_anom(region) = tempelev
    dens_anom(region) = tempdens
endfor
close, 20
stop
index = sort(elev_anom) ;sort
elevation anomalies least to greatest
sorted_elev = elev_anom(index)
sorted_dens = dens_anom(index)

high = num * 0.75
low = num * 0.4
bottom = ceil(high) ;bottom
index of upper 25%
top = floor(low) ;top index of
lower 40%

upper = sorted_dens(bottom:num-1)
lower = sorted_dens(0:top)

```

```
result = TM_TEST(upper, lower, /unequal)
print, '      T-stat      P-value'
print, result(0), result(1)

end
```

```

pro thetae_anal

; this program reads the upper air data files, consolidates them to one
file, extracts the four classes
; of events (high_active, high_inactive, low_active, and low_inactive,
; and analyzes the data for Theta_E at 500mb, 700mb, 850mb, and the
surface

close, /all

;ua_file ='C:\My Documents\sphill\upper_air\9000ua_SW.txt'
;ua_file ='C:\My Documents\sphill\upper_air\9000ua_BR.txt'
ua_file ='C:\My Documents\sphill\upper_air\9000ua_AL.txt'

;date_file = 'C:\My Documents\sphill\text\high_active_SW.txt'
;date_file = 'C:\My Documents\sphill\text\high_active_BR.txt'
;date_file = 'C:\My Documents\sphill\text\high_active_AL.txt'
;date_file = 'C:\My Documents\sphill\text\BRact_ALinact.txt'
;date_file = 'C:\My Documents\sphill\text\BRinact_ALact.txt'
;date_file = 'C:\My Documents\sphill\text\BRact_ALact.txt'
date_file = 'C:\My Documents\sphill\text\BRinact_ALinact.txt'
;date_file = 'C:\My Documents\sphill\text\BRact_Lowact.txt'
;date_file = 'C:\My Documents\sphill\text\BRinact_Lowact.txt'
;date_file = 'C:\My Documents\sphill\text\ALact_Lowact.txt'
;date_file = 'C:\My Documents\sphill\text\ALinact_Lowact.txt'

;outfile = 'C:\My Documents\sphill\upper_air\Theta_E_SW.txt'
;outfile = 'C:\My Documents\sphill\upper_air\Theta_E_BR.txt'
;outfile = 'C:\My Documents\sphill\upper_air\Theta_E_AL.txt'
;outfile = 'C:\My Documents\sphill\upper_air\Theta_E_BR_ALact.txt'
;outfile = 'C:\My Documents\sphill\upper_air\Theta_E_AL_BRact.txt'
;outfile = 'C:\My Documents\sphill\upper_air\ThetaE_BR_BRa_ALia.txt'
;outfile = 'C:\My Documents\sphill\upper_air\ThetaE_BR_BRia_ALa.txt'
;outfile = 'C:\My Documents\sphill\upper_air\ThetaE_BR_BRa_ALa.txt'
;outfile = 'C:\My Documents\sphill\upper_air\ThetaE_BR_BRia_ALia.txt'
;outfile = 'C:\My Documents\sphill\upper_air\ThetaE_AL_BRa_ALa.txt'
;outfile = 'C:\My Documents\sphill\upper_air\ThetaE_AL_BRia_ALia.txt'
;outfile = 'C:\My Documents\sphill\upper_air\ThetaE_AL_BRa_ALia.txt'
;outfile = 'C:\My Documents\sphill\upper_air\ThetaE_AL_BRia_ALa.txt'
;outfile = 'C:\My Documents\sphill\upper_air\ThetaE_BR_BRact_lowact.txt'
;outfile = 'C:\My
Documents\sphill\upper_air\ThetaE_BR_BRinact_lowact.txt'
;outfile = 'C:\My Documents\sphill\upper_air\ThetaE_AL_ALact_lowact.txt'
;outfile = 'C:\My
Documents\sphill\upper_air\ThetaE_AL_ALinact_lowact.txt'

openr, 7, ua_file

missing = 32767
header_date = ''
header = ''

```

```

i = 0L                                ;sets the looping index
to 0
date = strarr(29179)
time = strarr(29179)
wmo = intarr(29179)
press_sfc = intarr(29179)
hgt_sfc = intarr(29179)
tmp_sfc = fltarr(29179)
dewpt_sfc = fltarr(29179)
press_850 = intarr(29179)
hgt_850 = intarr(29179)
tmp_850 = fltarr(29179)
dewpt_850 = fltarr(29179)
press_700 = intarr(29179)
hgt_700 = intarr(29179)
tmp_700 = fltarr(29179)
dewpt_700 = fltarr(29179)
press_500 = intarr(29179)
hgt_500 = intarr(29179)
tmp_500 = fltarr(29179)
dewpt_500 = fltarr(29179)

while not eof(7) do begin           ;reading the daily upper air data

    readf, 7, header_date
    skip:
    ; Converts the 'dates' value into a different format for file name
setup
    date_broke=STRSPLIT(header_date(0), ' ', /extract)
    ; Extracts the year from file info
    year_num=string(date_broke(4))
    if (strlen(year_num) NE 4) then stop
    ; Extracts and reformats the month from file info
    mon_num=string(2)
    mon_name=STRLOWCASE(date_broke(3))
    if (strlen(mon_name) NE 3) then stop
    if (mon_name EQ 'jan') then mon_num='01'
    if (mon_name EQ 'feb') then mon_num='02'
    if (mon_name EQ 'mar') then mon_num='03'
    if (mon_name EQ 'apr') then mon_num='04'
    if (mon_name EQ 'may') then mon_num='05'
    if (mon_name EQ 'jun') then mon_num='06'
    if (mon_name EQ 'jul') then mon_num='07'
    if (mon_name EQ 'aug') then mon_num='08'
    if (mon_name EQ 'sep') then mon_num='09'
    if (mon_name EQ 'oct') then mon_num='10'
    if (mon_name EQ 'nov') then mon_num='11'
    if (mon_name EQ 'dec') then mon_num='12'
    ; Extracts the day from file info
    day_num=string(date_broke(2))
    if (strlen(day_num) LT 2) then day_num = '0'+day_num
    ; Extracts the hour from file info
    hour_num=string(date_broke(1))
    if (strlen(hour_num) LT 2) then hour_num = '0'+hour_num
    ; Setup the file name for output file
    year_numb = strmid(year_num, 2,2)

```

```

date(i) = mon_num+'/'+day_num+'/'+year_num
time(i) = hour_num

temp = strarr(7)
readf, 7, format = "(a7,2x,a5,2x,a5,2f7.2,4x,a3,2x,a5)", temp
wmo(i) = fix(temp(2))

readf, 7, header
readf, 7, header

temp_sfc = strarr(7)
readf, 7, format = "(a7,3x,a4,5a7)",temp_sfc
type = fix(temp_sfc(0))
if type EQ 9 then begin
    press_sfc(i) = fix(temp_sfc(1))
    hgt_sfc(i) = fix(temp_sfc(2))
    tmp_sfc(i) = (float(temp_sfc(3)))/10
    dewpt_sfc(i) = (float(temp_sfc(4)))/10
endif
temp_850 = strarr(7)
readf, 7, header
readf, 7, format = "(a7,3x,a4,5a7)",temp_850      ;850mb / ridge top
wind
type = fix(temp_850(0))
if type EQ 4 then begin
    press_850(i) = fix(temp_850(1))
    hgt_850(i) = fix(temp_850(2))
    tmp_850(i) = (float(temp_850(3)))/10
    dewpt_850(i) = (float(temp_850(4)))/10
endif
temp_700 = strarr(7)
readf, 7, format = "(a7,3x,a4,5a7)",temp_700      ;500mb / steering
flow
if type EQ 4 then begin
    press_700(i) = fix(temp_700(1))
    hgt_700(i) = fix(temp_700(2))
    tmp_700(i) = (float(temp_700(3)))/10
    dewpt_700(i) = (float(temp_700(4)))/10
endif
temp_500 = strarr(7)
readf, 7, format = "(a7,3x,a4,5a7)",temp_500      ;500mb / steering
flow
type = fix(temp_500(0))
if type EQ 4 then begin
    press_500(i) = fix(temp_500(1))
    hgt_500(i) = fix(temp_500(2))
    tmp_500(i) = (float(temp_500(3)))/10
    dewpt_500(i) = (float(temp_500(4)))/10
endif
i = i+1
rept:
while not eof(7) do begin
    readf, 7, header
    header_broke=STRSPLIT(header(0), ' ', /extract)
    type = header_broke(0)
    if type NE '254' then begin
        stop
;

```

```

        goto, rept
    endif else begin
        if type EQ '254' then begin
            header_date = header
        stop
        goto, skip
    endif
    endelse
endwhile
endwhile
close, 7

date = date(where(press_sfc NE 0))
press_sfc = press_sfc(where(press_sfc NE 0))
hgt_sfc = hgt_sfc(where(press_sfc NE 0))
tmp_sfc = tmp_sfc(where(press_sfc NE 0))
dewpt_sfc = dewpt_sfc(where(press_sfc NE 0))
press_850 = press_850(where(press_sfc NE 0))
hgt_850 = hgt_850(where(press_sfc NE 0))
tmp_850 = tmp_850(where(press_sfc NE 0))
dewpt_850 = dewpt_850(where(press_sfc NE 0))
press_700 = press_700(where(press_sfc NE 0))
hgt_700 = hgt_700(where(press_sfc NE 0))
tmp_700 = tmp_700(where(press_sfc NE 0))
dewpt_700 = dewpt_700(where(press_sfc NE 0))
press_500 = press_500(where(press_sfc NE 0))
hgt_500 = hgt_500(where(press_sfc NE 0))
tmp_500 = tmp_500(where(press_sfc NE 0))
dewpt_500 = dewpt_500(where(press_sfc NE 0))

; check for missing data...throw out any obs with missing data
all_obs = [[press_sfc],[hgt_sfc],[tmp_sfc],[dewpt_sfc],$  

           [press_850],[hgt_850],[tmp_850],[dewpt_850],$  

           [press_700],[hgt_700],[tmp_700],[dewpt_700],$  

           [press_500],[hgt_500],[tmp_500],[dewpt_500]]

cols = n_elements(press_sfc)
rows = 16
column = intarr(cols)
for i = 0, cols-1 do begin
    for j = 0, rows-1 do begin
        if (all_obs(i,j) EQ 32767) or (all_obs(i,j) EQ 3276.7) then
begin
            column(i) = 1
        endif
    endfor
endfor

keep = where(column NE 1)
nc = n_elements(keep)
new_obs = fltarr(nc,rows)
new_obs = all_obs(keep,*)
date = date(keep)

;keep only dates within the given text files (format=01/13/90)

```

```

tempdate = strarr(8)
tempdate0 = ''
tempdate1 = ''
tempdate2 = ''
tempdate3 = ''
tempdate4 = ''
tempdate5 = ''
tempdate6 = ''
tempdate7 = ''
mult_dates = ''
final_obs = fltarr(1,16)
final_dates = strarr(1)
search_dates = strarr(8)

openr, 13, date_file
i = 0
while not eof(13) do begin
    readf, 13, mult_dates
    reads, mult_dates, tempdate0, tempdate1, tempdate2, tempdate3,
    tempdate4,$
                           tempdate5, tempdate6, tempdate7,
format = "(x,a8,x,a8,x,a8,x,a8,x,a8,x,a8,x,a8,x,a8)""

    search_dates(0) = tempdate0
    i = i+1
    search_dates(1) = tempdate1
    i = i+1
    search_dates(2) = tempdate2
    i = i+1
    search_dates(3) = tempdate3
    i = i+1
    search_dates(4) = tempdate4
    i = i+1
    search_dates(5) = tempdate5
    i = i+1
    search_dates(6) = tempdate6
    i = i+1
    search_dates(7) = tempdate7
    i = i+1

    for j = 0, 7 do begin
        for k = 0, nc-1 do begin
            if (search_dates(j) EQ date(k)) then begin
                final_dates = [final_dates, date(k)]
                final_obs = [final_obs, new_obs(k,*)]
            endif
        endfor
    endfor
endwhile
close, 13
index = where(final_dates NE '99/99/99' and final_dates NE '')
final_dates = final_dates(index)                                ;array of dates
with good ua_data for days in daily summary files
final_obs = final_obs(index,*)                                 ;array of
good observations for days in daily summary files

```

```

nc = n_elements(final_dates)

N = nc
count = 0
consol_date = strarr(1)
consol_date(0) = final_dates(0)
temp_date = final_dates

index = where(temp_date NE temp_date(0), count) ;begins
consolidating repeated dates
if count NE 0 then begin
    temp_date = temp_date(index)
    for i = 1, N-1 do begin
        consol_date = [consol_date, temp_date(0)]
        index = where(temp_date NE temp_date(0), count)
        if count NE 0 then begin
            temp_date = temp_date(index)
        endif else begin
            goto, done
        endelse
    ;N = n_elements(temp_date)
    endfor
endif else begin
    goto, done
endelse
done: ;done consolidating...list of unique dates is in

;consol_date
N = n_elements(consol_date)
;N is number of unique dates

sto_array = strarr(6)

obs_data = {obs_struct, $
            date: strarr(nc),      $;
            press_sfc: intarr(nc),  $;
            thetae_sfc: intarr(nc), $;
            hgt_850: intarr(nc),   $;
            thetae_850: intarr(nc), $;
            hgt_700: intarr(nc),   $;
            thetae_700: intarr(nc), $;
            hgt_500: intarr(nc),   $;
            thetae_500: intarr(nc)};;

consol_obs_array = {consol_obs_struct, $
                     date: strarr(N),      $;
                     thetae_sfc: fltarr(N),  $;
                     thetae_850: fltarr(N),  $;
                     thetae_700: fltarr(N),  $;
                     thetae_500: fltarr(N)};

consol_obs_array.date = consol_date

;calculate u, v components for sfc, rt, & upp...store in sto_array(0:5)

for i = 0, N-1 do begin ;for each distinct date

```

```

thetae_sfc = 0
total_thetae_sfc = 0.0
total_thetae_850 = 0.0
total_thetae_700 = 0.0
total_thetae_500 = 0.0

index = where(final_dates EQ consol_date(i), count)
for j = 0, count-1 do begin ; for each occurrance of a date
(in the daily summaries)
    ;read a dewpoint ob, and calculate equivalent potential
temperature
    T_sfc = final_obs(index(j),2)
    Td_sfc = final_obs(index(j),3)
    T_850 = final_obs(index(j),6)
    Td_850 = final_obs(index(j),7)
    T_700 = final_obs(index(j),10)
    Td_700 = final_obs(index(j),11)
    T_500 = final_obs(index(j),14)
    Td_500 = final_obs(index(j),15)
    sfc_p = final_obs(index(j),0)

    e_sfc = 6.11*exp(19.83-(5417/(Td_sfc+273)))
    e_850 = 6.11*exp(19.83-(5417/(Td_850+273)))
    e_700 = 6.11*exp(19.83-(5417/(Td_700+273)))
    e_500 = 6.11*exp(19.83-(5417/(Td_500+273)))
    thetae_sfc =
    ((1000/sfc_p)^0.28557)*(T_sfc+273)+((1547.88/sfc_p)*e_sfc)
    thetae_850 = (1.04750*(T_850+273))+(1.82104*e_850)
    thetae_700 = (1.10722*(T_700+273))+(2.21126*e_700)
    thetae_500 = (1.21889*(T_500+273))+(3.09577*e_500)
    total_thetae_sfc = total_thetae_sfc + thetae_sfc
    total_thetae_850 = total_thetae_850 + thetae_850
    total_thetae_700 = total_thetae_700 + thetae_700
    total_thetae_500 = total_thetae_500 + thetae_500
endfor

;calculate average equivalent potential temperature
avg_thetae_sfc = (total_thetae_sfc)/(count)
if (abs(avg_thetae_sfc) LT 0.000001) then avg_thetae_sfc = 0.0
avg_thetae_850 = (total_thetae_850)/(count)
if (abs(avg_thetae_850) LT 0.000001) then avg_thetae_850 = 0.0
avg_thetae_700 = (total_thetae_700)/(count)
if (abs(avg_thetae_700) LT 0.000001) then avg_thetae_700 = 0.0
avg_thetae_500 = (total_thetae_500)/(count)
if (abs(avg_thetae_500) LT 0.000001) then avg_thetae_500 = 0.0

;assign average wind observations for entire area for each day to
consol_obs_array
consol_obs_array.thetae_sfc(i) = avg_thetae_sfc
consol_obs_array.thetae_850(i) = avg_thetae_850
consol_obs_array.thetae_700(i) = avg_thetae_700
consol_obs_array.thetae_500(i) = avg_thetae_500
consol_obs_array.date(i) = consol_date(i)
endfor
;stop

```

```

mean_thetae_sfc =
total(consol_obs_array.thetae_sfc)/n_elements(consol_obs_array.thetae_sfc
)
mean_thetae_850 =
total(consol_obs_array.thetae_850)/n_elements(consol_obs_array.thetae_850
)
mean_thetae_700 =
total(consol_obs_array.thetae_700)/n_elements(consol_obs_array.thetae_700
)
mean_thetae_500 =
total(consol_obs_array.thetae_500)/n_elements(consol_obs_array.thetae_500
)
;stop
;store daily u, v
n = n_elements(consol_obs_array.thetae_sfc)
openw, 28, outfile
for i =0, n-1 do begin
    printf, 28,
consol_obs_array.thetae_sfc(i),consol_obs_array.thetae_850(i),$
    consol_obs_array.thetae_700(i),
consol_obs_array.thetae_500(i)
    printf, 28, consol_obs_array.date(i)
endfor

close, 28
openr, 20, outfile
thetae_sfc = fltarr(n)
thetae_850 = fltarr(n)
thetae_700 = fltarr(n)
thetae_500 = fltarr(n)
temp1 = fltarr(4)
temp2 = ''
date = strarr(n)

for i = 0,n-1 do begin
    readf, 20, temp1
    thetae_sfc(i) = temp1(0)
    thetae_850(i) = temp1(1)
    thetae_700(i) = temp1(2)
    thetae_500(i) = temp1(3)
    readf, 20, temp2
    date(i) = temp2
endfor

close, 20

;computes the mean, var
result1 = MOMENT(thetae_sfc)
result2 = MOMENT(thetae_850)
result3 = MOMENT(thetae_700)
result4 = MOMENT(thetae_500)

openw, 28, outfile, /append
printf, 28, 'Mean / Std Dev Sfc ThetaE: ',result1(0), ' /
',sqrt(result1(1))
printf, 28, 'Mean / Std Dev 850 ThetaE: ',result2(0), ' /
',sqrt(result2(1))

```

```
printf, 28, 'Mean / Std Dev 700 ThetaE: ',result3(0), ' /  
' ,sqrt(result3(1))  
printf, 28, 'Mean / Std Dev 500 ThetaE: ',result4(0), ' /  
' ,sqrt(result4(1))  
close, 28  
end
```

```

pro ua_anal

; this program reads the upper air data files, consolidates them to one
file, extracts the four classes
; of events (high_active, high_inactive, low_active, and low_inactive,
; and analyzes the data for mean u,v, and V winds at 500mb
; mean u,v, and V winds at
;
; ridge top
;
; surface

; Programmer: Stephen Phillips
; Last Update: 26 Oct 01
; Modified by: Me

close, /all

ua_file ='C:\My Documents\sphill\upper_air\9000ua_SE.txt'

;date_file = 'C:\My Documents\sphill\text\high_active.txt'
;date_file = 'C:\My Documents\sphill\text\high_inactive.txt'
;date_file = 'C:\My Documents\sphill\text\low_active.txt'
;date_file = 'C:\My Documents\sphill\text\low_inactive.txt'
;date_file = 'C:\My Documents\sphill\text\BRact_ALact.txt'
;date_file = 'C:\My Documents\sphill\text\BRact_ALinact.txt'
;date_file = 'C:\My Documents\sphill\text\BRinact_ALact.txt'
;date_file = 'C:\My Documents\sphill\text\BRinact_ALinact.txt'
;date_file = 'C:\My Documents\sphill\text\ALact_Lowact.txt'
;date_file = 'C:\My Documents\sphill\text\ALact_Lowinact.txt'
;date_file = 'C:\My Documents\sphill\text\ALinact_Lowact.txt'
;date_file = 'C:\My Documents\sphill\text\BRact_Lowact.txt'
;date_file = 'C:\My Documents\sphill\text\BRact_Lowinact.txt'
date_file = 'C:\My Documents\sphill\text\BRinact_Lowact.txt'

;outfile = 'C:\My Documents\sphill\upper_air\high_active_avg_wnds.txt'
;outfile = 'C:\My Documents\sphill\upper_air\high_inactive_avg_wnds.txt'
;outfile = 'C:\My Documents\sphill\upper_air\low_active_avg_wnds.txt'
;outfile = 'C:\My Documents\sphill\upper_air\low_inactive_avg_wnds.txt'
;outfile = 'C:\My Documents\sphill\upper_air\BRact_ALact_avg_wnds.txt'
;outfile = 'C:\My Documents\sphill\upper_air\BRact_ALinact_avg_wnds.txt'
;outfile = 'C:\My Documents\sphill\upper_air\BRinact_ALact_avg_wnds.txt'
;outfile = 'C:\My Documents\sphill\upper_air\BRinact_ALinact_avg_wnds.txt'
;outfile = 'C:\My Documents\sphill\upper_air\ALact_Lowact_avg_wnds.txt'
;outfile = 'C:\My Documents\sphill\upper_air\ALact_Lowinact_avg_wnds.txt'
;outfile = 'C:\My Documents\sphill\upper_air\ALinact_Lowact_avg_wnds.txt'
;outfile = 'C:\My Documents\sphill\upper_air\BRact_Lowact_avg_wnds.txt'
;outfile = 'C:\My Documents\sphill\upper_air\BRact_Lowinact_avg_wnds.txt'
outfile = 'C:\My Documents\sphill\upper_air\BRinact_Lowact_avg_wnds.txt'

openr, 7, ua_file

```

```

missing = 32767
header_date = ''
header = ''
i = 0L
to 0
date = strarr(29179)
time = strarr(29179)
wmo = intarr(29179)
sfc_press = intarr(29179)
sfc_hgt = intarr(29179)
sfc_tmp = fltarr(29179)
sfc_dewpt = fltarr(29179)
sfc_wnd_dir = intarr(29179)
sfc_wnd_spd = fltarr(29179)
rt_press = intarr(29179)
rt_hgt = intarr(29179)
rt_tmp = fltarr(29179)
rt_dewpt = fltarr(29179)
rt_wnd_dir = intarr(29179)
rt_wnd_spd = fltarr(29179)
upp_press = intarr(29179)
upp_hgt = intarr(29179)
upp_tmp = fltarr(29179)
upp_dewpt = fltarr(29179)
upp_wnd_dir = intarr(29179)
upp_wnd_spd = fltarr(29179)

while not eof(7) do begin ;reading the daily upper air data

    readf, 7, header_date
    skip:
    ; Converts the 'dates' value into a different format for file name
setup
    date_broke=STRSPLIT(header_date(0), ' ', /extract)
    ; Extracts the year from file info
    year_num=string(date_broke(4))
    if (strlen(year_num) NE 4) then stop
    ; Extracts and reformats the month from file info
    mon_num=string(2)
    mon_name=STRLOWCASE(date_broke(3))
    if (strlen(mon_name) NE 3) then stop
    if (mon_name EQ 'jan') then mon_num='01'
    if (mon_name EQ 'feb') then mon_num='02'
    if (mon_name EQ 'mar') then mon_num='03'
    if (mon_name EQ 'apr') then mon_num='04'
    if (mon_name EQ 'may') then mon_num='05'
    if (mon_name EQ 'jun') then mon_num='06'
    if (mon_name EQ 'jul') then mon_num='07'
    if (mon_name EQ 'aug') then mon_num='08'
    if (mon_name EQ 'sep') then mon_num='09'
    if (mon_name EQ 'oct') then mon_num='10'
    if (mon_name EQ 'nov') then mon_num='11'
    if (mon_name EQ 'dec') then mon_num='12'
    ; Extracts the day from file info
    day_num=string(date_broke(2))
    if (strlen(day_num) LT 2) then day_num = '0'+day_num

```

```

; Extracts the hour from file info
hour_num=string(date_broke(1))
if (strlen(hour_num) LT 2) then hour_num = '0'+hour_num
; Setup the file name for output file
year numb = strmid(year_num, 2,2)
date(i) = mon_num+'/'+day_num+'/'+year_numb
time(i) = hour_num

temp = strarr(7)
readf, 7, format = "(a7,2x,a5,2x,a5,2f7.2,4x,a3,2x,a5)", temp
wmo(i) = fix(temp(2))

readf, 7, header
readf, 7, header

temp_sfc = strarr(7)
readf, 7, format = "(a7,3x,a4,5a7)",temp_sfc
type = fix(temp_sfc(0))
if type EQ 9 then begin
    sfc_press(i) = fix(temp_sfc(1))
    sfc_hgt(i) = fix(temp_sfc(2))
    sfc_tmp(i) = (float(temp_sfc(3)))/10
    sfc_dewpt(i) = (float(temp_sfc(4)))/10
    sfc_wnd_dir(i) = fix(temp_sfc(5))
    sfc_wnd_spd(i) = (float(temp_sfc(6)))/10
endif
temp_850 = strarr(7)
readf, 7, header
readf, 7, format = "(a7,3x,a4,5a7)",temp_850      ;850mb / ridge top
wind
type = fix(temp_850(0))
if type EQ 4 then begin
    rt_press(i) = fix(temp_850(1))
    rt_hgt(i) = fix(temp_850(2))
    rt_tmp(i) = (float(temp_850(3)))/10
    rt_dewpt(i) = (float(temp_850(4)))/10
    rt_wnd_dir(i) = fix(temp_850(5))
    rt_wnd_spd(i) = (float(temp_850(6)))/10
endif
temp_500 = strarr(7)
readf, 7, header
readf, 7, format = "(a7,3x,a4,5a7)",temp_500      ;500mb / steering
flow
type = fix(temp_500(0))
if type EQ 4 then begin
    upp_press(i) = fix(temp_500(1))
    upp_hgt(i) = fix(temp_500(2))
    upp_tmp(i) = (float(temp_500(3)))/10
    upp_dewpt(i) = (float(temp_500(4)))/10
    upp_wnd_dir(i) = fix(temp_500(5))
    upp_wnd_spd(i) = (float(temp_500(6)))/10
endif
i = i+1
rept:
while not eof(7) do begin
    readf, 7, header
    header_broke=STRSPLIT(header(0), ' ', /extract)

```

```

type = header_broke(0)
if type NE '254' then begin
;
stop
    goto, rept
endif else begin
    if type EQ '254' then begin
        header_date = header
;
stop
    goto, skip
    endif
endelse
endwhile
;
for j = 0, 5 do begin
;
    readf, 7, header
;
;skips the remaining levels
;
endfor

endwhile
close, 7

date = date(where(sfc_press NE 0))
sfc_press = sfc_press(where(sfc_press NE 0))
sfc_hgt = sfc_hgt(where(sfc_press NE 0))
sfc_tmp = sfc_tmp(where(sfc_press NE 0))
sfc_dewpt = sfc_dewpt(where(sfc_press NE 0))
sfc_wnd_dir = sfc_wnd_dir(where(sfc_press NE 0))
sfc_wnd_spd = sfc_wnd_spd(where(sfc_press NE 0))
rt_press = rt_press(where(sfc_press NE 0))
rt_hgt = rt_hgt(where(sfc_press NE 0))
rt_tmp = rt_tmp(where(sfc_press NE 0))
rt_dewpt = rt_dewpt(where(sfc_press NE 0))
rt_wnd_dir = rt_wnd_dir(where(sfc_press NE 0))
rt_wnd_spd = rt_wnd_spd(where(sfc_press NE 0))
upp_press = upp_press(where(sfc_press NE 0))
upp_hgt = upp_hgt(where(sfc_press NE 0))
upp_tmp = upp_tmp(where(sfc_press NE 0))
upp_dewpt = upp_dewpt(where(sfc_press NE 0))
upp_wnd_dir = upp_wnd_dir(where(sfc_press NE 0))
upp_wnd_spd = upp_wnd_spd(where(sfc_press NE 0))

; check for missing data...throw out any obs with missing data
all_obs =
[[sfc_press],[sfc_hgt],[sfc_tmp],[sfc_dewpt],[sfc_wnd_dir],[sfc_wnd_spd],
$ [rt_press],[rt_hgt],[rt_tmp],[rt_dewpt],[rt_wnd_dir],[rt_wnd_spd],$ [upp_press],[upp_hgt],[upp_tmp],[upp_dewpt],[upp_wnd_dir],[upp_wnd_spd]]]

cols = n_elements(sfc_press)
rows = 18
column = intarr(cols)
for i = 0, cols-1 do begin
    for j = 0, rows-1 do begin
        if (all_obs(i,j) EQ 32767) or (all_obs(i,j) EQ 3276.7) then
begin
            column(i) = 1

```

```

        endif
    endfor
endfor

keep = where(column NE 1)
nc = n_elements(keep)
new_obs = fltarr(nc,rows)
new_obs = all_obs(keep,*)
date = date(keep)

;keep only dates within the given text files (format=01/13/90)

tempdate = strarr(8)
tempdate0 = ''
tempdate1 = ''
tempdate2 = ''
tempdate3 = ''
tempdate4 = ''
tempdate5 = ''
tempdate6 = ''
tempdate7 = ''
mult_dates = ''
final_obs = fltarr(1,18)
final_dates = strarr(1)
search_dates = strarr(8)

openr, 13, date_file
i = 0
while not eof(13) do begin
    readf, 13, mult_dates
    reads, mult_dates, tempdate0, tempdate1, tempdate2, tempdate3,
    tempdate4,$
                           tempdate5, tempdate6, tempdate7,
format = "(x,a8,x,a8,x,a8,x,a8,x,a8,x,a8,x,a8,x,a8)"

    search_dates(0) = tempdate0
    i = i+1
    search_dates(1) = tempdate1
    i = i+1
    search_dates(2) = tempdate2
    i = i+1
    search_dates(3) = tempdate3
    i = i+1
    search_dates(4) = tempdate4
    i = i+1
    search_dates(5) = tempdate5
    i = i+1
    search_dates(6) = tempdate6
    i = i+1
    search_dates(7) = tempdate7
    i = i+1

    for j = 0, 7 do begin
        for k = 0, nc-1 do begin
            if (search_dates(j) EQ date(k)) then begin
                final_dates = [final_dates, date(k)]

```

```

                final_obs  = [final_obs, new_obs(k,*)]
            endif
        endfor
    endfor
endwhile
close, 13
index = where(final_dates NE '99/99/99' and final_dates NE '')
;if (index NE -1) then begin
    final_dates = final_dates(index)                                ;array of
dates with good ua_data for days in daily summary files
    final_obs = final_obs(index,*)                                     ;array
of good observations for days in daily summary files
;endif
nc = n_elements(final_dates)

N = nc
count = 0
consol_date = strarr(1)
consol_date(0) = final_dates(0)
temp_date = final_dates

index = where(temp_date NE temp_date(0), count)                      ;begins
consolidating repeated dates
if count NE 0 then begin
    temp_date = temp_date(index)
    for i = 1, N-1 do begin
        consol_date = [consol_date, temp_date(0)]
        index = where(temp_date NE temp_date(0), count)
        if count NE 0 then begin
            temp_date = temp_date(index)
        endif else begin
            goto, done
        endelse
    ;N = n_elements(temp_date)
    endfor
endif else begin
    goto, done
endelse
done:                                                               ;done consolidating...list of unique dates is in
                ;consol_date
N = n_elements(consol_date)
;N is number of unique dates

sto_array = strarr(6)

obs_data = {obs_struct, $
            date: strarr(nc),      $;
            sfc_press: intarr(nc), $;
            sfc_u: fltarr(nc),    $;
            sfc_v: fltarr(nc),    $;
            sfc_dir: intarr(nc),  $;
            sfc_Vect: strarr(nc), $;
            rt_hgt: intarr(nc),   $;
            rt_u: fltarr(nc),    $;
            rt_v: fltarr(nc),    $;

```

```

        rt_dir: intarr(nc),      $;
        rt_Vect: strarr(nc),      $;
        upp_hgt: intarr(nc),      $;
        upp_u:  fltarr(nc),      $;
        upp_v:  fltarr(nc),      $;
        upp_dir: intarr(nc),      $;
        upp_Vect: strarr(nc)};

consol_obs_array = {consol_obs_struct, $
                     date: strarr(N),           $;
                     sfc_u: fltarr(N),          $;
                     sfc_v: fltarr(N),          $;
                     rt_u: fltarr(N),          $;
                     rt_v: fltarr(N),          $;
                     upp_u: fltarr(N),          $;
                     upp_v: fltarr(N),          $;
                     sfc_thetae: fltarr(N),      $;
                     rt_thetae: fltarr(N),      $;
                     upp_thetae: fltarr(N)};

consol_obs_array.date = consol_date

;calculate u, v components for sfc, rt, & upp...store in sto_array(0:5)

for i = 0, N-1 do begin                         ;for each distinct date

    avg_sfc_u = 0
    avg_sfc_v = 0
    avg_rt_u = 0
    avg_rt_v = 0
    avg_upp_u = 0
    avg_upp_v = 0
    thetae_sfc = 0
    total_sfc_u = 0
    total_sfc_v = 0
    total_rt_u = 0
    total_rt_v = 0
    total_upp_u = 0
    total_upp_v = 0
    total_thetae_sfc = 0.0
    total_thetae_rt = 0.0
    total_thetae_upp = 0.0

    index = where(final_dates EQ consol_date(i), count)
    for j = 0, count-1 do begin      ; for each occurrance of a date
    (in the daily summaries)
        ;read a wind ob, break it into components, and add ea
    component to previous ob for day
        sfc_dir = final_obs(index(j),4)
        sfc_dir = (sfc_dir-180) * !PI/180
        sfc_u = final_obs(index(j),5)*sin(sfc_dir)
        sfc_v = final_obs(index(j),5)*cos(sfc_dir)
        rt_dir = final_obs(index(j),10)
        rt_dir = (rt_dir-180) * !PI/180
        rt_u = final_obs(index(j),11)*sin(rt_dir)
        rt_v = final_obs(index(j),11)*cos(rt_dir)
        upp_dir = final_obs(index(j),16)

```

```

        upp_dir = (upp_dir-180) * !PI/180
        upp_u = final_obs(index(j),17)*sin(upp_dir)
        upp_v = final_obs(index(j),17)*cos(upp_dir)

        total_sfc_u = total_sfc_u + sfc_u
        total_sfc_v = total_sfc_v + sfc_v
        total_rt_u = total_rt_u + rt_u
        total_rt_v = total_rt_v + rt_v
        total_upp_u = total_upp_u + upp_u
        total_upp_v = total_upp_v + upp_v

        ;read a dewpoint ob, and calculate equivalent potential
        temperature
        T_sfc = final_obs(index(j),2)
        Td_sfc = final_obs(index(j),3)
        T_rt = final_obs(index(j),8)
        Td_rt = final_obs(index(j),9)
        T_upp = final_obs(index(j),14)
        Td_upp = final_obs(index(j),15)
        e_sfc = 6.11*exp(19.83-(5417/(Td_sfc+273)))
        e_rt = 6.11*exp(19.83-(5417/(Td_rt+273)))
        e_upp = 6.11*exp(19.83-(5417/(Td_upp+273)))
        sfc_p = final_obs(index(j),0)
        thetae_sfc =
        ((1000/sfc_p)^0.28557)*(T_sfc+273)+((1547.88/sfc_p)*e_sfc)
        thetae_rt = (1.04750*(T_rt+273))+(1.82104*e_rt)
        thetae_upp = (1.21889*(T_upp+273))+(3.09577*e_upp)
        total_thetae_sfc = total_thetae_sfc + thetae_sfc
        total_thetae_rt = total_thetae_rt + thetae_rt
        total_thetae_upp = total_thetae_upp + thetae_upp
    endfor

    ;calculate: u / v components of sfc / rt / upp winds
    avg_sfc_u = (total_sfc_u)/(count)
    if (abs(avg_sfc_u) LT 0.000001) then avg_sfc_u = 0.0
    avg_sfc_v = (total_sfc_v)/(count)
    if (abs(avg_sfc_v) LT 0.000001) then avg_sfc_v = 0.0
    avg_rt_u = (total_rt_u)/(count)
    if (abs(avg_rt_u) LT 0.000001) then avg_rt_u = 0.0
    avg_rt_v = (total_rt_v)/(count)
    if (abs(avg_rt_v) LT 0.000001) then avg_rt_v = 0.0
    avg_upp_u = (total_upp_u)/(count)
    if (abs(avg_upp_u) LT 0.000001) then avg_upp_u = 0.0
    avg_upp_v = (total_upp_v)/(count)
    if (abs(avg_upp_v) LT 0.000001) then avg_upp_v = 0.0
    avg_thetae_sfc = (total_thetae_sfc)/(count)
    if (abs(avg_thetae_sfc) LT 0.000001) then avg_thetae_sfc = 0.0
    avg_thetae_rt = (total_thetae_rt)/(count)
    if (abs(avg_thetae_rt) LT 0.000001) then avg_thetae_rt = 0.0
    avg_thetae_upp = (total_thetae_upp)/(count)
    if (abs(avg_thetae_upp) LT 0.000001) then avg_thetae_upp = 0.0

    ;assign average wind observations for entire area for each day to
    consol_obs_array
    consol_obs_array.sfc_u(i) = avg_sfc_u
    consol_obs_array.sfc_v(i) = avg_sfc_v
    consol_obs_array.rt_u(i) = avg_rt_u

```

```

    consol_obs_array.rt_v(i) = avg_rt_v
    consol_obs_array.upp_u(i) = avg_upp_u
    consol_obs_array.upp_v(i) = avg_upp_v
    consol_obs_array.sfc_thetae(i) = avg_thetae_sfc
    consol_obs_array.rt_thetae(i) = avg_thetae_rt
    consol_obs_array.upp_thetae(i) = avg_thetae_upp
    consol_obs_array.date(i) = consol_date(i)
endfor
;stop
mean_sfc_thetae =
total(consol_obs_array.sfc_thetae)/n_elements(consol_obs_array.sfc_thetae)
)
mean_rt_thetae =
total(consol_obs_array.rt_thetae)/n_elements(consol_obs_array.rt_thetae)
mean_upp_thetae =
total(consol_obs_array.upp_thetae)/n_elements(consol_obs_array.upp_thetae)
)
;stop
;store daily u, v
n = n_elements(consol_obs_array.sfc_u)
openw, 28, outfile
for i =0, n-1 do begin
    printf, 28,
    consol_obs_array.sfc_u(i), consol_obs_array.sfc_v(i), consol_obs_array.rt_u
    (i), $
        consol_obs_array.rt_v(i), consol_obs_array.upp_u(i), consol_obs_array
    .upp_v(i)
    printf, 28, consol_obs_array.date(i)
endfor

close, 28
openr, 20, outfile
sfc_u = fltarr(n)
sfc_v = fltarr(n)
rt_u = fltarr(n)
rt_v = fltarr(n)
upp_u = fltarr(n)
upp_v = fltarr(n)
temp1 = fltarr(6)
temp2 = ''
date = strarr(n)

for i = 0,n-1 do begin
    readf, 20, temp1
    sfc_u(i) = temp1(0)
    sfc_v(i) = temp1(1)
    rt_u(i) = temp1(2)
    rt_v(i) = temp1(3)
    upp_u(i) = temp1(4)
    upp_v(i) = temp1(5)
    readf, 20, temp2
    date(i) = temp2
endfor

close, 20

```

```

;computes the mean, var
result1 = MOMENT(sfc_u)
result2 = MOMENT(sfc_v)
result3 = MOMENT(rt_u)
result4 = MOMENT(rt_v)
result5 = MOMENT(upp_u)
result6 = MOMENT(upp_v)
sfc_wnd = ''
rt_wnd = ''
upp_wnd = ''
sfc_spd = sqrt(result1[0]^2 + result2[0]^2)
sfc_dir = (atan(result1[0] / result2[0])* (180/!PI)) + 180
sfc_wnd =
strcompress(string(round(sfc_dir)))+'/'+strcompress(string(sfc_spd))
rt_spd = sqrt(result3[0]^2 + result4[0]^2)
rt_dir = (atan(result3[0] / result4[0])* (180/!PI)) + 180
rt_wnd =
strcompress(string(round(rt_dir)))+'/'+strcompress(string(rt_spd))
upp_spd = sqrt(result5[0]^2 + result6[0]^2)
upp_dir = (atan(result5[0] / result6[0])* (180/!PI)) + 180
upp_wnd =
strcompress(string(round(upp_dir)))+'/'+strcompress(string(upp_spd))

openw, 28, outfile, /append
printf, 28, 'Mean, Std Dev of sfc wind, u component: ', result1[0],
sqrt(result1[1])
printf, 28, 'Mean, Std Dev of sfc wind, v component: ', result2[0],
sqrt(result2[1])
printf, 28, 'Mean, Std Dev of rt wind, u component: ', result3[0],
sqrt(result3[1])
printf, 28, 'Mean, Std Dev of rt wind, v component: ', result4[0],
sqrt(result4[1])
printf, 28, 'Mean, Std Dev of upp wind, u component: ', result5[0],
sqrt(result5[1])
printf, 28, 'Mean, Std Dev of upp wind, v component: ', result6[0],
sqrt(result6[1])
printf, 28, 'Mean wind dir/spd: sfc, rt, upp: ',sfc_wnd, rt_wnd, upp_wnd
printf, 28, 'Mean Sfc ThetaE: ',mean_sfc_thetae
printf, 28, 'Mean RT ThetaE: ',mean_rt_thetae
printf, 28, 'Mean Upp ThetaE: ',mean_upp_thetae
close, 28
end

```

**VITA**

Stephen Edward Phillips was born on the 15<sup>th</sup> day of November 1972 to Mr. and Mrs. James W. Phillips of Wichita Falls, Texas. He graduated from Burk Burnett High School in May of 1991.

On the 21<sup>st</sup> day of December 1996, Captain Phillips graduated from Texas A&M University with a B.S. in Meteorology, and was commissioned as a second lieutenant in the United States Air Force. After serving tours of duty with 55<sup>th</sup> Operations Support Squadron at Offutt Air Force Base, Nebraska, and with the 2<sup>nd</sup> Infantry Division at Camp Red Cloud Army Installation, Republic of Korea, he was assigned to the Air Force Institute of Technology to attend Texas A&M University as a masters' degree candidate.

Captain Phillips is currently assigned to the Air Force Combat Climatology Center in Asheville, North Carolina. His permanent address is:

22G Ascension Dr.

Ashville, NC 28806